EIGENVALUE PLACEMENT FOR VARIABLE STRUCTURE CONTROL SYSTEMS

by

Catherine Anne Woodham

A Thesis submitted for the
degree of Doctor of Philosophy

The Department of Applied and Computational Mathematics
University of Sheffield

October 1991

ORIGINAL COPY TIGHTLY BOUND

To Jan

"Work hard ... Rock hard ... Eat hard ... Sleep hard ...
Grow big ... Wear glasses if you need 'em "

Webb Wilder 1986

ACKNOWLEDGMENTS

I would like to thank Dr Alan Zinober, my supervisor, for all his enthusiasm, help and encouragement during the last three years, and for his advice during the preparation of this thesis. I would also like to acknowledge the financial support of the Science and Engineering Research Council.

My grateful thanks are also due to Judith Ellis, Madeleine Floy and Christine Barker, for all their help, cups of tea, and for the use of their printer. I would also like to thank Linda Wilkinson for all her help and support.

Finally, I would like to acknowledge the excellent music of Joe Ely, which kept me going during the period of preparing this thesis.

SUMMARY

Variable Structure Control is a well-known solution to the problem of deterministic control of uncertain systems, since it is invariant to a class of parameter variations. A central feature of VSC is that of sliding motion, which occurs when the system state repeatedly crosses certain subspaces in the state space. These subspaces are known as sliding hyperplanes, and it is the design of these hyperplanes which is considered in this thesis.

A popular method of hyperplane design is to specify eigenvalues in the left-hand half-plane for the reduced order equivalent system, and to design the control matrix to yield these eigenvalues. A more general design approach is to specify some region in the left-hand half-plane within which these eigenvalues must lie. Four regions are considered in this thesis, namely a disc, an infinite vertical strip, a sector and a region bounded by two intersecting sectors.

The methods for placing the closed-loop eigenvalues within these regions all require the solution of a matrix Riccati equation : discrete or continuous, real or complex. The choice of the positive definite symmetric matrices in these Riccati equations affects the positioning of the eigenvalues within the region. Suitable selection of these matrices will therefore lead to real or complex eigenvalues, as required, and will influence their position within the chosen region.

The solution of the hyperplane design problem by a more general choice of the closed-loop eigenvalues lends itself to the minimization of the linear part of the control. A suitable choice of the position of the eigenvalues within the required region enables either the 2-norm of the linear part of the control, or the condition number of the linear feedback to be minimized. The choice of the range space eigenvalues may also be used, more effectively, in this minimization.

CONTENTS

1. INTRODUCTION

The problem of controlling uncertain dynamical systems has been studied increasingly in recent years. One solution to this problem is the Variable Structure controller, and it is this solution which will be considered in this thesis. Variable Structure Control (VSC) with a sliding mode was first introduced by Soviet authors in the early sixties, and a survey paper of this early work was written in the seventies (Utkin, 1977). The early results on the invariance of VSC systems to a class of parameter variations and disturbances were established by Drazenovic in 1969. In the 1970's and 1980's the method was extended to multivariable control systems, and model-following control (Young, 1977 & 1978, Zinober, El-Ghezawi and Billings, 1982) and CAD packages were developed (Dorling, 1985). Current applications include robotics, and flight control.

A Variable Structure Control system is a system for which the structure of the state feedback control is altered, or switched, in a preordained way, as the system state crosses certain subspaces in the state space. These subspaces are generally known as the sliding hyperplanes, the discontinuity surfaces, the switching manifolds, or the switching surfaces. The controller generally consists of the sum of a linear part and a non-linear part; the non-linear part contains the discontinuous elements of the control. A non-linear system whose structure alters on the switching surfaces, due to control of this form is generally known as a Variable Structure System (VSS).

The central characteristic of a Variable Structure System is the sliding motion which occurs when the system state crosses and then recrosses a switching surface. This sliding motion depends on the form of the control law, and may occur on individual switching surfaces, or on all of the switching surfaces together. If the latter case occurs, then the system is said to be in the sliding mode, and its motion is then effectively constrained to lie within a subspace of the full state space. The system is therefore equivalent to a system of lower order, known as the reduced order equivalent system, and this lower order system must be asymptotically stable to ensure that the state slides down the switching surfaces to the origin.

The objective of the design of a VSC system is to drive the state from some arbitrary initial condition onto the intersection of the switching surfaces, and then to maintain it on, or in the neighbourhood of, this intersection. The design process consists of two separate parts, the existence problem and the reachability problem. The choice of a set of hyperplanes to give the system the required behaviour in the sliding mode is called the existence problem. The hyperplanes must be chosen so that the sliding mode on their intersection gives the desired performance of the reduced order equivalent system. The solution of the existence problem is completely independent of the form of the control functions. Once the existence problem has been satisfactorily solved, the second stage of the design process, which consists of the design of controls which ensure the attainment of the desired sliding mode, is considered.

This part of the design process is called the reachability problem, and since its solution depends on the choice of the sliding hyperplanes, it cannot be solved until the existence problem has been solved.

The transient motion of a VSC regulator system consists of two independent stages :

1) a preferably rapid motion to bring the system to the intersection of the switching surfaces, where the sliding motion will occur.
2) a slower sliding motion of (possibly) infinite duration during which the state slides towards the state space origin, whilst remaining in or in the neighbourhood of, the sliding subspace.

This independent two stage motion can help to solve the problem of opposing design requirements, which occurs between static and dynamic accuracy, when designing a linear control. A Variable Structure Controller may be designed to give a rapid response with no loss of stability, and with insensitivity to parameter variations, and invariance to certain external disturbances. A controller designed in this way compares well with other design methods, for instance that of the Lyapunov controller (Garofalo and Glielmo, 1988), and a comparison of these two methods is contained in Chapter 2.

The solution of the existence problem requires the sliding hyperplanes to be chosen, to give an asymptotically stable reduced order equivalent system. The transient response of a linear system is given by a linear combination of the modes of the

system. The time response of the system is also determined by its eigenstructure, and so it is clearly important to choose a suitable structure for a satisfactory solution of the control problem.

In this thesis, we are particularly concerned with the choice of the closed-loop eigenvalues, and hence the sliding hyperplanes. The system will have a mode of unforced behaviour for each closed-loop eigenvalue, and these modes will be excited to various degrees by an arbitrary initial condition, and will behave independently of each other. Clearly then, the choice of the closed-loop eigenvalues of a system fixes the possible modes of unforced behaviour of that system, and so choosing suitable eigenvalues, in some way, is clearly important.

The simplest method is to specify the exact eigenvalues required, and this method is used by the VASSYD CAD package, which will be discussed in Chapter 2. However, it would clearly be advantageous to be able to specify the eigenvalues in a more general way, and one which is more closely linked to the modes of unforced behaviour of the system. Two possibilities for eigenvalue positioning are to place them within a strip or a disc, and these will be discussed, with regard to a Variable Structure controller, in Chapter 3. Another possibility is to place the eigenvalues within a sector, or a damping region, linked to the damping ratio of the system. The damping ratio, together with the closed-loop eigenvalues, determines the transient response of the system. This will be discussed in Chapter 4, again with regard to a Variable Structure controller. These methods require the

solution of a matrix Riccati equation, either discrete or continuous, with a real or complex solution. The choice of the positive definite symmetric matrices in the Riccati equation has an effect on the positioning of the eigenvalues within the chosen region, and this is investigated in Chapters 5 and 6.

The control effort required to reach the required subspace is also an important factor. It would clearly be advantageous to be able to design the controller so that the required control effort is minimized in some way. The linear part of the control lends itself to being minimized, rather than the non-linear part, which is discontinuous. This will be investigated in Chapter 7.

The research undertaken in this thesis is arranged in six chapters. Chapter 2 contains a description of the design of both a Variable Structure controller and a Lyapunov controller, and a comparison of their performance with regard to a robot arm tracking problem. The design of the sliding hyperplanes by placing the closed-loop eigenvalues of the reduced order equivalent system within a disc or a strip in the left-hand half-plane is contained in Chapter 3, and numerical examples of the hyperplane design process are given. In Chapter 4, a method for placing the closed loop eigenvalues of a system within a sector is developed, again with numerical examples of the hyperplane design process. Chapter 5 is concerned with the dependence of the eigenvalue placement within a disc or a strip to the design of the positive definite symmetric matrices, while Chapter 6 contains a similar investigation for the sector, and an investigation into the range of sectors available. The numerical examples given in

both of these chapters have again been chosen to demonstrate the hyperplane design process. In Chapter 7 the effect of minimizing the linear part of the control is investigated, and the results of the minimization are assessed by considering the robot arm tracking problem outlined in Chapter 2.

2. COMPARISON OF VSC AND LYAPUNOV METHODS

2.1 Introduction

There are many approaches to the problem of deterministic control of uncertain time-varying systems, and two possibilities which will be considered in this work are Variable Structure Control (see for example, Drazenovic, 1969, Itkis, 1976, Utkin, 1977 & 1978, De Carlo, Zak & Matthews, 1988, Zinober, El-Ghezawi & Billings, 1981 & 1982, Dorling & Zinober, 1986 & 1988), and Lyapunov control (see for example, Gutman & Palmor, 1982, Corless & Leitmann, 1981, Barmish & Leitmann, 1982, Ryan, 1988, Garofalo & Glielmo, 1988). The essential feature of VSC is that the non-linear feedback control has a discontinuity on one or more subspaces in the state space. The controller is designed so that the chosen sliding subspace, the null space of the sliding hyperplane matrix, is quickly reached, and thereafter the state remains within this subspace. The two parts of a VSC design procedure, the existence problem and the reachability problem, have been explained in Chapter 1. In Lyapunov control, a nonlinear function is developed using a Lyapunov function and specified bounds on the uncertainties, to give uniform boundedness and ultimate boundedness of the closed-loop feedback trajectory.

In Section 2.2, the existence problem for a VSC system is outlined, with respect to the regulator system. The design strategy of the CAD package VASSYD (Dorling, 1985) is also briefly outlined. Section 2.3 briefly outlines the Lyapunov approach

theoretically developed by Garofalo and Glielmo, 1988. Section 2.4 contains the numerical example being used in this comparison. The robot arm under consideration is described, and its equations are adapted for use with the two methods. The Lyapunov method requires some development from its theoretical formulation for use with a numerical example. The constants have to be chosen, and a method developed to ensure that the closed-loop eigenvalues of the two systems are the same (Zinober & Woodham, 1989). Section 2.5 contains a brief discussion of the results.

2.2 The Regulator System and VSC Method

A general form of the regulator system is given by

$$\dot{x}(t) = \left(A+\Delta A\right)x(t) + \left(B+\Delta B\right)u(t) + Df(t,x(t)) \qquad (2.2.1)$$

where x is the state n-vector, u is the control m-vector, and f is the disturbance p-vector. A and ΔA are $n \times n$ matrices, and ΔA represents the uncertainties in the plant values. B and ΔB are $n \times m$ matrices, ΔB represents the plant/control interface uncertainties and D is a $n \times p$ matrix representing the external disturbance effects. During the ideal sliding mode, motion is constrained to lie within a subspace of the full state space, which is designed to be a complementary subspace to the range space of B. Thus, during sliding, any uncertainties and disturbances acting in the range space of B will have no effect on the solution.

It is therefore sufficient to consider the *ideal* system, with no uncertainties and disturbances, given by

$$\dot{x}(t) = Ax(t) + Bu(t) \qquad (2.2.2)$$

where x, u, A and B are as defined above.

Matched uncertainties are handled by suitable choice of the control function. We assume that $m < n$, B is of full rank m and the pair (A,B) is completely controllable. The sliding mode may be determined from the condition

$$Cx(t) = 0 \qquad \forall\ t \geq t_s \qquad (2.2.3)$$

where t_s is the time when the sliding subspace is reached and C is an $m \times n$ matrix. Differentiating equation (2.2.3) with respect to time, and substituting for $\dot{x}(t)$ from (2.2.2) gives

$$C\dot{x}(t) = CAx(t) + CBu(t) = 0 \qquad \forall\ t \geq t_s \qquad (2.2.4)$$

Equation (2.2.4) may be rearranged to give

$$CBu(t) = -CAx(t) \qquad (2.2.5)$$

C is designed so that $|CB| \neq 0$, and therefore the product CB is invertible,and hence equation (2.2.5) may be rearranged to give the following expression

$$u(t) = -(CB)^{-1}CAx(t) = -Kx(t) \qquad (2.2.6)$$

where u(t), the equivalent control, is the open-loop control which forces the trajectory to remain in the null space of C, during sliding.

Substituting for u(t) from equation (2.2.6) into equation (2.2.2) gives

$$\dot{x}(t) = (I - B(CB)^{-1}C)Ax(t) \qquad \forall\ t \geq t_s \qquad (2.2.7)$$
$$= (A - BK)x(t)$$

which is the system equation for the closed-loop system dynamics during sliding.

It can be seen that this motion is independent of the actual control u and depends only on the choice of C, which determines the matrix K. The function of the control u is to drive the state into the sliding subspace $\mathcal{M}$, and thereafter to maintain it within the subspace $\mathcal{M}$.

The convergence of the state vector to the origin is ensured by suitable choice of the feedback matrix K. The determination of the matrix K or alternatively, the determination of the matrix C defining the subspace $\mathcal{M}$ may be achieved without prior knowledge of the form of the control vector u. (The reverse is not true). The null space of C, $\mathcal{N}(C)$, and the range space of B, $\mathcal{R}(B)$, are, under the hypotheses given earlier, complementary subspaces, so $\mathcal{N}(C) \cap \mathcal{R}(B) = \{0\}$. Since motion lies entirely within $\mathcal{N}(C)$ during the ideal sliding mode, the dynamic behaviour of the system during sliding is unaffected by the controls, as they act only within $\mathcal{R}(B)$. The development of the theory and design principles is simplified by using a particular canonical form for the system, which is closely related to the Kalman canonical form for a multivariable linear system.

By assumption, the matrix B has full rank m, so that there exists an orthogonal n×n transformation matrix T such that

$$TB = \begin{bmatrix} 0 \\ B_2 \end{bmatrix} \tag{2.2.8}$$

where B_2 is m×m and nonsingular.

Let $B = QR$, where Q is an n×n orthogonal matrix and R is n×m and upper triangular. Partitioning this expression for B gives

$$\begin{bmatrix} B_1 \\ B_2 \end{bmatrix} = \begin{bmatrix} Q_{11} & Q_{12} \\ Q_{21} & Q_{22} \end{bmatrix} \begin{bmatrix} R_1 \\ 0 \end{bmatrix} \tag{2.2.9}$$

Premultiplying both sides of equation (2.2.9) by Q^T, since Q is orthogonal, and hence $Q^T = Q^{-1}$, gives

$$\begin{bmatrix} Q_{11}^T & Q_{21}^T \\ Q_{12}^T & Q_{22}^T \end{bmatrix} \begin{bmatrix} B_1 \\ B_2 \end{bmatrix} = \begin{bmatrix} R_1 \\ 0 \end{bmatrix} \tag{2.2.10}$$

Since we require T to be chosen so that equation (2.2.8) holds, it is clear from equation (2.2.10) that T is given by

$$T = \begin{bmatrix} Q_{12}^T & Q_{22}^T \\ Q_{11}^T & Q_{21}^T \end{bmatrix} \tag{2.2.11}$$

The orthogonality restriction is imposed on T for reasons of numerical stability, and to remove the problem of inverting T when transforming back to the original system. The transformed state is y=Tx, so $T\dot{x} = \dot{y}$, and the state equation (2.2.2) becomes

$$\dot{y}(t) = TAT^T y(t) + TBu(t) \tag{2.2.12}$$

The sliding condition is $CT^T y(t) = 0$, $\forall\ t \geq t_s$. If the transformed state y is now partitioned as

$$y^T = (y_1^T \quad y_2^T); \qquad y_1 \in \mathcal{R}^{n-m}, \quad y_2 \in \mathcal{R}^m \tag{2.2.13}$$

and the matrices TAT^T, TB and CT^T are partitioned accordingly, then equation (2.2.12) may be written as a pair of equations :

$$\dot{y}_1(t) = A_{11}y_1(t) + A_{12}y_2(t) \tag{2.2.14a}$$

$$\dot{y}_2(t) = A_{12}y_1(t) + A_{22}y_2(t) + B_2u(t) \tag{2.2.14b}$$

The sliding condition becomes

$$C_1y_1(t) + C_2y_2(t) = 0 \tag{2.2.15}$$

where

$$TAT^T = \begin{bmatrix} A_{11} & A_{12} \\ A_{21} & A_{22} \end{bmatrix} \qquad CT^T = \begin{bmatrix} C_1 & C_2 \end{bmatrix}.$$

and C_2 is nonsingular (from CB nonsingular).

The canonical form is central to hyperplane design methods and it plays a significant role in the solution of the reachability problem, i.e. the determination of the control form ensuring the attainment of the sliding mode in $\mathcal{M}$ (Zinober, 1984). Equation (2.2.15) defining the sliding mode is equivalent to

$$y_2(t) = -Fy_1(t) \tag{2.2.16}$$

where the $m \times (n-m)$ matrix F is defined by

$$F = C_2^{-1}C_1 \tag{2.2.17}$$

so that in the sliding mode y_2 is related linearly to y_1.

The sliding mode satisfies equation (2.2.16) and

$$\dot{y}_1 = A_{11}\, y_1(t) + A_{12}\, y_2(t) \qquad (2.2.18)$$

This represents an $(n-m)^{th}$ order system in which y_2 plays the role of a state feedback control. So we get

$$\dot{y}_1(t) = (A_{11} - A_{12}F)y_1(t) \qquad (2.2.19)$$

which is known as the reduced order equivalent system, with system matrix $(A_{11} - A_{12}F)$. The design of a stable sliding mode such that $y \to 0$ as $t \to \infty$ requires the determination of the gain matrix F such that $(A_{11} - A_{12}F)$ has n-m left-hand half-plane eigenvalues.

The CAD package **VASSYD** (Dorling, 1985) will design the sliding hyperplanes, either by assignment of the sliding mode spectrum, or by quadratic minimization. The design of the sliding mode spectrum requires the exact specification of the closed-loop eigenvalues of the reduced order equivalent system $A_{11} - A_{12}F$. The eigenvectors may be assigned explicitly, or designed by the package to give maximally robust eigenvalues, using the theory that the sensitivity of an eigenvalue is inversely proportional to the angle between its left and right eigenvectors (Wilkinson, 1965), and a suitable design method (Kautsky, Nichols and Van Dooren, 1985). The hyperplane matrix C is calculated, by reversing the transformation process (see Chapter 3, Section 3.2), and then the remaining m left-hand half-plane arbitrary eigenvalues of the full-order linear feedback system must be chosen.

The *feedback* matrices are then calculated (see Chapter 7, Section 7.2) to give a controller of the form

$$u(x) = Lx + \frac{\hat{\rho} Nx}{\|Mx\| + \delta} \qquad (2.2.20)$$

where $\hat{\rho}$ is an arbitrary constant, δ is a constant used to smooth the control, and $\| \ \|$ is the matrix 2-norm.

2.3 Lyapunov Control

The Lyapunov control approach requires the closed-loop system error trajectories to be ultimately bounded and the convergence of the error norm to be arbitrarily close to exponential convergence with a desired time constant (Garofalo & Glielmo, 1988).

Consider a multi-input multi-output system of the form

$$y^{(\upsilon)} = f(y,.....y^{(\upsilon-1)}) + F(y,.....,y^{(\upsilon-1)})\underset{\sim}{u} \qquad (2.3.1)$$

$$y(t_o) = y_o,.....,y^{(\upsilon-1)}(t_o) = y_o{}^{(\upsilon-1)} \qquad (2.3.2)$$

where $y \in \mathcal{R}^m$ is the output, $u \in \mathcal{R}^m$ is the input, and υ is a positive integer.

Suppose the following :

i) Let $f(y,..,y^{(\upsilon-1)})$ be continuous and cone-bounded with respect to $y,...,y^{(\upsilon-1)}$, so that there exists k_i $i = 1,...,\nu$ such that

$$\|f(y,..,y^{(\upsilon-1)})\| \leq k_0 + k_1\|y\| + .. + k_\upsilon\|y^{(\upsilon-1)}\| \qquad (2.3.3)$$

ii) Let there exist a known matrix $W(y,....,y^{(\upsilon-1)}) \in \mathcal{R}^m$ and a scalar λ_D such that, for any $(y,...,y^{(\upsilon-1)}) \in \mathcal{R}^{m\upsilon}$, the matrix D, defined as follows

$$D(y,...,y^{(\upsilon-1)}) = F(y,...,y^{(\upsilon-1)})W(y,...,y^{(\upsilon-1)}) \tag{2.3.4}$$

is positive definite and norm bounded, in other words it satisfies the following inequality

$$\left\| D(y,.....,y^{(\upsilon-1)}) \right\| \leq \bar{\lambda}_D \tag{2.3.5}$$

It is possible to find a function $g : \mathcal{R}^{m\upsilon} \rightarrow \mathcal{R}^+$ satisfying the following inequality

$$g(y,.....,y^{(\upsilon-1)}) \geq \max \left\| f(y,.....,y^{(\upsilon-1)}) \right\| \tag{2.3.6}$$

for all $(y,...,y^{(\upsilon-1)})$. There also exists a positive scalar λ_D satisfying

$$\lambda_D \leq \min \lambda_i \left[\frac{D + D^T}{2} \right], \forall (y,...,y^{(\upsilon-1)}) \tag{2.3.7}$$

where min λ_i represents the minimum eigenvalue out of the set of m.

The objective of the control is to make the tracking error

$$\underset{\sim}{\varepsilon} = \underset{\sim}{\hat{y}} - \underset{\sim}{y} \tag{2.3.8}$$

ultimately bounded in a ball around $\varepsilon = 0$. The radius of this ball can be made small by a suitable choice of the controller parameters.

Let $\underset{\sim}{W}$ be given by

$$\underset{\sim}{W} = f + F\underset{\sim}{u} - \underset{\sim}{\hat{y}}^{(\upsilon)} - k_{\upsilon}\underset{\sim}{\varepsilon} - k_{\upsilon-1}\underset{\sim}{\varepsilon}^{(1)} \ \ldots \ - k_1\underset{\sim}{\varepsilon}^{(\upsilon-1)} \qquad (2.3.9)$$

where k_i, $i = 1,\ldots,\nu$ are arbitrary $m \times m$ matrices.

From equations (2.3.1), (2.3.8) and (2.3.9), the error dynamics equation may be written

$$\underset{\sim}{\varepsilon}^{(\upsilon)} + k_1\underset{\sim}{\varepsilon}^{(\upsilon-1)} + \ldots\ldots\ldots + k_{\upsilon}\underset{\sim}{\varepsilon} = -\underset{\sim}{W} \qquad (2.3.10)$$

Define $\underset{\sim}{e}$ to be

$$\underset{\sim}{e}^T = \begin{bmatrix} \underset{\sim}{\varepsilon}^T & \underset{\sim}{\varepsilon}^{(1)T} & \ldots\ldots & \underset{\sim}{\varepsilon}^{(\upsilon-1)T} \end{bmatrix} \qquad (2.3.11)$$

Then the state space representation of the dynamic equation of the tracking error may be written

$$\dot{\underset{\sim}{e}} = E\underset{\sim}{e} - B_1\underset{\sim}{W} \qquad (2.3.12)$$

where

$$E = \begin{bmatrix} 0 & I_m & \ldots\ldots\ldots & 0 & 0 \\ 0 & 0 & I_m & \ldots\ldots & 0 & 0 \\ 0 & \ldots\ldots\ldots\ldots\ldots & & & I_m \\ -k_{\nu} & \ldots\ldots\ldots\ldots\ldots & & & -k_1 \end{bmatrix} \qquad B_1 = \begin{bmatrix} 0 \\ \cdot \\ \cdot \\ I_m \end{bmatrix} \qquad (2.3.13)$$

The k_i matrices are chosen so that E is asymptotically stable.

Let P be the unique positive definite solution of the Lyapunov equation

$$E^T P + PE = -Q \tag{2.3.14}$$

where Q is a symmetric positive definite matrix.

If ρ_v is chosen to be smaller than zero, and $\underset{\sim}{W}$ is such that

$$\underset{\sim}{v}^T \left[\underset{\sim}{W} - (B_1^T P B_1)^{-1} B_1^T P E \underset{\sim}{e} \right] \geq \ell(\|\underset{\sim}{v}\|) > 0 \tag{2.3.15}$$

for any $\underset{\sim}{e}$: $\|\underset{\sim}{v}\| > \rho_v$, where $\underset{\sim}{v} = B_1^T P \underset{\sim}{e}$, then the error, $\underset{\sim}{e}$, is uniformly bounded and globally ultimately bounded in ball of known radius (Garofalo & Glielmo, 1988).

In addition, if $\underset{\sim}{v}^T \underset{\sim}{W} \geq 0$ for any $\underset{\sim}{e}$: $\|\underset{\sim}{v}\| > \rho_v$ then the norm of the trajectories of the system given in equation (2.3.12) is upper bounded by a time function which is close to an exponential one, with a known time constant.

Define the following function

$$\gamma(y,\ldots,y^{(\upsilon-1)},e,\hat{y}^{(\upsilon)}) = g(y,\ldots,y^{(\upsilon-1)}) + \max\left[\|K\| ; \left\| K + (B_1 P B_1)^{-1} B_1^T P E \right\| \right] \|e\| + \|\hat{y}\| \tag{2.3.16}$$

where $K = \left[K_\upsilon \ \ldots\ K_1 \right]$

The controller is then given by

$$\underset{\sim}{u} = h\mathcal{G}W \frac{B_1^T P \underset{\sim}{e}}{\left\| B_1^T P \underset{\sim}{e} \right\| + \delta} \qquad (2.3.17)$$

where

$$\delta > 0 \qquad h > (1 + \delta/\rho_v)/\lambda_D \qquad \rho_v < \|\underset{\sim}{v}\|$$

$$0 < \mathcal{G} \leq \gamma(y, \ldots, y^{(\upsilon-1)}, \underset{\sim}{e}, \hat{\underset{\sim}{y}}^{(m)})$$

The most straightforward choice for the arbitrary matrices in equation (2.3.13) is an identity matrix in each case. However, since this chapter is concerned with comparing the results from the Lyapunov method and the VSC method, it would clearly be better to choose the arbitrary matrices so that the closed-loop eigenvalues of the full order system are the same for both controllers. A method of choosing the arbitrary matrices to give the specific closed-loop eigenvalues required, with reference to the particular example being considered, is developed in the next section.

2.4 The Robot Manipulator

The example being used to compare these two methods is that of a robot manipulator tracking a particular trajectory, which is an example of a nonlinear uncertain model-following system. Both the methods outlined in this chapter will be used to define a model following control, and the effectiveness of the designs may then easily be seen by comparing the actual track of the robot arm with the desired track.

The robot manipulator under consideration is a two link robot arm, which moves in a horizontal plane (see Fig 2.1). The nonlinear equations governing its movements are as follows

$$\ddot{\theta}_r = g\left[-J_2 v_1 \dot{\theta}_r + a v_2 \dot{\phi}_r + ab\dot{\theta}_r^2 + J_2 b\dot{\phi}_r^2 + 2J_2 b\dot{\theta}_r\dot{\phi}_r + J_2 u_1 - a u_2\right] \qquad (2.4.1)$$

$$\ddot{\phi}_r = g\left[a v_1 \dot{\theta}_r - h v_2 \dot{\phi}_r - bh\dot{\theta}_r^2 - ab\dot{\phi}_r^2 + 2ab\dot{\theta}_r\dot{\phi}_r - a u_1 + h u_2\right] \qquad (2.4.2)$$

where J_i is the moment of inertia of link i about axis i, m_i is the mass of link i, v_i is the viscous friction constant for axis i and $\tilde{I}$ is the moment of inertia of the axis 1 motor. These parameters are given the nominal values listed below.

$J_2 = 0.000412$ $\qquad$ $a = J_2 + 2m_2 l_1 l_2 \cos\phi_r$

$b = 2m_2 l_1 l_2 \sin\phi_r$ $\qquad$ $h = J_1 + J_2 + 4m_2 l_1^2 + \tilde{I} + 4m_2 l_1 l_2 \cos\phi_r$

$\qquad\qquad\qquad\qquad\quad = 0.008819 + 0.00118\cos\phi_r$

$g = 1/(J_2 h - a^2)$ $\qquad$ $l_1 = l_2 = 2$ $\qquad$ $m_2 = 6.9875\times10^{-5}$

$\tilde{I} = 6.877\times10^{-3}$ $\qquad$ $v_1 = 0.0025$ $\qquad$ $v_2 = 6.07\times10^{-5}$

Equations (2.4.1) and (2.4.2) are required to be converted to the form of equation (2.2.1), so that a Variable Structure controller may be designed, and to the form of equation (2.3.1) so that a Lyapunov controller may be designed. The cross terms in equations (2.4.1) and (2.4.2) will be ignored during the controller design process, for simplicity, but will be included in the model-following simulation which is carried out for each controller. It is clear from the results obtained for both controllers, that this strategy enables suitable controllers to be designed on a decoupled system, for effective control of the full robot arm system.

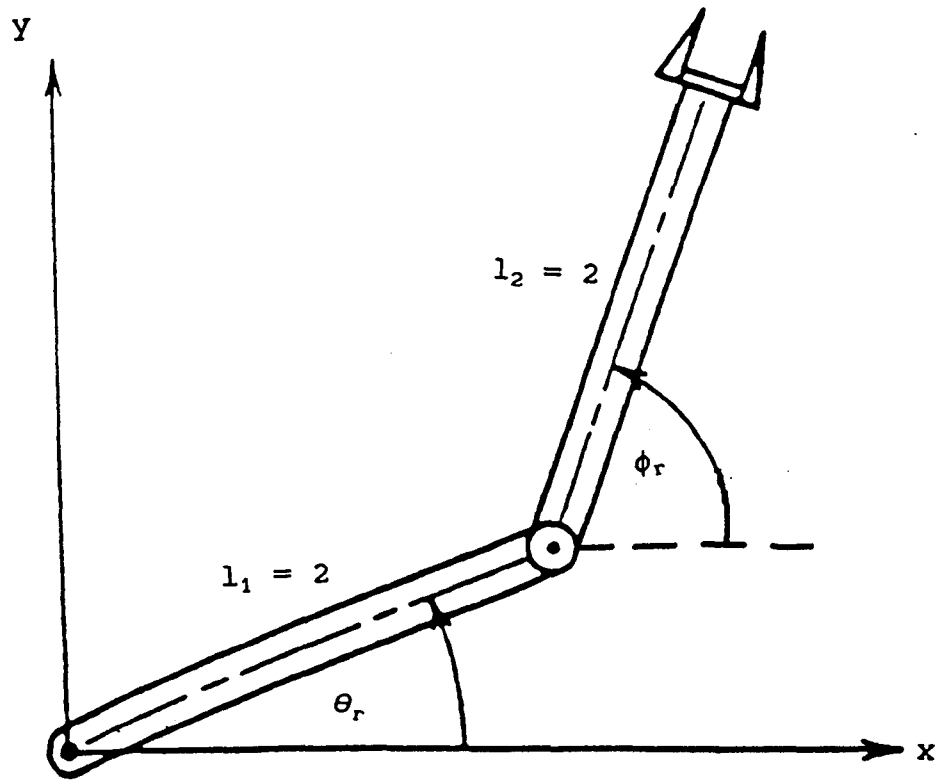

Fig 2.1 The two-link robot arm

If the cross terms are ignored, equations (2.4.1) and (2.4.2) may be written in the following matrix form

$$\begin{bmatrix} \ddot{\theta}_r \\ \ddot{\phi}_r \end{bmatrix} = \begin{bmatrix} -gJ_2v_1 & gav_2 \\ gav_1 & -ghv_2 \end{bmatrix} \begin{bmatrix} \dot{\theta}_r \\ \dot{\phi}_r \end{bmatrix} + \begin{bmatrix} gJ_2 & -ga \\ -ga & gh \end{bmatrix} \begin{bmatrix} u_1 \\ u_2 \end{bmatrix} \qquad (2.4.3)$$

Equation (2.4.3) is clearly of the form of equation (2.3.1) with the function f and the matrix F given by

$$f = \begin{bmatrix} -gJ_2v_1\dot{\theta}_r + gav_2\dot{\phi}_r \\ gav_1\dot{\theta}_r - ghv_2\dot{\phi}_r \end{bmatrix} \qquad F = \begin{bmatrix} gJ_2 & -ga \\ -ga & gh \end{bmatrix} \qquad (2.4.4)$$

To convert equation (2.4.3) to the standard form for VSC, consider the substitutions

$$\theta_r = y_1 \qquad \dot{\theta}_r = y_2 \qquad \phi_r = y_3 \qquad \dot{\phi}_r = y_4$$

Differentiating these expressions with respect to time gives

$$\dot{\theta}_r = \dot{y}_1 = y_2 \qquad \dot{\phi}_r = \dot{y}_3 = y_4$$

$$\ddot{\theta}_r = \ddot{y}_1 = \dot{y}_2 \qquad \ddot{\phi}_r = \ddot{y}_3 = \dot{y}_4$$

Substituting for θ_r, ϕ_r, and their first and second derivatives in equation (2.4.3) gives

$$\begin{bmatrix} \dot{y}_1 \\ \dot{y}_2 \\ \dot{y}_3 \\ \dot{y}_4 \end{bmatrix} = \begin{bmatrix} 0 & 0 & 1 & 0 \\ 0 & -gJ_2v_1 & 0 & gav_2 \\ 0 & 0 & 0 & 0 \\ 0 & gav_1 & 0 & -ghv_2 \end{bmatrix} \begin{bmatrix} y_1 \\ y_2 \\ y_3 \\ y_4 \end{bmatrix} + \begin{bmatrix} 0 & 0 \\ gJ_2 & -ga \\ 0 & 0 \\ -ga & gh \end{bmatrix} \begin{bmatrix} u_1 \\ u_2 \\ u_3 \\ u_4 \end{bmatrix} \qquad (2.4.5)$$

Equation (2.4.5) is clearly in the form required for a Variable Structure control problem.

A linear system of the form $\dot{x} = A_d x$, where A_d is a diagonalizable matrix has a solution of the form $x=x_o e^{A_d t}$. If A_d is diagonalizable, then $A_d\Gamma = \Gamma\Lambda$, where Λ has the eigenvalues of A_d on the leading diagonal, and zeros elsewhere, and the columns of Γ are the corresponding right eigenvectors. If the eigenvalues of A_d are distinct, then the corresponding eigenvectors will be linearly independent, and the matrix Γ will be non-singular, and so $A_d = \Gamma\Lambda\Gamma^{-1} = \Gamma\Lambda G$, where G is the matrix of left eigenvectors. The solution may therefore be written $x = x_o\Gamma e^{\Lambda t}G$, and it can be seen that a suitable choice of eigenvectors can lead to the decoupling of the components of the vector x. If, for example, both Γ and G were equal to the identity matrix, then the states of x would all be independent of each other, and depend only on the exponential of the appropriate eigenvalue, and the initial state value.

For the VSC case, the open-loop eigenvalues of the full order system, $\lambda(A)$, are [0 0 -0.4016 -0.1218]. The closed-loop eigenvalues of the reduced order system, the null space eigenvalues were chosen to be -5 and -7, to ensure rapid decay of the error states to zero, and the system is of the form given above, with $A_d = A_{11} - A_{12}F$. The respective eigenvectors of these eigenvalues were chosen to be $[1\ \xi\ 0\ 0]^T$ and $[0\ 0\ 1\ \xi]^T$, where ξ is arbitrary, to yield decoupling between θ_r (y_1 and y_2) and ϕ_r (y_3 and y_4), as explained above.

The m remaining eigenvalues for the full order linear feedback of the system were chosen to be -12 and -14, and the resulting controller matrices from the VASSYD package are

$$L = \begin{bmatrix} -3.6800 & -0.2360 & -0.4710 & -0.0346 \\ -0.3640 & -0.0233 & -0.1600 & -0.0124 \end{bmatrix}$$

$$M = \begin{bmatrix} -0.3500 & -0.0184 & 0.1330 & 0.0078 \\ -0.1610 & -0.0085 & -0.3400 & -0.0200 \end{bmatrix}$$

$$N = \begin{bmatrix} -1.22\times10^{-1} & -6.42\times10^{-3} & -7.96\times10^{-3} & -4.68\times10^{-4} \\ -1.18\times10^{-2} & -6.21\times10^{-4} & -4.48\times10^{-3} & -2.64\times10^{-4} \end{bmatrix}$$

The state trajectories to be tracked by the robot arm have been chosen to be those of the model plant with plant matrix A_m and input matrix B_m :

$$A_m = \begin{bmatrix} 0 & 1 & 0 & 0 \\ -100 & -20 & 0 & 0 \\ 0 & 0 & 0 & 1 \\ 0 & 0 & -36 & -12 \end{bmatrix} \qquad B_m = \begin{bmatrix} 0 & 0 \\ 100 & 0 \\ 0 & 0 \\ 0 & 36 \end{bmatrix} \qquad (2.4.6)$$

This model plant has the same basic structure as the robot arm, since it has eigenvalues [-10 -10 -6 -6] which correspond to the two modes of the robot arm motion. The trajectory under consideration is illustrated in figure 2.2.

The results for the Variable Structure controller for a simulated run, of 40 seconds, using the full, coupled, equations of the robot arm, with the arm following the trajectory illustrated in figure 2.2, are shown in figure 2.3.

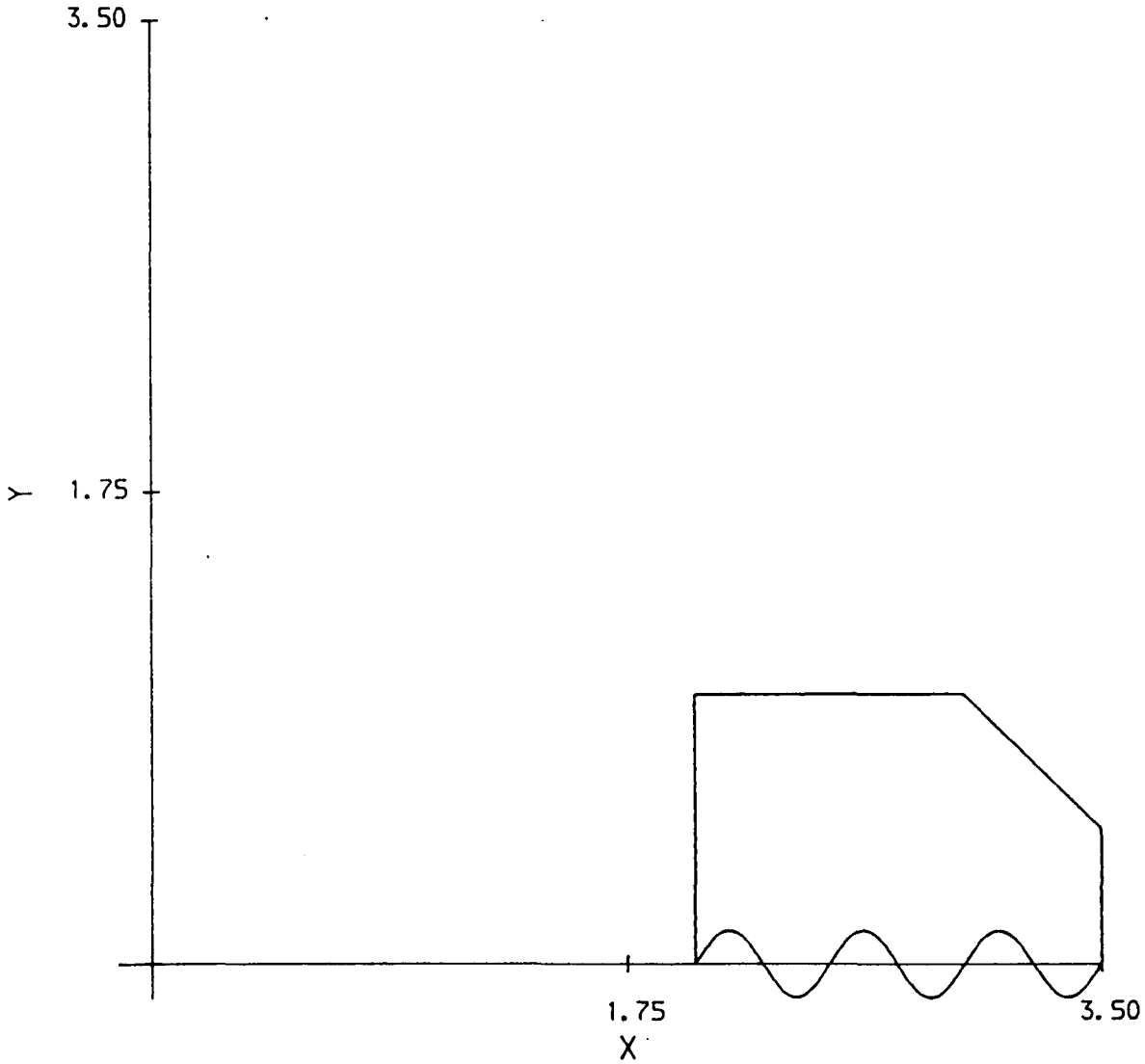

Fig 2.2 The trajectory to be followed by the robot arm in the plane

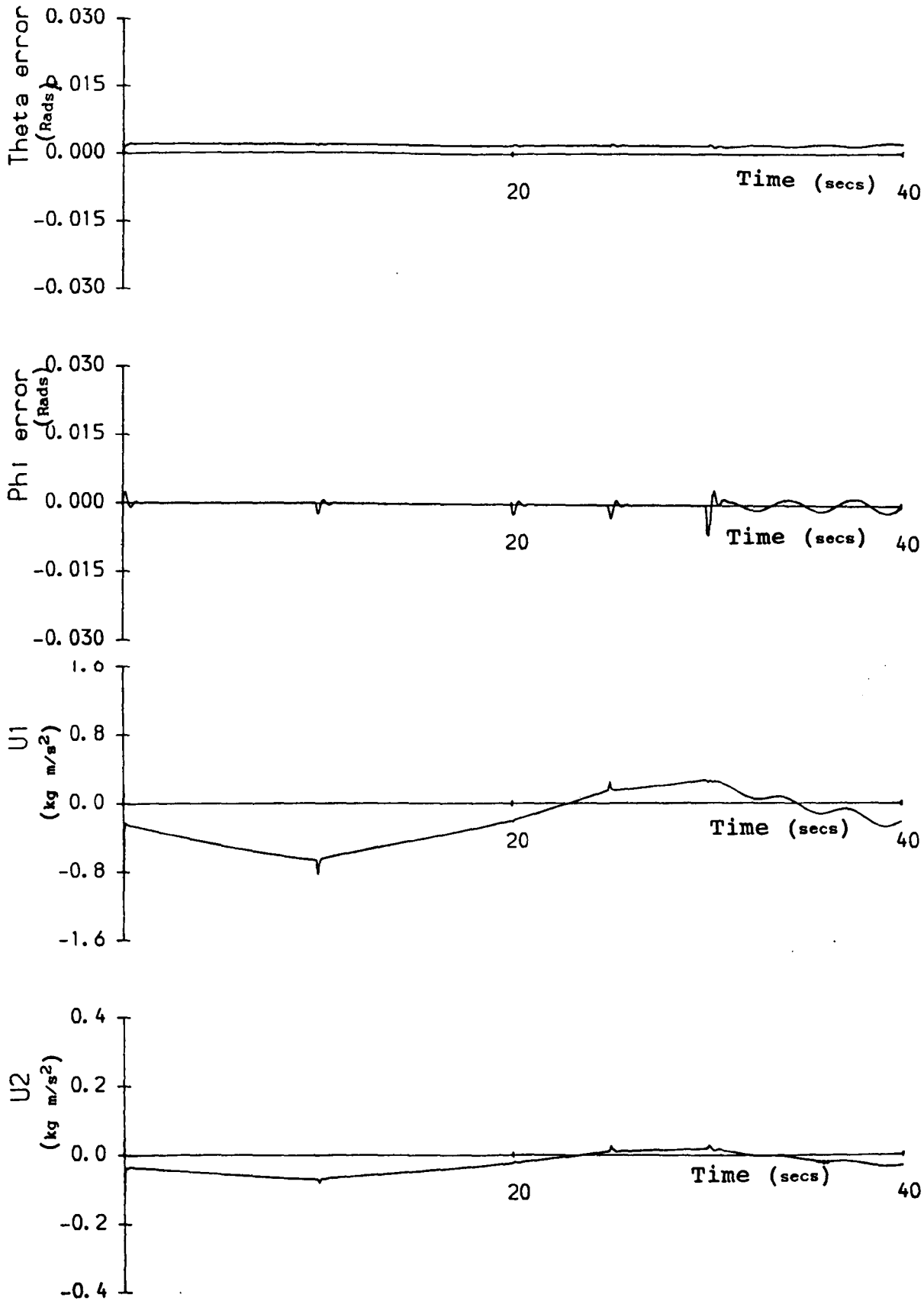

Fig 2.3 Results for the Variable structure controller

It can be seen from figure 2.3 that the errors in θ_r and ϕ_r are less than 0.5°, and very steady. By comparing the angle error plots with the required robot trajectory (Fig 2.2), it can be seen that the small "blips" in the results occur when the arm changes direction. The changes of direction occur at the corners of the trajectory and the sinusoid starts 30 seconds into the simulation. The ϕ_r errors are generally negligible, except at the corners of the trajectory, since most of the movement occurs in the lower arm. They increase during the sinusoidal part of the trajectory, since the upper part of the arm is moving as much as the lower part at this point. The θ_r error remains at about 0.2° since the lower arm is moving constantly throughout the simulation. The two parts of the control are very smooth, apart from the small "blips" which occur when the robot arm is required to change direction. The control effort clearly decreases in magnitude after the first 10 seconds of the simulation, which is as would be expected, and it becomes less smooth during the sinusoidal part of the trajectory. It can be seen from these results that a variable structure controller gives a good model-following performance for this problem.

For the Lyapunov approach, the eigenvalues in the null space are required to be the same as those for the Variable Structure controller during sliding. The discontinuous part of the Variable Structure control is approximated by a continuous control, which brings the trajectory close to the sliding subspace.

The motion during sliding is controlled by $K = -(CB)^{-1}CA$, (Equation (2.2.5)), where $u^N = \dfrac{\hat{\rho}Cx}{\|Cx\| + \delta}$. The Lyapunov controller is of this form, with C replaced by B_1^TP (Equation (2.3.16)), and so the closed-loop system during sliding is defined as

$$\begin{bmatrix} \ddot{\theta}_r \\ \ddot{\phi}_r \end{bmatrix} = \left[I + F(B_1^TPF)^{-1}B_1^TP \right] f \qquad (2.4.7)$$

since $\underset{\sim}{v} = B_1^T P \underset{\sim}{e}$

As explained in the previous section, to enable a comparison of the two methods to be made, the closed-loop eigenvalues of the system in the null space are required to be the same in each case (Zinober and Woodham, 1989). The closed-loop eigenvalues for the reduced order equivalent system of the VSC problem were chosen to be -5 and -7, and so the closed-loop eigenvalues of the full order system given in equation (2.2.7) are [-5 -7 0 0]. The strategy for choosing the arbitrary k_1 matrices in equation (2.3.13) so that the closed-loop eigenvalues of the system have the required values will now be outlined.

For the Lyapunov method, let us consider a general form of the E matrix

$$E = \begin{bmatrix} 0 & 0 & 1 & 0 \\ 0 & 0 & 0 & 1 \\ -k_1 & 0 & -k_3 & 0 \\ 0 & -k_2 & 0 & -k_4 \end{bmatrix}$$

Solving equation (2.3.14) for the general E matrix gives

$$P=\begin{bmatrix} -(k_3^2+k_1^2+k_1)/2k_3k_1 & 0 & -1/2k_2 & 0 \\ 0 & -(k_2^2+k_4^2+k_2)/2k_2k_4 & 0 & -1/2k_2 \\ -1/2k_1 & 0 & -(k_1+1)/2k_1k_3 & 0 \\ 0 & -1/2k_2 & 0 & -(k_2+1)/2k_2k_4 \end{bmatrix}$$

Multiplying out the left-hand side of equation (2.4.7) gives

$$\begin{bmatrix} 0 & 1 & 0 & 0 \\ 0 & -1.9\times10^{-7}-k_3/(k_1+1) & 0 & 4.7\times10^{-8}-2.4\times10^{-7}k_4/(k_2+1) \\ 0 & 0 & 0 & 0 \\ 0 & -6.8\times10^{-6}+2.1\times10^{-5}k_3/(k_1+1) & 0 & 3.9\times10^{-7}-k_4/(k_2+1) \end{bmatrix}$$

The eigenvalues of this matrix are given by

$$\lambda^2\left[\left(\lambda + k_3/(k_1+1)\right)\left(\lambda + k_4/(k_2+1)\right)\right] = 0$$

So $\lambda^2 = 0$ or $\lambda = -k_3/(k_1+1)$ or $\lambda = -k_4/(k_2+1)$

Since for this particular example we require the two non-zero eigenvalues to be -5 and -7, the values of the k_i must be

$$k_3 = 10 \quad k_4 = 14 \qquad \text{and} \qquad k_1 = k_2 = 1$$

The Lyapunov controller consists only of a non-linear part, given in equation (2.3.16), and so the control matrix B_1^TP is given by

$$B_1^TP = \begin{bmatrix} -0.5 & 0 & -0.1 & 0 \\ 0 & -0.5 & 0 & -0.1429 \end{bmatrix}$$

The other variables required by the Lyapunov method will now be chosen. From equation (2.3.4) and equation (2.3.7), we have

$$D = FW \qquad \lambda_D = \min \lambda_i \left[\frac{D + D^T}{2} \right]$$

Let us choose the following matrix W

$$W = \begin{bmatrix} 1/g & 0 \\ 0 & 1/g \end{bmatrix}$$

Then D is given by

$$D = \begin{bmatrix} J & -a \\ -a & h \end{bmatrix}$$

and hence, λ_D becomes

$$\lambda_D = \left[(h + J) \pm \sqrt{((h+J)^2 - 4hJ + 4a^2)} \right]/2$$

The matrix D will alter as the robot arm moves, since both a and h depend on ϕ_r, as can be seen from equation (2.4.2) and will therefore not remain constant. The values of a and h are however bounded since $\cos\phi_r$ and $\sin\phi_r$ are bounded, and so the matrix D is bounded. Clearly, λ_D will not remain constant, but will vary as the robot arm moves. From equation (2.3.16) we have

$\rho_v < \|\underset{\sim}{v}\|$ so choose $\rho_v = 0.1\|\underset{\sim}{v}\|$

$\delta > 0$ so choose $\delta = 1.0 \times 10^{-6}$ $\qquad h = (1 + \delta/\rho_v)/\lambda_D$

choose $\gamma(y,\ldots,y^{(\upsilon-1)}, \underset{\sim}{e}, \underset{\sim}{\hat{y}}^{(m)}) = \left\| f(y,\ldots,y^{(\upsilon-1)}) \right\|$

Since f varies as ϕ_r varies, λ_D varies, and v varies as the error, $\underset{\sim}{e}$, varies, ρ_v, γ and h will not remain constant, but will alter as the robot arm moves. If the matrix D was chosen so that λ_D was constant, ρ_v would still vary with v, but some alterations in the gain would be removed.

The results for the Lyapunov controller for a simulated run of 40 seconds, with the full, coupled, robot arm equations, and with the arm following the trajectory illustrated in figure 2.2 are shown in figure 2.4. It can be seen from figure 2.4 that the errors in θ_r and ϕ_r are larger than those for the Variable Structure controller, although they are still less than 1°. Again, changes in these values occur when the robot arm is required to change direction, and the largest errors occur during the sinusoidal part of the trajectory. In this case, the error plots for θ_r and ϕ_r are very similar, unlike the plots for the Variable Structure controller, and this is presumably due to the differences in the two controllers. It can also be seen that the control is not smooth, but continually oscillating, and this is due to the effect of the gain term in the control, $h\mathcal{P}W$, which is altered at every time step. The two parts of the control in this case remain bounded, and constant within the bounds, as would be expected from the design, and do not alter at different points of the trajectory. However, despite the control not being smooth, the Lyapunov controller does give a good model-following performance.

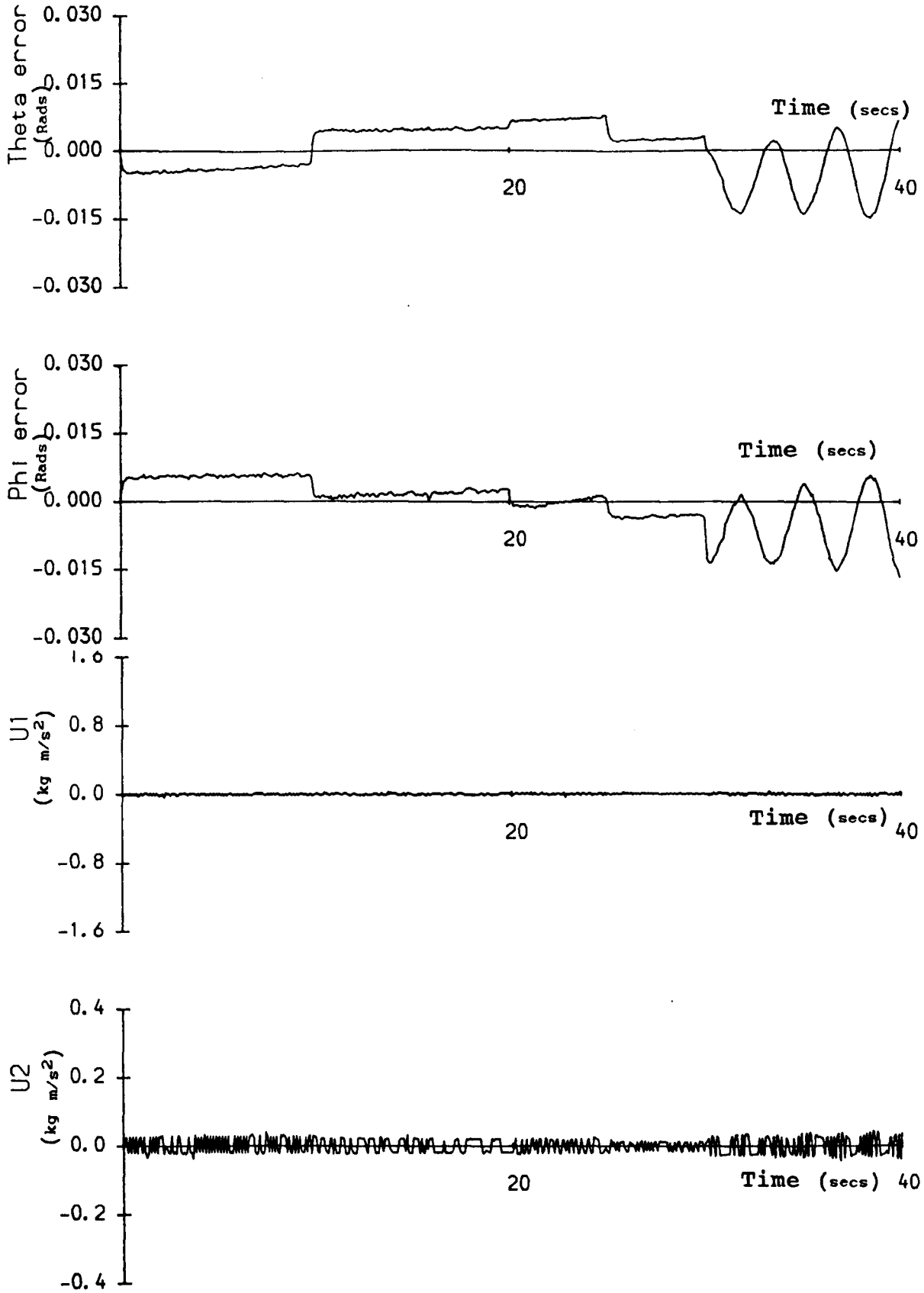

Fig 2.4 Results for the Lyapunov controller

2.5 Discussion

As can be seen from the results in Figures 2.3 and 2.4, the errors during the model-following simulation for both controllers are small. The smoothness of the Lyapunov controller could be improved by altering the choice of the gain term, $h\mathcal{P}W$, so that it does not change with every time step. A plot of the results for the Lyapunov controller for the first second of the simulation, including a plot of the gain, is given in figure 2.5. It can be seen from this plot the very large variations in the value of $h\mathcal{P}W$, and the effect this is having on the two control components. However, the components of the control are clearly bounded, and remain small throughout the simulation.

It would appear from these results that a Variable Structure controller leads to more accurate model-following control than this particular Lyapunov controller. The control effort for a Variable Structure controller is initially larger in magnitude, but much smoother, than that of the Lyapunov controller, but its magnitude decreases with time whereas that of the Lyapunov controller remains approximately constant.

The Lyapunov controller could be smoothed by altering the way in which the gain term, $h\mathcal{P}W$, is calculated. If h and $\mathcal{P}$ were not calculated at each time step, or if their mean value over several time steps was used, then the gain term would not alter at every time step. This would result in fewer calculations per time step, and a smoother control.

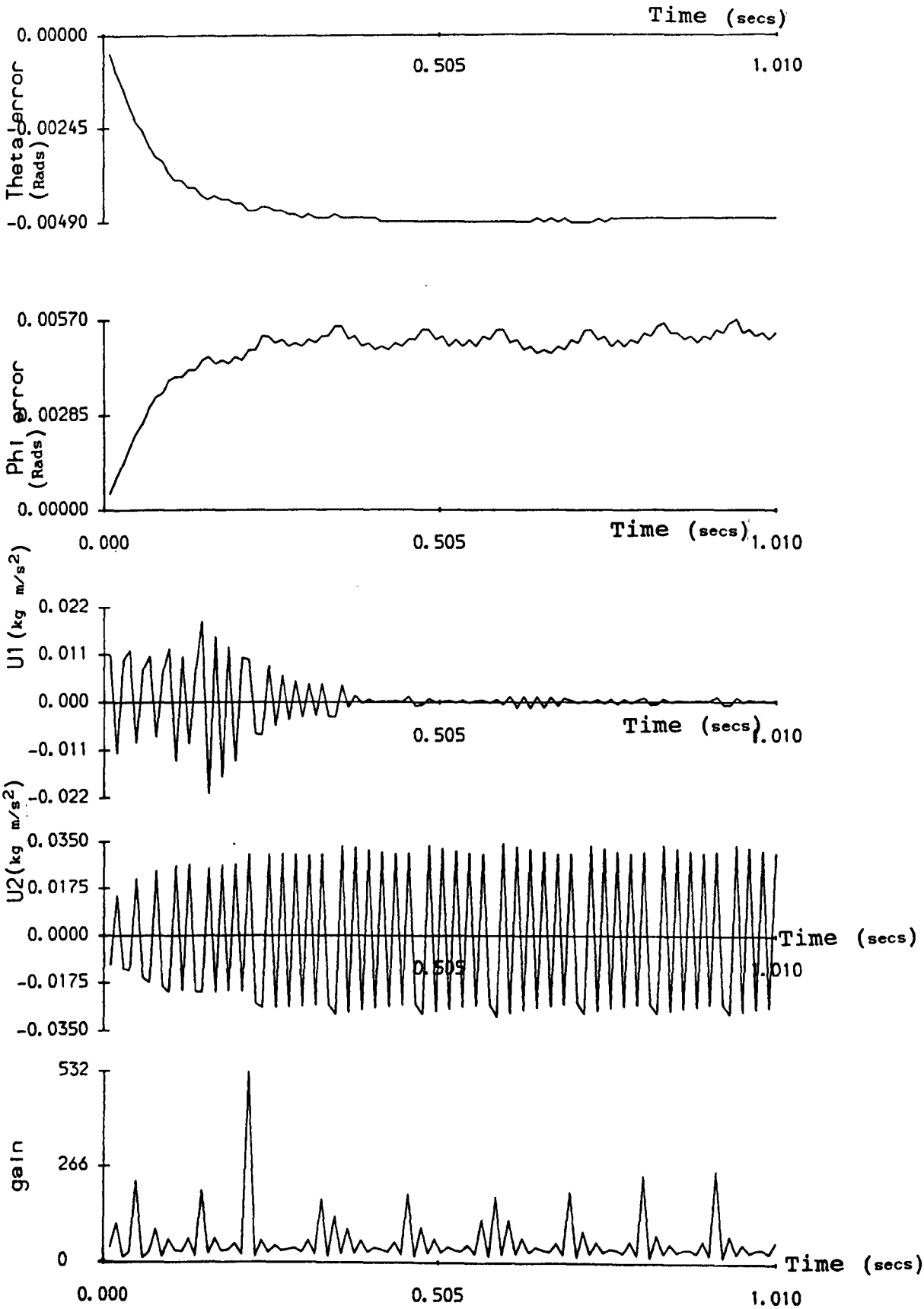

Fig 2.5 The results for the first second, including the gain variation, for the Lyapunov controller

3. EIGENVALUE PLACEMENT IN A DISC OR STRIP APPLIED TO VSC

3.1 Introduction

The problem of selecting the eigenvalues of a closed-loop Variable Structure Control system, and hence directly specifying the sliding hyperplanes, is an important one, since the choice of the eigenvalues affects the stability and response of the system. A popular method for designing the sliding hyperplane matrix (Dorling & Zinober, 1986) requires the exact specification of the desired closed-loop eigenvalues. This is a very rigid design requirement, since in many practical examples, exact eigenvalue specification may not be required; the eigenvalues may simply required to be in a certain region of the left-hand half-plane. In general, the desired exact eigenvalues for the closed-loop system will not be known, so it would clearly be advantageous in certain problems to be able to specify a general region of the left-hand half-plane within which the eigenvalues should lie.

Some work has been done on the placing of the closed-loop eigenvalues in a particular region by linear state feedback methods, rather than VSC methods. One method is the placing of the eigenvalues in a hyperbola with major and minor axes at 45° to the x and y axes, by selecting the weighting matrices of the LQ problem in an iterative way (Kawasaki and Shimemura, 1983). This method has been extended for other hyperbolic regions, and small sectors, using a similar approach with a modified Riccati equation being used to design the controller (Kawasaki & Shimemura, 1988).

Some work has also been done on root clustering using a Lyapunov type approach with Kronecker product matrices (Abdul-Wahab, 1990). An eigenvalue location method involving mapping onto a region of the complex plane has also been considered (Bogachev, Grigor'ev, Drozdov and Korov'yakov, 1980). This method involves the solution of a modified Lyapunov equation in the design of the control law. All of the above methods are fairly complicated to use, since they either involve iterative processes, or calculations of Kronecker matrix products, or complicated transformations, and they all involve rigidly specified regions in the left-hand half-plane.

In this chapter we shall consider two regions in the left-hand half-plane which are specified in a straightforward manner. The first region under consideration is that of a disc in the left-hand half-plane, which is specified by its radius, r, and its centre, $-\alpha + 0j$. The second region under consideration is that of an infinite vertical strip in the left-hand half plane, which is specified by its real axis crossing points. In Chapter 4 a more general region of the left-hand half-plane will be considered.

In section 3.2 the general theory for placing eigenvalues in a disc (Furuta and Kim, 1987) is described, and is then extended for application to a Variable Structure Control System. In section 3.3 the general theory for placing eigenvalues in a vertical strip (Shieh, Dib and McInnis, 1986) is described, and is then extended for application to a VSC system. This section also includes some discussion of three of the methods of solution of the continuous Riccati equation with the Q matrix equal to the

null matrix. Section 3.4 contains some illustrative numerical examples for the two methods, and a brief discussion of the results is presented in section 3.5.

3.2 Controller Design For Eigenvalues in a Disc

The technique of placing all the closed-loop eigenvalues of a system within a specified disc with centre $-\alpha + 0j$ and radius r (Fig 3.1) has been adapted for use with a VSC system. In this case the n-m closed-loop eigenvalues of the reduced order equivalent system are required to be placed within the specified disc.

Furuta and Kim (1987) have studied the standard linear regulator problem for systems of the form (2.2.2) with linear feedback u = Fx. Consider the matrix equation

$$-\alpha A^{*}P - \alpha PA + A^{*}PA + (\alpha^2 - r^2)P = -Q \qquad (3.2.1)$$

where Q is an arbitrary symmetric positive definite matrix, * denotes the matrix conjugate transpose, and α and r are scalars.

Let λ and ν be an eigenvalue and right eigenvector of A, then

$$A\nu = \lambda\nu \quad \text{and} \quad \nu^{*}A^{*} = \bar{\lambda}\nu^{*} \qquad (3.2.2)$$

Premultiplying equation (3.2.1) by ν^{*}, postmultiplying it by ν and substituting for $A\nu$ and $\nu^{*}A^{*}$ from equation (3.2.2) gives

$$(-\alpha(\bar{\lambda} + \lambda) + |\lambda|^2 + \alpha^2 - r^2)\nu^{*}P\nu = -\nu^{*}Q\nu \qquad (3.2.3)$$

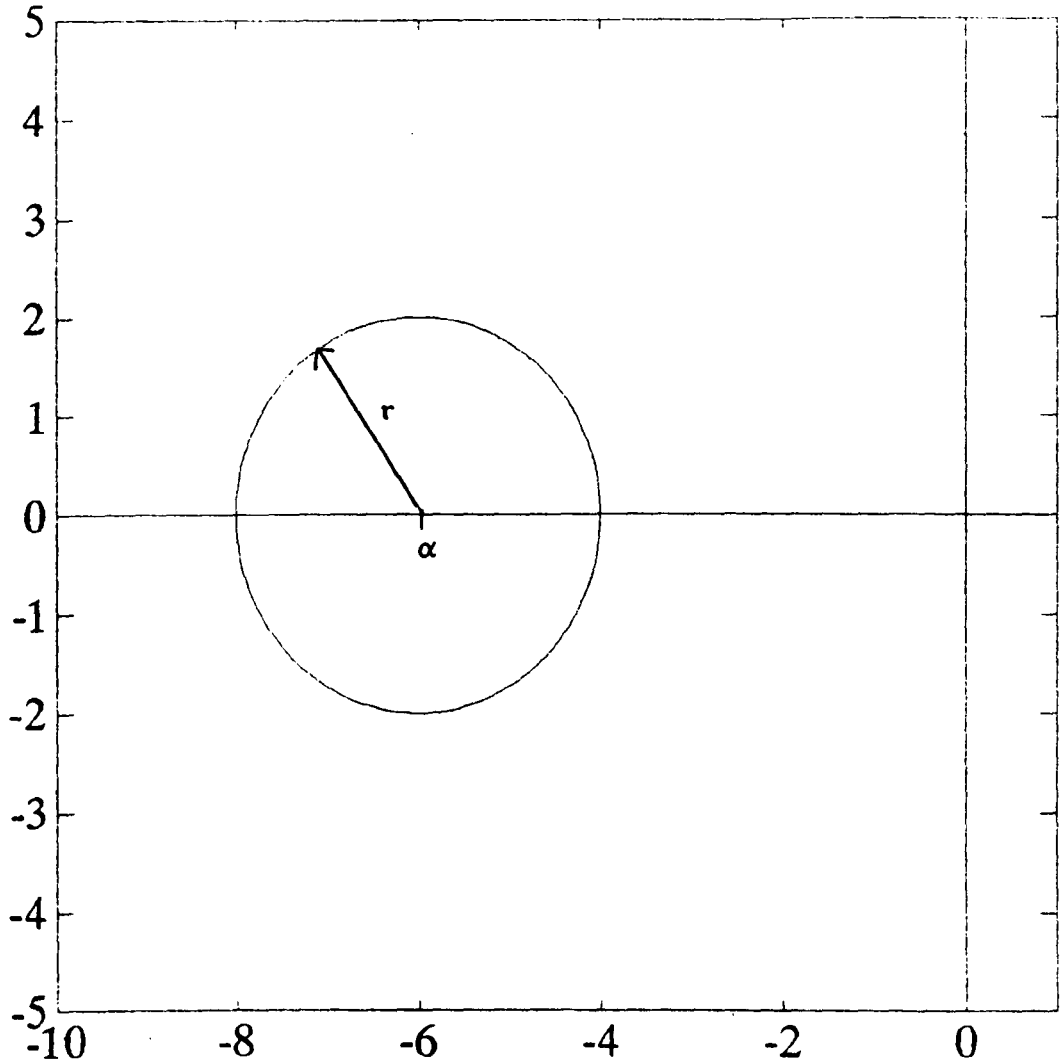

Fig 3.1 Disc of radius r and centre α + 0j

Now let $\lambda = x + jy$ with $\bar{\lambda} = x - jy$. Substituting for λ and $\bar{\lambda}$ in equation (3.2.3) gives

$$\{(x - \alpha)^2 + y^2 - r^2\}v^*Pv = -v^*Qv \qquad (3.2.4)$$

Since Q is positive definite, and we require P to be positive definite, it follows that

$$(x - \alpha)^2 + y^2 - r^2 < 0 \qquad (3.2.5)$$

So, if there exists a positive definite solution P of (3.2.1), all the eigenvalues of A will lie within the disc with centre $-\alpha + 0j$ and radius r. This is the necessary condition for the eigenvalues of A to lie within the disc, and the proof of sufficiency is contained in Furuta and Kim (1987).

In this case, the eigenvalues of the closed-loop system A + BF, where F is a control gain matrix, are required to be within the disc, so equation (3.2.1) becomes

$$-\alpha(A+BF)^*P-\alpha P(A+BF)+(A+BF)^*P(A+BF)+(\alpha^2+r^2)P = -Q \qquad (3.2.6)$$

with

$$F = -(r^2R + B^TPB)^{-1}B^TP(A - \alpha I)$$

This matrix Riccati equation may be solved using the discrete method, which takes the iterative form for s = 0,1,2,...

$$P_{s+1} = \left[\begin{array}{l} (A-\alpha I)^T P_s (A-\alpha I) + r^2 Q - \\ \qquad (A-\alpha I)^T P_s B (r^2 R + B^T P_s B)^{-1} B^T P_s (A-\alpha I) \end{array} \right] / r^2 \qquad (3.2.7)$$

where R and Q are arbitrary symmetric positive definite matrices.

The desired P in equation (3.2.6) is the steady state solution P_s from equation (3.2.7), since in the limit, as $k \to \infty$, $P_k = P$ (Furuta and Kim, 1987).

For the sliding mode design, we require the (n-m) left-hand half-plane closed-loop eigenvalues of the reduced order equivalent system, $A_{11} - A_{12}F$, to lie within the specified disc (Woodham and Zinober, 1990). The discrete matrix Riccati equation to be solved for the reduced order system is therefore

$$P_{s+1} = \frac{1}{r^2}\left\{(A_{11} - \alpha I)^T P_s (A_{11} - \alpha I) + r^2 Q \right.$$
$$\left. (A_{11}-\alpha I)^T P_s A_{12}(r^2 R + A_{12}^T P_s A_{12})^{-1} A_{12}^T P_s (A_{11}-\alpha I)\right\} \qquad (3.2.8)$$

where Q and P are (n-m)×(n-m) matrices.

The control matrix is given by

$$F = (r^2 R + A_{12}^T P A_{12})^{-1} A_{12}^T P (A_{11} - \alpha I) \qquad (3.2.9)$$

The control matrix will have the opposite sign to that for the general system (A + BF) for the obvious reason that the system now under consideration is of the form A - BF.

The eigenvalues of the reduced order system $(A_{11} - A_{12}F)$ will then lie in the specified disc, and the sliding hyperplane matrix C may now be obtained.

Recall from Section 2.2 that

$$CT^T = \begin{bmatrix} C_1 & C_2 \end{bmatrix} \qquad \text{and} \qquad F = C_2^{-1}C_1$$

Since the product CB is non-singular, CT^TTB, B_2 and C_2 are nonsingular, and CT^T may be written

$$CT^T = C_2\begin{bmatrix} C_2^{-1}C_1 & I_m \end{bmatrix}$$

where I_m is the m-dimensional identity matrix.

Now $(T^T)^{-1} = T$, and choosing $C_2 = I_m$, since the product CB is not critical to the design, (Utkin and Yang, 1978), the sliding hyperplane matrix C is given by

$$C = \begin{bmatrix} F & I_m \end{bmatrix} T \tag{3.2.10}$$

So (n - m) of the closed-loop eigenvalues of the full order system

$$\dot{x} = [I_n - B(CB)^{-1}C]Ax \tag{3.2.11}$$

will lie in the required region and the remaining m eigenvalues will be zero (Dorling and Zinober, 1986).

The choice of the two arbitrary matrices, Q and R, in equation (3.2.8) will affect the positioning of the eigenvalues within the specified disc, and this will be discussed in more detail in Chapter 6.

3.3 Controller Design for Eigenvalues in a Vertical Strip

The problem of placing all the closed-loop eigenvalues of a system within an infinite vertical strip (Fig 3.2) in the left-hand half-plane (Shieh, Dib and McInnis, 1986) has been extended for use with the sliding mode.

Consider the general system given in equation (2.2.2), and two positive real numbers h_1 and h_2 with $h_2 > h_1$. These two positive values specify the open vertical strip crossing the negative real axis at the points $-h_2$ and $-h_1$.

Define the matrix $\hat{A}$

$$\hat{A} = A + h_1 I \tag{3.3.1}$$

Suppose that (Shieh, Dib and McInnis, 1986)

$$u = -R^{-1}B^T P x \tag{3.3.2}$$

where R is an arbitrary m×m positive definite matrix, P is the positive definite solution of the continuous matrix Riccati equation with its right-hand side equal to zero

$$PBR^{-1}B^T P - \hat{A}^T P - P\hat{A} = 0 \tag{3.3.3}$$

and the constant gain μ is chosen to be

$$\mu = 0.5 + \frac{(h_2 - h_1)}{2Tr(\hat{A}^+)} \tag{3.3.4}$$

where $Tr(\hat{A}^+)$ is the sum of the positive eigenvalues of $\hat{A}$.

Then the resulting closed-loop system is

$$\dot{x}(t) = (A - \mu BK)x(t) \tag{3.3.5}$$

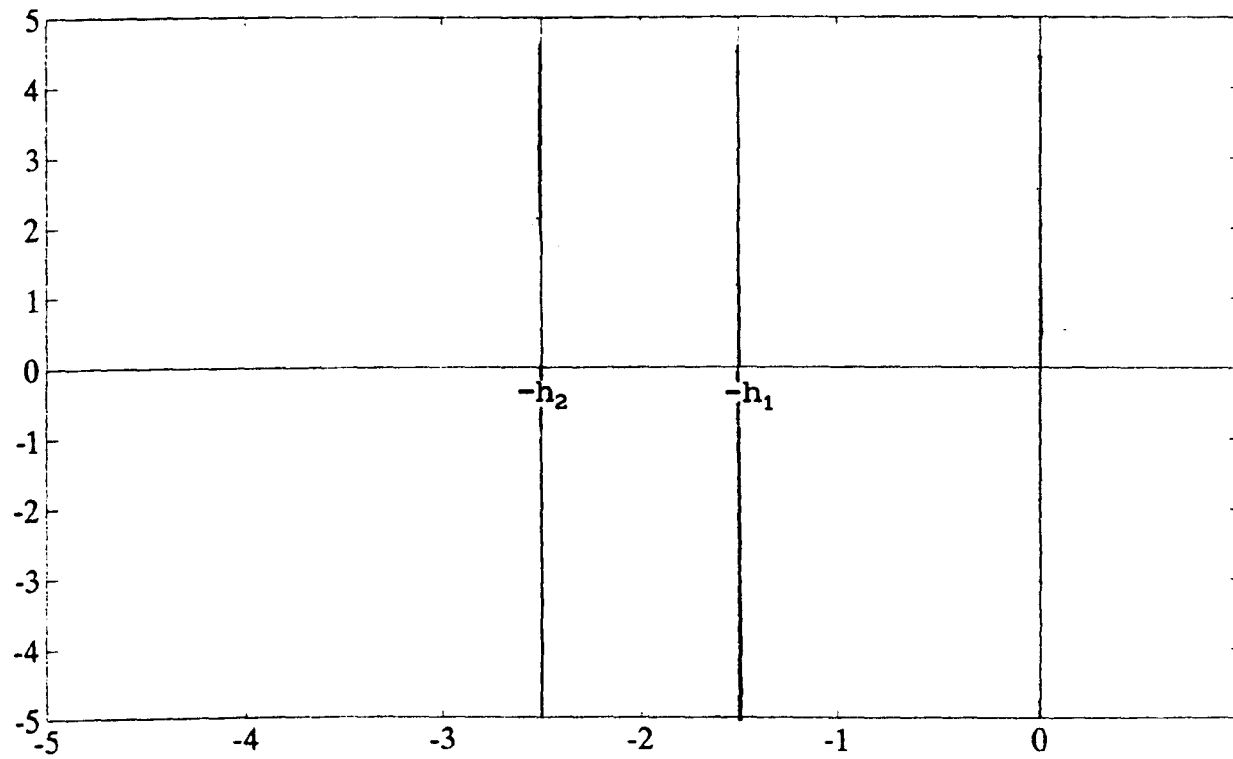

Fig 3.2 Strip with limits $-h_1$ and $-h_2$

If A has pure left-hand half-plane eigenvalues λ_i^- (i = 1,..,n^-), and pure right-hand half-plane eigenvalues λ_i^+ (i = 1,..,n^+), then the eigenvalues of the closed-loop system $(A - BR^{-1}B^TP)$ will be λ_i^- (i = 1,..,n^-) and $-\lambda_i^+$ (i = 1,..,n^+), where P is the positive definite solution of the Riccati equation given in equation (3.3.3). The eigenvalues of $(A - \mu BR^{-1}B^TP)$, where $\mu \neq 1$, will be λ_i^- (i = 1,..,n^-), and n^+ pure left-hand half-plane eigenvalues.

If $h_2 > \max\{|Re(\tilde{\lambda}_i)|\}$ for all i, where $\tilde{\lambda}_i$ are the negative eigenvalues of A, then the eigenvalues of $(A- \mu BK)$ will all lie within the vertical strip which crosses the real axis at the points $[-h_2, -h_1]$ (Shieh, Dib & McInnis, 1986).

For the sliding mode design, we require the (n - m) left-hand half-plane closed-loop eigenvalues of $(A_{11} - A_{12}F)$ to lie within the specified vertical strip (Woodham and Zinober, 1990). The matrix Riccati equation to be solved is therefore

$$PA_{12}R^{-1}A_{12}^TP - \hat{A}^TP - P\hat{A} = 0 \qquad (3.3.6)$$

where $\hat{A}$ is given by

$$\hat{A} = A_{11} + h_1I \qquad (3.3.7)$$

and A_{11} and A_{12} are as given in Section 2.2, (page 11). The control matrix F is given by

$$F = \mu R^{-1}A_{12}^TP$$

which has the opposite sign to the control matrix for the system (A + BF) for the reason stated earlier (Section 3.2). The constant μ is defined in equation (3.3.4) with $\hat{A}$ as defined in

equation (3.3.7). So all the closed-loop eigenvalues of the reduced order system will lie in the vertical strip which crosses the real axis at $-h_2$ and $-h_1$. The sliding hyperplane matrix, C, is then obtained from equation (3.2.10) and (n-m) of the closed-loop eigenvalues of the full order system given in equation (3.2.11) will also lie in the required region. The remaining m eigenvalues will be zero (Dorling and Zinober, 1986).

It should be noted that it is not possible to move the original eigenvalues (those of A_{11}) towards the right-hand half plane, so the value of h_2 is limited by the eigenvalues of A_{11} (Shieh, Dib and McInnis, 1986). This is because of the invariance of the negative open-loop eigenvalues to the closed-loop transformation.

In practice, it has been found that if equation (3.3.3) is solved using the lqr program from MATLAB, a difficulty arises, since the right-hand side is zero. This leads to a divide by zero warning and some inaccuracies in the resulting P matrix. The problem arises because the trivial solution of equation (3.3.6) is $P = 0$. A straightforward way round this problem is to set the Q matrix to be of the form qI, where q is a very small positive scalar, of the order of 10^{-20},which gives an acceptable result. The results for both Q equal to zero and Q equal to qI are contained in section 3.4.

A better solution to the problem, mathematically speaking,

would be to use a method of solving the continuous Riccati equation which works even if Q is the null matrix, if such a method exists. Several different methods will now be considered for the solution of this problem.

The method used in the MATLAB toolbox is that of eigenvalue decomposition of an associated Hamiltonian matrix, which is known as the Macfarlane-Potter-Fath method (Kailath, 1980). Two other methods for solving the continuous matrix Riccati equation, which may be considered, are an iterative method and a Schur method (Laub, 1979) which allows Q to be greater than or equal to zero. These three methods will be described briefly below, and their suitability for this particular problem (that of a null Q matrix) will be discussed.

Consider the iterative method (Anderson & Moore, 1971) for the continuous matrix Riccati equation

$$A^TP + PA - PBR^{-1}B^TP + Q = 0 \qquad (3.3.12)$$

This method uses the following transformations

$$\Phi = \frac{1}{2}(I - A^T)P(I - A) \qquad (3.3.13)$$

$$\tilde{E} = (I - A)^{-1}(I + A) \qquad \tilde{F} = 2(I - A)^{-2}B$$

$$\tilde{G} = R + B^T(I - A^T)^{-1}Q(I - A)^{-1}B \qquad \tilde{H} = Q(I - A)^{-1}B$$

Using these transformations, equation (3.3.12) may be written

$$\tilde{E}^T\Phi\tilde{E} - \Phi - \left[\tilde{E}^T\Phi\tilde{F} + \tilde{H}\right]\left[\tilde{G} + \tilde{F}^T\Phi\tilde{F}\right]^{-1}\left[\tilde{E}^T\Phi\tilde{F} + \tilde{H}\right]^T + Q = 0 \qquad (3.3.14)$$

The existence of a unique non-negative definite solution P of equation (3.3.12) implies the existence of a unique non-negative definite solution Φ of equation (3.3.14). This solution may be obtained by solving equation (3.3.14) using a discrete method, as follows

$$\Phi_{i+1} = \tilde{E}^T\Phi_i\tilde{E} - \left[\tilde{E}^T\Phi_i\tilde{F}+\tilde{H}\right]\left[\tilde{G}+\tilde{F}^T\Phi_i\tilde{F}\right]^{-1}\left[\tilde{E}^T\Phi_i\tilde{F}+\tilde{H}\right]^T + Q \qquad (3.3.15)$$

where

$$\Phi = \lim_{i\to\infty} \Phi_i \quad \text{and} \quad \Phi_o = 0$$

P is then determined from

$$P = 2(I - A^T)^{-1}\Phi(I - A)^{-1} \qquad (3.3.16)$$

At first sight, this would seem to be a good method to use, as a null Q matrix will clearly not give rise to any zero divide warnings. However, it becomes clear on closer inspection that if Q is the null matrix, then $\tilde{H}$ is zero and so the first step with $\Phi_o = 0$ leads to $\Phi_1 = 0$. Therefore, in the limit, as $i \to \infty$, $\Phi = 0$. It is possible that it is not necessary for Φ_o to be equal to zero, and this will be investigated in the next section. It is also clear from equations (3.3.13) that the method will not work if the matrix (I - A) is singular, and so care must be taken with the choice of the matrix A.

An approximate answer can perhaps be obtained by setting Q to be of the form qI, where q is a very small positive scalar, but this may again lead to an approximate answer. This approximation will also be investigated in the next section.

The Macfarlane-Potter-Fath method (Kailath, 1980), which is used by the MATLAB routine for solving the continuous matrix Riccati equation, solves equation (3.3.12) by considering its associated Hamiltonian matrix

$$\mathfrak{M} = \begin{bmatrix} A & -BR^{-1}B^T \\ -Q & -A^T \end{bmatrix} \qquad (3.3.17)$$

Assuming that equation (3.3.12) is an n-dimensional matrix equation, the Hamiltonian matrix, $\mathfrak{M}$, will be a 2n-dimensional matrix.

Let $J = \begin{pmatrix} 0 & I \\ -I & 0 \end{pmatrix}$, so $J^T = J^{-1} = -J$, then :

$\mathfrak{M}$ is Hamiltonian if $J^{-1}\mathfrak{M}^TJ = -\mathfrak{M}$

$\mathfrak{M}$ is symplectic if $J^{-1}\mathfrak{M}^TJ = \mathfrak{M}^{-1}$

Two important properties of Hamiltonian matrices are :

i) If λ is an eigenvalue of $\mathfrak{M}$, then $-\lambda$ will also be an eigenvalue of $\mathfrak{M}$, with the same multiplicity.

ii) If $\mathfrak{M}$ is Hamiltonian and U is symplectic, then $U^{-1}\mathfrak{M}U$ is Hamiltonian (or symplectic).

Suppose that $\mathfrak{M}$ has 2n distinct eigenvalues and that its eigenvectors may be partitioned as follows

$$\mathfrak{M}\begin{bmatrix} \ell_i \\ q_i \end{bmatrix} = \lambda_i \begin{bmatrix} \ell_i \\ q_i \end{bmatrix} \qquad i = 1,2,\ldots,2n \qquad (3.3.18)$$

where $\{\ell_i\}$ and $\{q_i\}$ are sets of n vectors.

Choose the eigenvalues with negative real parts, $\{\lambda_i^- \; i=1,\ldots,n\}$ and let $\{\bar{\ell}_1, \bar{q}_1\}$ be the corresponding eigenvectors. Then P can be calculated as

$$P = \left[\bar{q}_1, \ldots, \bar{q}_n\right]\left[\bar{\ell}_1, \ldots, \bar{\ell}_n\right]^{-1} \qquad (3.3.19)$$

There are two problems which can occur with this method, when Q is the null matrix. The first problem is that there may not be sufficient negative eigenvalues of $\mathfrak{M}$ to form the P matrix. Suppose that there are n_1 negative eigenvalues of $\mathfrak{M}$, where $n_1 < n$. This problem may be overcome by using the eigenvectors of $n-n_1$ of the zero eigenvalues, thus enabling the P matrix to be formed. The second, more common, problem is that the 2n eigenvalues of $\mathfrak{M}$ are not distinct, in which case the method is not valid. A possible approach to this problem is to assemble the P matrix in the usual way, with generalized eigenvectors in the case of non-distinct eigenvalues. This modified version of the Macfarlane-Potter-Fath method may lead to an inaccurate P matrix. Numerical results for this modified method are contained in Section 3.4.

Laub (1979) claims that the Schur method will solve the continuous matrix Riccati equation (3.3.12) for $Q \geq 0$. Consider again the associated Hamiltonian matrix $\mathfrak{M}$ given in equation (3.3.17). Let $\mathfrak{M}$ have eigenvalues $\lambda_1, \ldots, \lambda_n$, then there exists a unitary transformation U such that $U^{-1}\mathfrak{M}U$ is upper triangular with diagonal elements $\lambda_1, \ldots, \lambda_n$.

There also exists an orthogonal transformation, U, such that $U^T \mathcal{M} U$ is quasi-upper triangular, with the 2×2 and 1×1 diagonal blocks in any order, with a suitable choice of U. The Hamiltonian matrix $\mathcal{M}$ may therefore be represented as

$$\mathcal{M} = USU^T \qquad \text{with } S = \begin{bmatrix} S_{11} & S_{12} \\ 0 & S_{22} \end{bmatrix} \tag{3.3.20}$$

where the S_{ij} are all n×n matrices.

The orthogonal transformation U may also be partitioned into n×n blocks to give

$$U = \begin{bmatrix} U_{11} & U_{12} \\ U_{21} & U_{22} \end{bmatrix} \tag{3.3.21}$$

Then the solution of equation (3.3.12), P, is given by

$$P = U_{21}U_{11}^{-1} \tag{3.3.22}$$

The problem with this method is that when Q is equal to zero, the Hamiltonian matrix, $\mathcal{M}$, given in equation (3.3.17) is already in Schur form as can be seen from equation (3.3.20), and so U_{21} is zero, and hence, trivially, P is zero. Again, it may be possible to use a Q matrix of the form qI, where q is a very small positive scalar to force U_{21} to be non-zero, and hence P to be non-zero, and this will be investigated in the next section.

3.4 Numerical Examples

For the first example, consider the following system which has five states (n = 5) and two control inputs (m = 2). The system matrix A and the interface matrix B are given by

$$A = \begin{bmatrix} -1 & 1 & 0 & 0 & 0 \\ 0 & -2 & 1 & 0 & 0 \\ 0 & 0 & 0 & 1 & 0 \\ 0 & 0 & 0 & 0 & 1 \\ 0 & 0 & 0 & 0 & 0 \end{bmatrix} \qquad B = \begin{bmatrix} 0 & 0 \\ 0 & 0 \\ 0 & 1 \\ 0 & 1 \\ 1 & 0 \end{bmatrix}$$

The transformation matrix T is taken as

$$T = -0.5 \begin{bmatrix} 2 & 0 & 0 & 0 & 0 \\ 0 & \sqrt{2} & 1 & -1 & 0 \\ 0 & \sqrt{2} & -1 & 1 & 0 \\ 0 & 0 & 0 & 0 & 2 \\ 0 & 0 & \sqrt{2} & \sqrt{2} & 0 \end{bmatrix}$$

Partitioning the product TAT^T, as outlined in Section 2.2, (p.11) gives

$$A_{11} = 0.25 \begin{bmatrix} -4 & 2\sqrt{2} & 2\sqrt{2} \\ 0 & -5+\sqrt{2} & -3-\sqrt{2} \\ 0 & -3+\sqrt{2} & -5-\sqrt{2} \end{bmatrix} \qquad A_{12} = 0.25 \begin{bmatrix} 0 & 0 \\ -2 & 2+\sqrt{2} \\ 2 & 2-\sqrt{2} \end{bmatrix}$$

For the disc, choose r = 2 and $\alpha = -6 + 0j$. Solving the discrete Riccati equation gives

$$P = \begin{bmatrix} 3471.4500 & 589.4871 & 626.9800 \\ 589.4871 & 123.8504 & 103.0881 \\ 626.9800 & 103.0881 & 171.0469 \end{bmatrix}$$

So the control matrix is

$$F = \begin{bmatrix} 7.1830 & -0.8451 & 7.6267 \\ 24.2803 & 7.9984 & 6.5819 \end{bmatrix}$$

The (n-m) closed-loop eigenvalues of $(A_{11} - A_{12}F)$ are -5.2958, -5.1979 and -5.0332.

After transforming back to the full state space, the sliding hyperplane matrix, C, is found to be

$$C = \begin{bmatrix} -7.1830 & -4.7953 & 4.2359 & -4.2359 & -1 \\ -24.2803 & -10.3098 & -1.4154 & 0.0011 & 0 \end{bmatrix}$$

Of course, (n-m) of the closed-loop eigenvalues of the full order system given in equation (3.2.11) are found to be the same as those for the reduced order system. The remaining m eigenvalues of the full order system are found to be zero.

For the strip, choose $h_1 = 1.5$. The eigenvalues of A_{11} are -2, -1 and -0.5, and choosing $h_2 = 2.5$ gives $\mu = 0.8333$.

As discussed in section 3.3, there are problems when solving the continuous matrix Riccati equation with the right-hand side set to zero. The iterative method will only give the trivial solution if Q = 0, and will not give a solution with Q set to qI, since when $h_1 = 1.5$, the matrix (I - 1.5A) is almost singular. Choosing $h_1 = 1$ solves this problem, and gives $\mu = 2$, and the following P matrix, after 100 steps

$$Q = 1.0e^{-20}\begin{bmatrix} 1 & 0 & 0 \\ 0 & 1 & 0 \\ 0 & 0 & 1 \end{bmatrix} \qquad P = 1\times10^{3}\begin{bmatrix} 0 & 0 & 0 \\ 1.0928 & 1.6396 & -0.0942 \\ 1.0928 & -1.6396 & 0.0942 \end{bmatrix}$$

This P matrix is clearly not acceptable, since not only is it not a symmetric matrix, but it is not positive definite.

Consider the same example, with $h_1 = 1$, but with $\Phi_o = I_{n-m}$, which gives the following solution

$$Q = 1.0e^{-2o}\begin{bmatrix}1 & 0 & 0\\ 0 & 1 & 0\\ 0 & 0 & 1\end{bmatrix} \qquad P = \begin{bmatrix}0.44 & 0.4063 & 0.2160\\ 0.4063 & 1.0490 & -0.4744\\ 0.2160 & -0.4744 & 0.7798\end{bmatrix}$$

This P matrix is clearly symmetric, and has no zero elements, and the control matrix is given by

$$F = \begin{bmatrix}-0.1903 & -1.5234 & 1.2534\\ 0.7568 & 1.6517 & -0.5815\end{bmatrix}$$

The closed-loop eigenvalues of $A_{11}-A_{12}F$ are -1.374, -2 and -2.839.

It is clear the the smallest eigenvalue is not within the vertical strip with bounds -1 and -2.5, and so despite giving an acceptable-looking P matrix, the iterative method with Φ_o non-zero and Q = qI appears not to work.

Returning to the original strip, $h_1 = 1.5$, the precise Macfarlane-Potter-Fath method will not give a solution since the eigenvalues of the Hamiltonian matrix $\mathfrak{M}$ are not distinct. Using the modified version of this method outlined in section 3.3 gives the following P matrix

$$P = \begin{bmatrix}1.8762 & 1.1182 & 1.5351\\ 1.4159 & 2.1772 & -0.1748\\ 1.2374 & -0.5958 & 2.3458\end{bmatrix}$$

It can be seen that this P matrix is not symmetric; the differences between the corresponding symmetric elements are of the order of 10^{-1}. Calculating the control matrix from this P matrix gives

$$F = \begin{bmatrix} -0.0744 & -1.1554 & 1.0503 \\ 1.1582 & 1.4759 & 0.1619 \end{bmatrix}$$

and the (n-m) closed-loop eigenvalues of $(A_{11} - A_{12}F)$ are $-1.9432 \pm 0.1274j$ and -2.

These eigenvalues are clearly within the vertical strip crossing the real axis at the points -2.5 and -1.5, and so it appears that the inaccuracy of the P matrix is not too critical for this particular example. Therefore, the modified version of the Macfarlane-Potter-Fath method gives a sufficiently accurate result. After transforming back to the full state space, the sliding hyperplane matrix is found to be

$$C = \begin{bmatrix} 0.0744 & 0.0744 & 1.1028 & -1.1028 & -1 \\ -1.1582 & -1.1582 & -1.3641 & -0.0501 & 0 \end{bmatrix}$$

A further improvement to this modified Macfarlane-Potter-Fath method would be to force P to be symmetric by choosing the off diagonal terms to be of the form

$$\tilde{P}_{ij} = \frac{P_{ij} + P_{ji}}{2} \qquad i \neq j \qquad (3.4.1)$$

For this example, P would become

$$P = \begin{bmatrix} 1.8762 & 1.2671 & 1.3863 \\ 1.2671 & 2.1772 & -0.3853 \\ 1.3863 & -0.3853 & 2.3458 \end{bmatrix}$$

The resulting control matrix is

$$F = \begin{bmatrix} 0.0497 & -1.0677 & 1.1380 \\ 1.0704 & 1.5016 & 0.0122 \end{bmatrix}$$

and the (n-m) closed-loop eigenvalues of $(A_{11} - A_{12}F)$ are -1.7119, -2 and -2.1745.

These eigenvalues are clearly within the vertical strip, crossing the real axis at the points -2.5 and -1.5. After transforming back to the full state space, the sliding hyperplane matrix is found to be

$$C = \begin{bmatrix} -0.0497 & -0.0497 & 1.1028 & -1.1028 & -1 \\ -1.0704 & -1.0704 & -1.4518 & 0.0376 & 0 \end{bmatrix}$$

If instead of setting Q to be the null matrix, it is set to be a matrix of the form qI, where q is a small positive scalar, the eigenvalues of the Hamiltonian matrix $\mathfrak{M}$ are distinct, and the Macfarlane-Potter-Fath method works without any modifications. The following solutions result from this method :

$$Q = 1.0e^{-20}\begin{bmatrix} 1 & 0 & 0 \\ 0 & 1 & 0 \\ 0 & 0 & 1 \end{bmatrix} \qquad P = \begin{bmatrix} 2.4373 & 1.4526 & 1.9942 \\ 1.4526 & 2.1991 & -0.1448 \\ 1.9942 & -0.1448 & 2.9695 \end{bmatrix}$$

As would be expected from this method, the P matrix is clearly completely symmetric. The control matrix is

$$F = \begin{bmatrix} 0.2257 & -0.9766 & 1.2958 \\ 1.2766 & 1.5465 & 0.2589 \end{bmatrix}$$

and the (n-m) closed-loop eigenvalues of $(A_{11} - A_{12}F)$ are -2 and $-1.9971 \pm 0.1462j$.

These values are clearly very close to the ones obtained with Q set to the null matrix since the complex pair differ only in the second decimal place, and the real value is the same. The results from this method are accurate since the method used was the unmodified Macfarlane-Potter-Fath method, but of course Q was not set to the null matrix. After transforming back to the full state space, the sliding hyperplane matrix is found to be

$$C = \begin{bmatrix} -0.2257 & -0.2257 & 1.1362 & -1.1362 & -1 \\ -1.2766 & -1.2766 & -1.3509 & -0.0633 & 0 \end{bmatrix}$$

Another solution to the problem of solving the continuous matrix Riccati equation when Q is the null matrix is to use the Schur method described in section 3.2, with the Q matrix set to qI where q is a small positive scalar. This gives the following results

$$Q = 1.0e^{-20}\begin{bmatrix} 1 & 0 & 0 \\ 0 & 1 & 0 \\ 0 & 0 & 1 \end{bmatrix} \qquad P = \begin{bmatrix} 0 & 0 & 0 \\ 0 & 0.9142 & -2.5 \\ 0 & -2.5 & 1.942 \end{bmatrix}$$

Although this P matrix is symmetric, it is clearly not a satisfactory result, since P is not positive definite.

It is unlikely that a P matrix of this form will give the required eigenvalues. It is presumed that the inaccuracies in the P matrix arise because although U_{21} is not zero, it is very small.
The control matrix is

$$F = \begin{bmatrix} 0 & -1.4226 & 0.2441 \\ 0 & 0.3452 & -2.0118 \end{bmatrix}$$

and the (n-m) closed-loop eigenvalues of $(A_{11} - A_{12}F)$ are -1, -1.1666 and -2.1666. Clearly, only one of these eigenvalues is within the strip with limits -2.5 and -1.5, and so, as was surmised from the form of P, this method does not work when Q is close to the null matrix.

For the second example, consider the robot arm discussed in Chapter 2. This system has four states (n = 4) and two control inputs (m = 2). The system matrix A and the interface matrix B are given by

$$A = \begin{bmatrix} 0 & 1 & 0 & 0 \\ 0 & -0.332 & 0 & 0.0187 \\ 0 & 0 & 0 & 0 \\ 0 & 0.783 & 0 & -0.1914 \end{bmatrix} \qquad B = \begin{bmatrix} 0 & 0 \\ 130.83 & -308.33 \\ 0 & 0 \\ -308.33 & 3155.39 \end{bmatrix}$$

The transformation matrix T is taken as

$$T = \begin{bmatrix} 1 & 0 & 0 & 0 \\ 0 & 0 & 1 & 0 \\ 0 & -0.3906 & 0 & 0.9206 \\ 0 & -0.9206 & 0 & -0.3906 \end{bmatrix}$$

Partitioning the product TAT^T, as outlined in Section 2.2 gives

$$A_{11} = \begin{bmatrix} 0 & 0 \\ 0 & 0 \end{bmatrix} \qquad A_{12} = \begin{bmatrix} -0.3906 & -0.9206 \\ 0.9206 & -0.3906 \end{bmatrix}$$

For the disc, choose $r = 2$ and $\alpha = -4 + 0j$. Solving the discrete matrix Riccati equation gives

$$P = \begin{bmatrix} 13.3007 & 0 \\ 0 & 13.3007 \end{bmatrix}$$

So the control matrix is

$$F = \begin{bmatrix} -1.2012 & 2.8309 \\ -2.8309 & -1.2012 \end{bmatrix}$$

The (n-m) closed-loop eigenvalues of $(A_{11} - A_{12}F)$ are a double root at -3.0752, which are clearly within the specified disc. After transforming back to the full state space, the sliding hyperplane matrix is found to be

$$C = \begin{bmatrix} -1.2012 & -0.3906 & 2.8309 & 0.9206 \\ -2.8309 & -0.9206 & -1.2012 & -0.3906 \end{bmatrix}$$

For the strip, choose $h_1 = 2.0$, which gives rise to a matrix $\hat{A}$ whose eigenvalues are both 0. Choosing $h_2 = 3$ gives $\mu = 0.625$ and the strip crosses the real axis at the points [-3,-2]. Solving the continuous matrix Riccati equation with the right-hand side set to zero by the Macfarlane-Potter Fath method again gives a Hamiltonian matrix with non-distinct eigenvalues. Using the modified version of this method to overcome this problem gives the following P matrix

$$P = \begin{bmatrix} 4 & 0 \\ 0 & 4 \end{bmatrix}$$

This P matrix is clearly symmetric, and may be shown to be an exact solution of (3.3.6) for this example, and so despite the eigenvalues of the Hamiltonian matrix not being distinct, there are no obvious errors. The control matrix is

$$F = \begin{bmatrix} -0.9765 & 2.3014 \\ -2.3014 & -0.9765 \end{bmatrix}$$

and the (n-m) closed-loop eigenvalues of $(A_{11} - A_{12}F)$ are a double root at -2.5. After transforming back to the full state space, the sliding hyperplane matrix is found to be

$$C = \begin{bmatrix} -0.9765 & -0.3906 & 2.3014 & 0.9206 \\ -2.3014 & -0.9206 & -0.9765 & -0.3906 \end{bmatrix}$$

Solving the continuous Riccati equation by this method, but with the Q matrix of the form qI, where q is a small positive scalar, still results in the Hamiltonian matrix having indistinct eigenvalues, and gives the following results

$$Q = 1.0e^{-20}\begin{bmatrix} 1 & 0 \\ 0 & 1 \end{bmatrix} \qquad P = \begin{bmatrix} 4 & 0 \\ -0.002 & 4 \end{bmatrix}$$

These results are almost the same as those for Q equal to the null matrix, but in this case, the P matrix is not quite symmetric, as there is an error of order 10^{-3} on P_{21}. The control matrix is given by

$$F = \begin{bmatrix} -0.9766 & 2.3014 \\ -2.3009 & -0.9765 \end{bmatrix}$$

The (n-m) closed-loop eigenvalues of $(A_{11} - A_{12}F)$ are again a double root at -2.5. After transforming back to the full state space, the sliding hyperplane matrix is found to be

$$C = \begin{bmatrix} -0.9776 & -0.3906 & 2.3014 & 0.9206 \\ -2.3009 & -0.9206 & -0.9765 & -0.3906 \end{bmatrix}$$

The results from this method with the P matrix forced to be symmetric, but with errors of the order 10^{-3} on both P_{21} and P_{12}, as outlined in equation (4.3.1) are

$$P = \begin{bmatrix} 4 & -0.001 \\ -0.001 & 4 \end{bmatrix} \qquad F = \begin{bmatrix} -0.9771 & 2.3016 \\ -2.3012 & -0.9760 \end{bmatrix}$$

The (n-m) closed-loop eigenvalues of the reduced order system $(A_{11} - A_{12}F)$ are -2.4994 and -2.5006, which are clearly within the strip. After transforming back to the full state space, the sliding hyperplane matrix is given by

$$C = \begin{bmatrix} -0.9771 & -0.3906 & 2.3016 & 0.9206 \\ -2.3012 & -0.9206 & -0.9760 & -0.3906 \end{bmatrix}$$

3.5 Discussion

It can be seen that the method of placing eigenvalues in a specified disc can be successfully applied to the problem of eigenvalue placement in a Variable Structure Control System. It is clear that this method is less restrictive than a method of choosing precise eigenvalues. The sensitivity of this method to changes in the arbitrary matrices will be considered in Chapter 6, along with the problem of positioning eigenvalues within the disc.

With regard to the placement of eigenvalues in an infinite vertical strip, it can be seen that this theory may be successfully applied to a Variable Structure Control System. This method also allows a much less rigid specification of the eigenvalues and therefore gives more flexibility of solution. The robustness of this method to changes in the arbitrary matrix is also discussed in Chapter 6.

Some difficulties arise with the solution of the continuous matrix Riccati equation when Q is the null matrix. The Macfarlane-Potter-Fath method uses the associated Hamiltonian matrix of the system, and it appears that when Q is null, this results in the eigenvalues of this matrix not being distinct.

As has been outlined in section 3.3 and illustrated in section 3.4, some modifications to the Macfarlane-Potter-Fath method enable this problem to be overcome, and also force the resulting P matrix to be symmetric. Both the iterative method and the Schur method outlined in section 3.3 will give either a null P matrix or a P matrix which is not positive definite, which is clearly unsatisfactory. The reason for the problems connected with the solution of the continuous matrix Riccati equation with the right-hand side equal to zero can be seen by looking at equation (3.3.6), since it is clear that the trivial solution is a null P. The only method discussed in this work in which this inherent problem can be overcome is that of the modified Macfarlane-Potter-Fath method. There may possibly be a better way of solving equation (3.3.6), and this will be considered in the future.

4. EIGENVALUE PLACEMENT IN A SPECIFIED SECTOR

4.1 Introduction

In this chapter the problem of placing eigenvalues in a region other than a disc or a vertical strip will be considered, and a new method will be developed to place the closed-loop eigenvalues of a system within a sector in the left-hand half-plane (Woodham and Zinober, 1991). Some work has been done recently on a similar problem for the very specific case of rotational systems (Kim and Lee, 1990). This method enables the system to be described by complex matrices, and the method used to place the eigenvalues within the chosen region results in a complex control matrix. There is no indication in this work of how to map this result back to the "real world".

The selection of weighting matrices to give the required eigenstructure has been considered (Harvey and Stein, 1978), and numerical methods for robust eigenstructure assignment have been studied (see for example, Kautsky, Nichols & Van Dooren, 1985, Burrows and Patton, 1990,a & b). The problem of root clustering for real and complex matrices has been addressed (Gutman, 1979, Gutman and Vaisberg, 1984) and the conditions for the eigenvalues of a matrix to lie within a particular sector are obtained from particular classes of matrices. However, this work does not give any indication of how to move the eigenvalues into the sector. Methods to determine whether the roots of a polynomial lie to the left of a vertical line (Soh, 1990), or in a sector in the left-

hand half-plane (Foo & Soh, 1990) have been developed. Again, no method is given for moving roots into the required region.

Some work has also been done on the robustness of eigenvalue assignment in regions bounded by straight lines (Juang, Hong and Wang, 1989). Once again, there is no strategy given to place the eigenvalues of a system within a particular region.

The method which will be described in this chapter, and illustrated with a numerical example (Woodham & Zinober, 1991), has no restrictions on the real system matrices. The method for ensuring that the eigenvalues will lie in the required region is developed in detail, and involves the solution of a complex continuous matrix Riccati equation. The resulting control matrix is also real, and thus possible to implement in a physical problem. The region which will be considered is an open ended sector bounded by a straight line cutting the left-hand half-plane, and its reflection in the real axis (Fig 4.1).

In section 4.2 the approach will be developed using the standard regulator theory, and it will then be applied to the particular problem of Variable Structure Control systems. In section 4.3 the extension of this work to a region bounded by two intersecting sectors is considered, and some of the problems are highlighted. Section 4.4 contains some examples of the method, applied to the two systems described in Chapter 3. In section 4.5 the effect on the method of particular pairs of α and θ values is investigated. It can be seen that there are limiting values of θ for each α value, and a possible method of predicting these values is outlined. Section 4.6 contains a discussion of the results.

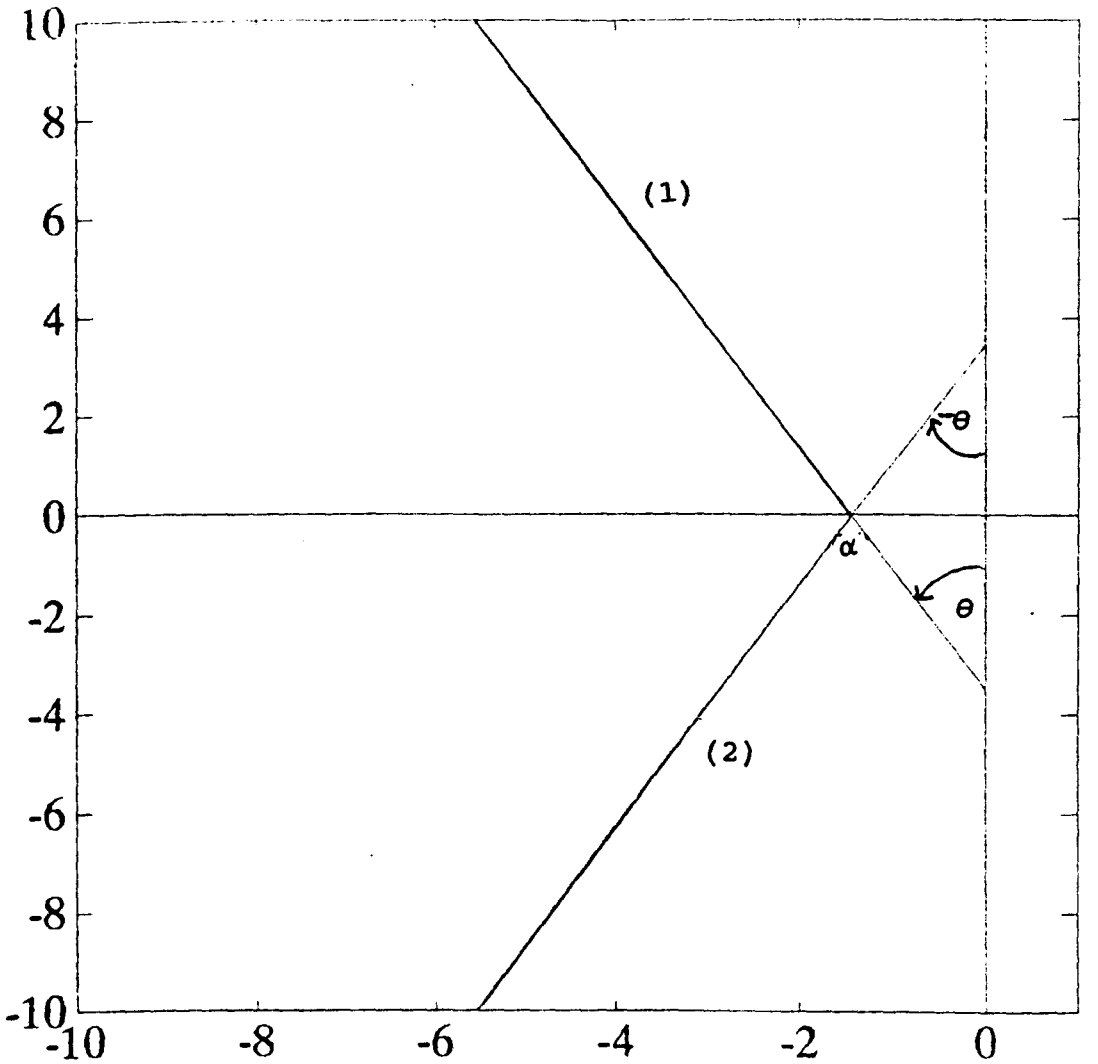

Fig 4.1 Sector with angle θ and real axis crossing point α

4.2 Technique for the Regulator System

The technique for placing all the closed loop eigenvalues of a system within a specified sector in the left-hand half-plane will now be developed (Woodham and Zinober, 1990).

Let us define a region bounded by a line at an angle θ to the imaginary axis, and crossing the real axis at α, where α is any real number, and the reflection of this line in the real axis (Fig 4.1). The angle θ is measured in an anti-clockwise direction from the imaginary axis, and lies between 0° and 90°.

We want to determine the state feedback, $u = Fx$, such that all the eigenvalues of the closed loop system lie within the required region.

The equation of line (1) is given by

$$l_1 \quad : \quad y\sin\theta + (x - \alpha)\cos\theta = 0 \qquad 0^\circ \le \theta \le 90^\circ \qquad (4.2.1)$$

The region we are considering is to the left of this line, and excludes the origin, so we require

$$y\sin\theta + (x - \alpha)\cos\theta < 0 \qquad (4.2.2)$$

The equation of line (2) is given by

$$l_2 \quad : \quad y\sin\theta - (x - \alpha)\cos\theta = 0 \qquad 0^\circ \le \theta \le 90^\circ \qquad (4.2.3)$$

The region we are considering is to the left of this line, and excludes the origin, so we require

$$y\sin\theta - (x - \alpha)\cos\theta > 0 \qquad (4.2.4)$$

Let us now consider the general system (2.2.2) and the matrix equation

$$e^{j\theta}A^{*}P + e^{-j\theta}PA - 2\alpha P\cos\theta = -Q \qquad (4.2.5)$$

Q is an arbitrary positive definite matrix and * denotes the complex conjugate transpose. Let λ and ν be an eigenvalue and corresponding right eigenvector of A, so that

$$A\nu = \lambda\nu \qquad \text{and} \qquad \nu^{*}A^{*} = \bar{\lambda}\nu^{*}$$

Premultiply equation (4.2.5) by ν^{*} and postmultiply by ν to give :

$$e^{j\theta}\nu^{*}A^{*}P\nu + e^{-j\theta}\nu^{*}PA\nu - 2\alpha\nu^{*}P\nu\cos\theta = -\nu^{*}Q\nu \qquad (4.2.6)$$

Substituting for $A\nu$ and $\nu^{*}A^{*}$, and rearranging gives

$$\nu^{*}P\nu\left[e^{j\theta}\,\bar{\lambda} + e^{-j\theta}\lambda - 2\alpha\cos\theta\right] = -\nu^{*}Q\nu \qquad (4.2.7)$$

Let $\lambda = x + jy$ and hence $\bar{\lambda} = x - jy$. Substituting into equation (4.2.7) gives

$$2\left[(x - \alpha)\cos\theta + y\sin\theta\right]\nu^{*}P\nu = -\nu^{*}Q\nu \qquad (4.2.8)$$

Since Q is positive definite and we require P to be positive definite it follows that

$$(x - \alpha)\cos\theta + y\sin\theta < 0 \qquad (4.2.9)$$

In other words, if there exists a positive definite solution P to equation (4.2.5), all the eigenvalues of the matrix A lie to the left of the line defined by

$$(x - \alpha)\cos\theta + y\sin\theta = 0.$$

Consider the state feedback u = Fx. The conditions for the eigenvalues of the closed loop system A + BF to lie within the region are required. Consider the following equation

$$e^{j\theta}(A + BF)^{*}P + e^{-j\theta}P(A + BF) - 2\alpha P\cos\theta = -\tilde{Q} \qquad (4.2.10)$$

where $\tilde{Q}$ is an arbitrary positive definite symmetric matrix.

It will now be shown that the eigenvalues of A + BF all lie in the required region if there exists a positive definite solution P satisfying (4.2.10). Let us now consider a continuous matrix Riccati equation of the form

$$e^{j\theta}(A - \alpha I)^{*}P + e^{-j\theta}P(A - \alpha I) - e^{-j\theta}PB\tilde{R}^{-1}B^{T}P = -\tilde{Q} \qquad (4.2.11)$$

Let $F = -\tilde{R}^{-1}B^{T}P$, where R is an m×m positive definite symmetric weighting matrix, and substitute for F in equation (4.2.11) to give

$$e^{j\theta}(A - \alpha I)^{*}P + e^{-j\theta}P(A - \alpha I) + e^{-j\theta}PBF = -\tilde{Q} \qquad (4.2.12)$$

Expanding equation (4.2.12) gives

$$e^{j\theta}A^{*}P - \alpha e^{j\theta}P + e^{-j\theta}P(A + BF) - \alpha Pe^{-j\theta} = -\tilde{Q} \qquad (4.2.13)$$

Rearranging equation (4.2.13) gives

$$e^{j\theta}A^{*}P + e^{-j\theta}P(A + BF) - \alpha P(e^{j\theta} + e^{-j\theta}) = -\tilde{Q} \qquad (4.2.14)$$

Now $e^{j\theta} + e^{-j\theta} = 2\cos\theta$, so substituting for this expression in equation (4.2.14) gives

$$e^{j\theta}A^{*}P + e^{-j\theta}P(A + BF) - 2\alpha P\cos\theta = -\tilde{Q} \qquad (4.2.15)$$

Comparing equations (4.2.10) and (4.2.15), it is clear that we must add $e^{j\theta}(BF)^{*}P$ to both sides of equation (4.2.15) to obtain the left-hand side of equation (4.2.10). So equation (4.2.15) becomes

$$e^{j\theta}(A+BF)^{*}P+e^{-j\theta}P(A+BF)-2\alpha P\cos\theta = -\tilde{Q}+e^{j\theta}(BF)^{*}P \qquad (4.2.16)$$

Now $(BF)^{*}P = F^{T}B^{T}P = -F^{T}\tilde{R}F$ (since F and B are real), so substituting for $(BF)^{*}P$ in equation (4.2.16) gives

$$e^{j\theta}(A+BF)^{*}P+e^{-j\theta}P(A+BF)-2\alpha P\cos\theta = -\tilde{Q} - e^{j\theta}F^{T}\tilde{R}F \qquad (4.2.17)$$

Since $\tilde{Q}$ and $\tilde{R}$ are arbitrary positive definite symmetric matrices, we can choose positive definite symmetric matrices Q and R such that

$$Q = \tilde{Q} + e^{j\theta}F^{T}\tilde{R}F \qquad \text{and} \qquad R = e^{j\theta}\tilde{R}$$

Then equation (4.2.17) may be written

$$e^{j\theta}(A + BF)^{*}P + e^{-j\theta}P(A + BF) - 2\alpha P\cos\theta = -Q \qquad (4.2.18)$$

It is clear that equation (4.2.18) and equation (4.2.10) are identical.

The eigenvalues of (A + BF) will, therefore, lie in the required region if there exists a positive definite solution P to equation (4.2.18) satisfying

$$e^{j\theta}(A - \alpha I)^{*}P + e^{-j\theta}P(A - \alpha I) - PBR^{-1}B^{T}P = -Q \qquad (4.2.19)$$

where $F = -R^{-1}B^{T}P$.

Since the eigenvalues of (A + BF) will be either real, or complex conjugate pairs, they will lie in the region bounded by line (1), and its reflection in the real axis, line (2). Conditions (4.2.2) and (4.2.4) will therefore be satisfied, and the eigenvalues of (A + BF) will lie in the required sector in the left-hand half-plane.

In general, the solution matrix P of equation (4.2.19) has complex elements except on the leading diagonal, unless the angle θ is zero. If θ is zero, then equation (4.2.19) is not a complex equation and so P will be a real positive definite matrix. The general form of the P matrix when θ is not equal to zero is

$$P = \begin{bmatrix} P_{11} & P_{12}-\tilde{P}_{12}j & P_{13}-\tilde{P}_{13}j & \cdots\cdots & P_{1n}-\tilde{P}_{1n}j \\ P_{12}+\tilde{P}_{12}j & P_{22} & P_{23}+\tilde{P}_{23}j & \cdots\cdots & P_{2n}+\tilde{P}_{2n}j \\ P_{13}+\tilde{P}_{13}j & P_{23}-\tilde{P}_{23}j & P_{33} & \cdots\cdots & P_{3n}-\tilde{P}_{3n}j \\ \cdot & \cdot & \cdot & \cdots\cdots & \cdot \\ \cdot & \cdot & \cdot & \cdots\cdots & \cdot \\ \cdot & \cdot & \cdot & \cdots\cdots & \cdot \\ \cdot & \cdot & \cdot & \cdots\cdots & \cdot \\ P_{1n}+\tilde{P}_{1n}j & P_{2n}-\tilde{P}_{2n}j & P_{3n}+\tilde{P}_{3n}j & \cdots\cdots & P_{nn} \end{bmatrix} \qquad (4.2.20)$$

The P matrix is a Hermitian matrix, since $P^* = P$, which can be seen from equation (4.2.19).

Now consider equation (4.2.19) with θ replaced by $-\theta$

$$e^{-j\theta}(A - \alpha I)^* P_1 + e^{j\theta} P_1 (A - \alpha I) - P_1 B R^{-1} B^T P_1 = -Q \qquad (4.2.21)$$

This gives rise to a solution P_1 which is also a Hermitian positive definite matrix and is the complex conjugate transpose of the solution P of equation (4.2.19). Substituting P^* for P_1 in equation (4.2.21) gives

$$e^{-j\theta}(A - \alpha I)^* P^* + e^{j\theta} P^* (A - \alpha I) - P^* B R^{-1} B^T P^* = -Q \qquad (4.2.22)$$

The complex conjugate transpose of equation (4.2.19) is

$$e^{-j\theta} P^* (A - \alpha I) + e^{j\theta}(A - \alpha I)^* P^* - P^* B^T R^{-1} B P^* = -Q \qquad (4.2.23)$$

It can be seen that equation (4.2.22) and equation (4.2.23) are very similar, and so clearly the solutions of equation (4.2.19) and equation (4.2.21) are very closely related. Since we require the control matrix to be real, and since the solutions of equations (4.2.19) and (4.2.21) are so closely related we shall define the control matrix to be

$$F = -R^{-1} B^T \hat{P} \qquad (4.2.24)$$

where $\hat{P}$ is defined to contain the modulus of the elements of the Hermitian positive definite matrix P. In other words, $\hat{P}$ is defined to be

$$\hat{P}_{ij} = \sqrt{\left(P_{ij} \bar{P}_{ij}\right)} \qquad (4.2.25)$$

If there exists a Hermitian positive definite solution P to equation (4.2.19) and if the control matrix is defined by equation (4.2.24), then it is postulated that the closed-loop eigenvalues of the system will lie between the line specified by α and θ and its reflection in the real axis. This will be illustrated numerically in Section 4.4.

For the sliding mode design we require the (n-m) left-hand half-plane closed-loop eigenvalues of the reduced order equivalent system ($A_{11} - A_{12}F$) to lie within the specified region. The matrix Riccati equation to be solved is therefore

$$e^{j\theta}(A_{11}-\alpha I)^{*}P + e^{-j\theta}P(A_{11}-\alpha I) - PA_{12}R^{-1}A_{12}^{T}P = -Q \qquad (4.2.26)$$

and the control matrix, F, is given by

$$F = R^{-1}A_{12}^{T}\hat{P}$$

where $\hat{P}$ is as defined in equation (4.2.25). The control matrix has the opposite sign to that of the system A + BF, since the system now under consideration is of the form A - BF.

The eigenvalues of the reduced order system $A_{11} - A_{12}F$ will then lie in the required region. The sliding hyperplane matrix, C, is obtained in the same way as before, and is given by

$$C = \left[F \; I_m\right]T$$

where T is the transformation matrix defined in Chapter 2.

The choice of the weighting matrix R has an effect on the positioning of the eigenvalues within the region, and also enables them to be placed within a region at an angle greater than the limiting θ value (Section 4.5). This effect will be discussed in the chapter on dependence of eigenvalue placement techniques on the design of the R matrix, Chapter 6.

4.3 Technique for a Region Bounded by Two Sectors

The extension of the technique for placing all the closed-loop eigenvalues of a system within a region bounded by one sector to a technique for placing all the closed-loop eigenvalues in a region bounded by the intersection of two sectors will now be considered.

The first sector is defined to be bounded by a line at an angle θ to the imaginary axis, crossing the real axis at α, and the reflection of this line in the real axis. The second sector is defined to be bounded by a line at an angle ϕ to the imaginary axis, crossing the real axis at β, and its reflection in the real axis (Fig 4.2). Both θ and ϕ are assumed to lie between 0° and 90°.

We want to determine the state feedback u = Fx such that all of the eigenvalues of the closed-loop system lie in this region of the left-hand half-plane.

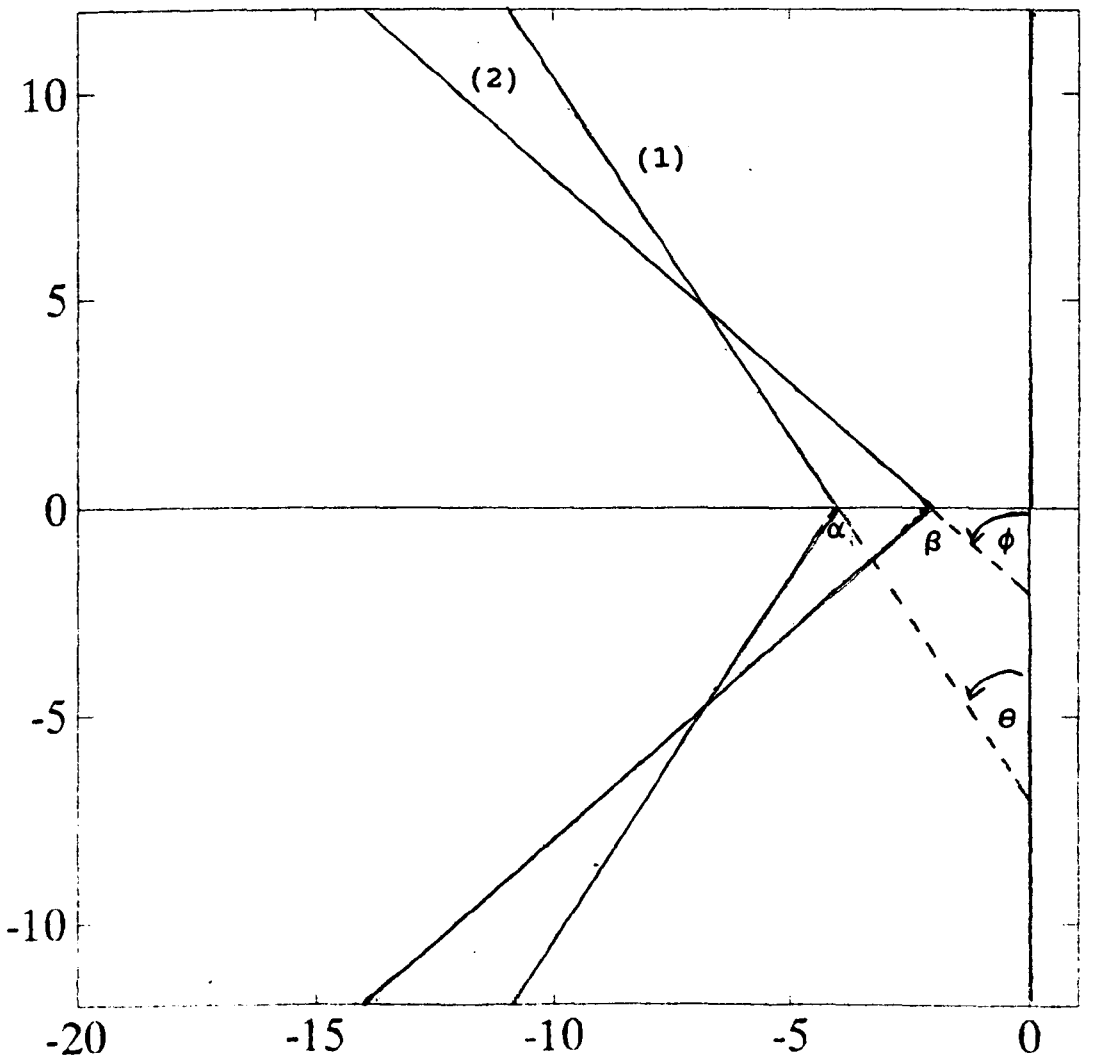

Fig 4.2 Two intersecting sectors with angles θ and ϕ and real axis crossing points α and β

From section 4.2 we may recall that for line (1) and its reflection in the real axis we have the following conditions

$$y\sin\theta + (x - \alpha)\cos\theta < 0 \tag{4.3.1}$$

$$y\sin\theta - (x - \alpha)\cos\theta > 0 \tag{4.3.2}$$

Similarly, for line (2) and its reflection in the real axis, we get the following conditions

$$y\sin\phi + (x - \beta)\cos\phi < 0 \tag{4.3.3}$$

$$y\sin\phi - (x - \beta)\cos\phi > 0 \tag{4.3.4}$$

As shown in the previous section, due to the symmetry of the eigenvalues of a matrix about the real axis, all of the closed-loop eigenvalues of the system will lie in sector 1 if there exists a positive definite matrix, P_1 satisfying

$$e^{j\theta}(A - \alpha I)^{*}P_1 + e^{-j\theta}P_1(A - \alpha I) - P_1BR_1^{-1}B^{T}P_1 = -Q_1 \tag{4.3.5}$$

All of the closed-loop eigenvalues of the system will lie in sector 2 if there exists a positive definite matrix, P_2 satisfying

$$e^{j\phi}(A - \beta I)^{*}P_2 + e^{-j\phi}P_2(A - \beta I) - P_2BR_2^{-1}B^{T}P_2 = -Q_2 \tag{4.3.6}$$

If all the closed-loop eigenvalues of the system are to lie in the region bounded by the intersection of the two sectors, then P_1 and P_2 must be positive definite, and satisfy equations (4.3.5) and (4.3.6).

Let us consider the general system (2.2.2) and the following matrix equation, which is a combination of equation (4.3.5) and equation (4.3.6)

$$(e^{j\theta}+e^{j\phi})A^{*}P + (e^{-j\theta}+e^{-j\phi})PA-2P(\alpha\cos\theta + \beta\cos\phi) = -Q \qquad (4.3.7)$$

where Q is an arbitrary positive definite matrix, and * denotes the complex conjugate transpose.

Let λ and ν be an eigenvalue and the corresponding right eigenvector of A, as defined in section 4.2. Premultiply equation (4.3.7) by ν^{*} and postmultiply it by ν to give

$$(e^{j\theta} + e^{j\phi})\nu^{*}A^{*}P\nu + (e^{-j\theta} + e^{-j\phi})\nu^{*}PA\nu - 2(\alpha\cos\theta + \beta\cos\phi)\nu^{*}P\nu = -\nu^{*}Q\nu \qquad (4.3.8)$$

Substituting for $A\nu$ and $\nu^{*}A^{*}$, and rearranging gives

$$\nu^{*}P\nu\left[(e^{j\theta}+e^{j\phi})\bar{\lambda}+(e^{-j\theta}+e^{-j\phi})\lambda-2(\alpha\cos\theta+\beta\cos\phi)\right] = -\nu^{*}Q\nu \qquad (4.3.9)$$

Let $\lambda = x + jy$ and hence $\bar{\lambda} = x - jy$. Substituting into equation (4.3.9) gives

$$\nu^{*}P\nu\left[\begin{array}{l}(\cos\theta+\cos\phi+j(\sin\phi+\sin\phi))(x-jy)+(\cos\theta+\\ \cos\phi-j(\sin\theta+\sin\phi))(x+jy)-2(\alpha\cos\theta+\beta\cos\phi)\end{array}\right]=-\nu^{*}Q\nu \qquad (4.3.10)$$

Expanding the expression in the brackets in equation (4.3.10), and rearranging gives

$$\nu^{*}P\nu\left[\begin{array}{r}2x(\cos\theta + \cos\phi) + 2y(\sin\theta + \sin\phi) - \\ 2(\alpha\cos\theta + \beta\cos\phi)\end{array}\right] = -\nu^{*}Q\nu \qquad (4.3.11)$$

Since Q is positive definite, and we require P to be positive definite, it follows that

$$x(\cos\theta+\cos\phi) + y(\sin\theta+\sin\phi) - (\alpha\cos\theta+\beta\cos\phi) < 0 \qquad (4.3.12)$$

Equation (4.3.12) may be rewritten in the form

$$(x - \alpha)\cos\theta + y\sin\theta + (x - \beta)\cos\phi + y\sin\phi < 0 \qquad (4.3.13)$$

However, equation (4.3.13) does not imply that conditions (4.3.1) and (4.3.3) hold, except in the particular case when $\alpha = \beta$ and $\theta = \phi$.

Consider the associated matrix Riccati equation

$$\left[(e^{j\theta}+e^{j\phi})A^* - (\alpha e^{j\theta}+\beta e^{j\phi})I\right]P - (e^{-j\theta}+e^{-j\phi})PBR^{-1}B^TP + P\left[(e^{-j\theta}+e^{-j\phi})A - (\alpha e^{-j\theta}+\beta e^{-j\phi})I\right] = -Q \qquad (4.3.14)$$

It can be seen that if both θ and ϕ are equal to 0, equation (4.3.14) becomes

$$\left[2A^* - (\alpha+\beta)I\right]P + \left[2A - (\alpha+\beta)I\right] - 2PBR^{-1}B^TP = -Q \qquad (4.3.15)$$

The solution of equation (4.3.15) will give a control matrix which it is postulated will place the closed-loop eigenvalues to the left of the line intersecting the real axis at the point

$$x = \frac{-(\alpha + \beta)}{2} \qquad (4.3.16)$$

It is clear that equation (4.3.7) does not lead to a solution which places the eigenvalues in the required region, except in the particular case when $\alpha = \beta$. The choice of a continuous matrix Riccati equation formed from the combination of equation (4.3.5) and equation (4.3.6) was clearly not entirely suitable for the solution of the problem of placing the eigenvalues in a region bounded by two intersecting sectors.

Consider instead a continuous matrix Riccati equation which is an approximation to the intersection of equation (4.3.5) and equation (4.3.6).

$$e^{j\theta}e^{j\phi}A^{*}P + e^{-j\theta}e^{-j\phi}PA - 2P(\alpha\cos(\theta+\phi) + \beta\cos\phi) = -Q \qquad (4.3.17)$$

Let λ and ν be an eigenvalue and the corresponding right eigenvector of A, with the same definition as before, and premultiply equation (4.3.17) by ν^{*} and postmultiply it by ν to give

$$e^{j(\theta+\phi)}\nu^{*}A^{*}P\nu + e^{-j(\theta+\phi)}\nu^{*}PA\nu - 2\nu^{*}P\nu(\alpha\cos(\theta+\phi) + \beta\cos\phi) = -\nu^{*}Q\nu \qquad (4.3.18)$$

Substituting in equation (4.3.18) for $\nu^{*}A^{*}$ and $A\nu$, and rearranging gives

$$\left(e^{j(\theta+\phi)}\bar{\lambda}+e^{-j(\theta+\phi)}\lambda-2(\alpha\cos(\theta+\phi)+\beta\cos\phi)\right)\nu^{*}P\nu = -\nu^{*}Q\nu \qquad (4.3.19)$$

Let $\lambda = x + jy$ and hence $\bar{\lambda} = x - jy$, and recall that

$$e^{j(\theta+\phi)} = \cos(\theta+\phi) + j\sin(\theta+\phi)$$
$$e^{-j(\theta+\phi)} = \cos(\theta+\phi) - j\sin(\theta+\phi)$$

Substituting in equation (4.3.19) for λ, $\bar{\lambda}$, $e^{j(\theta+\phi)}$ and $e^{-j(\theta+\phi)}$ and rearranging gives

$$\left(2x\cos(\theta+\phi)+2y\sin(\theta+\phi)-2\alpha\cos(\theta+\phi)-2\beta\cos\phi\right)\nu^{*}P\nu = -\nu^{*}Q\nu \qquad (4.3.20)$$

Since Q is positive definite, and we require P to be positive definite, it follows that

$$x\cos(\theta+\phi) + y\sin(\theta+\phi) - \alpha\cos(\theta+\phi) - \beta\cos\phi < 0 \qquad (4.3.21)$$

Equation (4.3.21) may be rearranged to give

$$(x - \alpha)\cos(\theta+\phi) + y\sin(\theta+\phi) - \beta\cos\phi \qquad (4.3.22)$$

Equation (4.3.22) is the equation of a straight line at an angle of $\theta+\phi$ to the imaginary axis which crosses the real axis at the point $\dfrac{\beta\cos\phi}{\cos(\theta+\phi)} + \alpha$.

It can be seen from Fig 4.3 that this region is a sector inside the required region, so that although the closed-loop eigenvalues will be within the required region, there is an area of this region in which they will not be placed, indicated by the shading.

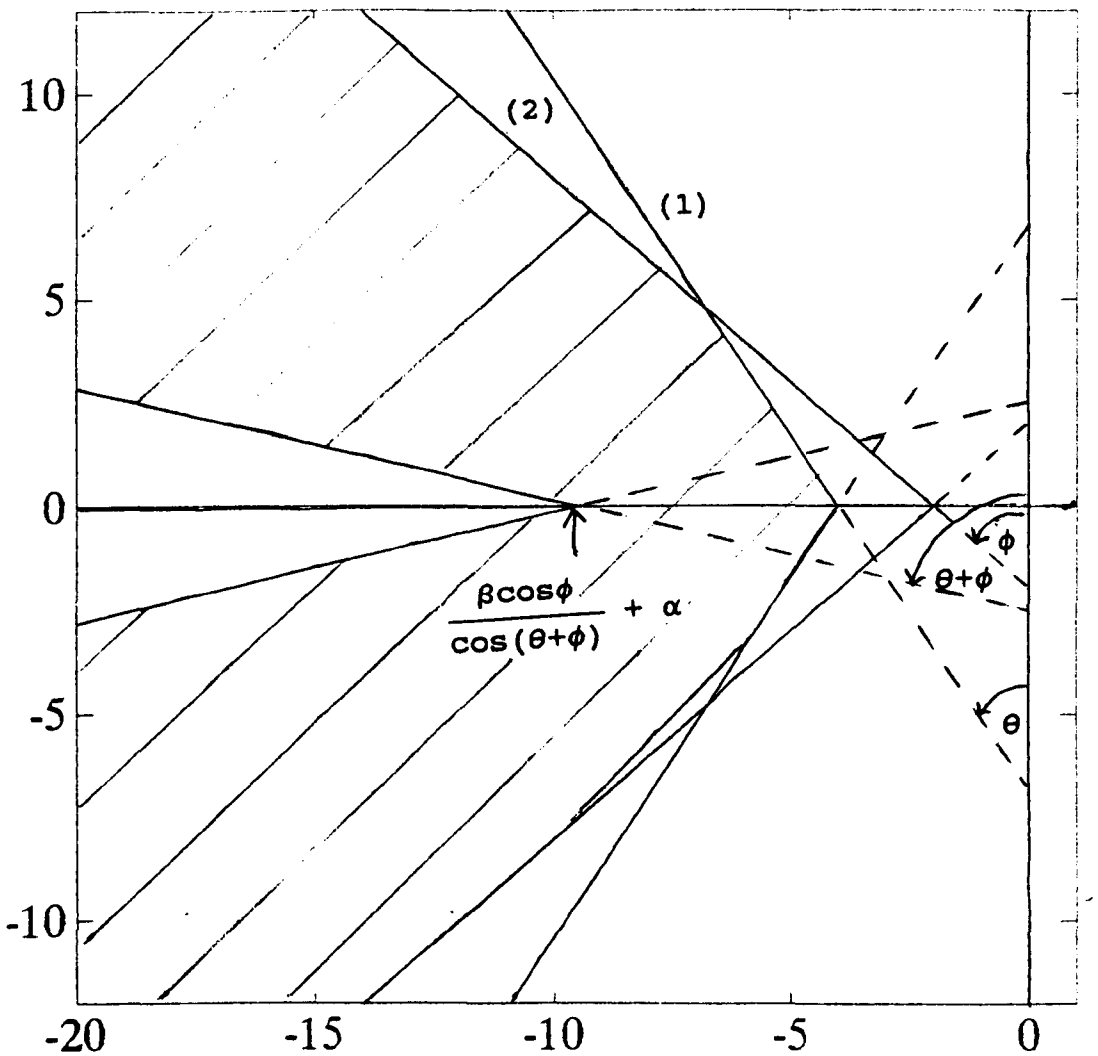

Fig 4.3 Sector within the required region

However, this method gives eigenvalues in a subregion of the required region, and so may be useful. The conditions for the eigenvalues of the closed-loop system A + BF to lie within the region are required. Consider the state feedback u = Fx and equation (4.3.17). We will now show that the eigenvalues of A + BF will lie in the required region if there exists a positive definite solution P to equation (4.3.17)

Consider a continuous matrix Riccati equation of the form

$$e^{j\phi}\left(e^{-j\theta}(A-\alpha I)-\beta I\right)^{*}P + e^{-j\phi}P\left(e^{-j\theta}(A-\alpha I)-\beta I\right) - e^{-j\phi}e^{-j\theta}PB\tilde{R}^{-1}B^{T}P = -\tilde{Q} \qquad (4.3.23)$$

Let $F = -\tilde{R}^{-1}B^{T}P$, where $\tilde{R}$ is an m×m positive definite symmetric weighting matrix, and substitute for F in equation (4.3.23) to give

$$e^{j\phi}\left(e^{-j\theta}(A-\alpha I)-\beta I\right)^{*}P + e^{-j\phi}P\left(e^{-j\theta}(A-\alpha I)-\beta I\right) + e^{-j\phi}e^{-j\theta}PBF = -\tilde{Q} \qquad (4.3.24)$$

Expanding equation (4.3.24) gives

$$e^{j\phi}e^{j\theta}A^{*}P-e^{j\phi}e^{j\theta}\alpha P-e^{j\phi}\beta P + e^{-j\phi}e^{-j\theta}P(A + BF) - e^{-j\phi}e^{-j\theta}\alpha P - e^{-j\phi}\beta P = -\tilde{Q} \qquad (4.3.25)$$

Rearranging equation (4.3.25) gives

$$e^{j\phi}e^{j\theta}A^{*}P + e^{-j\phi}e^{-j\theta}P(A + BF) - P\left(\alpha(e^{-j\phi}e^{-j\theta} + e^{j\phi}e^{j\theta}) + \beta(e^{-j\phi} + e^{j\phi})\right) = -\tilde{Q} \qquad (4.3.26)$$

Now $e^{-j\phi} + e^{j\phi} = 2\cos\phi$ and $e^{j\phi}e^{j\theta} + e^{-j\phi}e^{-j\theta} = 2\cos(\theta+\phi)$, so substituting for these expressions in equation (4.3.26) gives

$$e^{j\phi}e^{j\theta}A^{*}P + e^{-j\phi}e^{-j\theta}P(A+BF) - 2P\left[\alpha\cos(\theta+\phi)+\beta\cos\phi\right] \qquad (4.3.27)$$

Comparing equation (4.3.17) and equation (4.3.27), it is clear that we must add $e^{j\phi}e^{j\theta}(BF)^{*}P$ to both sides of equation (4.3.27) to obtain the left-hand side of equation (4.3.17). So equation (4.3.27) becomes

$$e^{j\phi}e^{j\theta}(A + BF)^{*}P + e^{-j\phi}e^{-j\theta}P(A + BF) - 2P\left[\alpha\cos(\theta + \phi) + \beta\cos\phi\right] = -\tilde{Q} + e^{j\phi}e^{j\theta}(BF)^{*}P \qquad (4.3.28)$$

Now $(BF)^{*}P = F^{T}B^{T}P = -F^{T}\tilde{R}F$ (since F and B are real), so substituting for $(BF)^{*}P$ in equation (4.3.28) gives

$$e^{j\phi}e^{j\theta}(A + BF)^{*}P + e^{-j\phi}e^{-j\theta}P(A + BF) - 2P\left[\alpha\cos(\theta + \phi) + \beta\cos\phi\right] = -\tilde{Q} - e^{j\phi}e^{j\theta}F^{T}\tilde{R}F \qquad (4.3.29)$$

Since $\tilde{Q}$ and $\tilde{R}$ are arbitrary positive definite symmetric matrices, we can choose positive definite symmetric matrices Q and R such that

$$Q = \tilde{Q} + e^{j\phi}e^{j\theta}F^{T}\tilde{R}F \qquad \text{and} \qquad R = e^{j\phi}e^{j\theta}\tilde{R}$$

Then equation (4.3.29) may be written

$$e^{j\phi}e^{j\theta}(A+BF)^{*}P+e^{-j\phi}e^{-j\theta}P(A+BF)-2P\left[\alpha\cos(\theta+\phi)+\beta\cos\phi\right]=-Q \qquad (4.3.30)$$

Clearly, equation (4.3.30) and equation (4.3.17) are identical, and so the eigenvalues of (A + BF) will lie in the required region if there exists a positive definite Hermitian solution P to equation (4.3.30) satisfying

$$e^{j\phi}\left[e^{-j\theta}(A-\alpha I)-\beta I\right]^{*}P + e^{-j\phi}P\left[e^{-j\theta}(A-\alpha I)-\beta I\right] - PBR^{-1}B^{T}P = -Q \qquad (4.3.31)$$

where $F = -R^{-1}B^{T}P$.

Again, the solution matrix P of equation (4.3.31) will be Hermitian, and so the control matrix will again be defined to be

$$F = R^{-1}B^{T}\hat{P} \qquad (4.3.32)$$

where $\hat{P}$ is again defined as

$$\hat{P}_{ij} = \sqrt{\left(P_{ij}\bar{P}_{ij}\right)} \qquad (4.3.33)$$

So, if there exists a Hermitian positive definite solution P to equation (4.3.31), and if the control matrix is defined by equation (4.3.32), then all the closed-loop eigenvalues of the system will lie in the required region.

For the sliding mode design, we require the (n-m) left-hand half-plane closed-loop eigenvalues of the reduced order equivalent system $(A_{11}-A_{12}F)$ to lie within the specified region. The control matrix will have the opposite sign to that for the system (A+BF).

The matrix Riccati equation to be solved is therefore

$$e^{j\phi}\left[e^{-j\theta}(A_{11}-\alpha I)-\beta I\right]^{*}P + e^{-j\phi}P\left[e^{-j\theta}(A_{11}-\alpha I)-\beta I\right] - PA_{12}R^{-1}A_{12}^{T}P = -Q \qquad (4.3.34)$$

and the control matrix, F, is given by

$$F = R^{-1}A_{12}^{T}\hat{P}$$

where $\hat{P}$ is as defined in equation (4.3.33).

The control matrix has the opposite sign to that for the system A + BF, since the reduced order equivalent system now being considered is of the form A - BF, as explained earlier.

The closed-loop eigenvalues of the reduced order equivalent system $A_{11} - A_{12}F$ will then lie in the required region. The sliding hyperplane matrix, C, is obtained in the same as in the previous section, and is given by

$$C = \left[F \quad I_m\right]T$$

where T is the transformation matrix defined in Chapter 2.

The effectiveness of this method will be illustrated with a numerical example in section 4.4.

4.4 Numerical Examples

As a first example, consider the five state system defined in Chapter 3, Section 3.4. The matrices for the reduced state system were obtained in that chapter, and are as follows

$$A_{11} = 0.25\begin{bmatrix} -4 & 2\sqrt{2} & 2\sqrt{2} \\ 0 & -5+\sqrt{2} & -3-\sqrt{2} \\ 0 & -3+\sqrt{2} & -5-\sqrt{2} \end{bmatrix} \qquad A_{12} = 0.25\begin{bmatrix} 0 & 0 \\ -2 & 2+\sqrt{2} \\ 2 & 2-\sqrt{2} \end{bmatrix}$$

Choose $\theta = 30^\circ$ and $\alpha = -2$. The Hermitian positive definite solution of the continuous matrix Riccati equation is

$$P = \begin{bmatrix} 13.5643 & 4.1713-1.5824j & 6.6808-0.9462j \\ 4.1713+1.5824j & 3.8012 & 1.0911+0.5761j \\ 6.6808+0.9462j & 1.0911-0.5761j & 7.1139 \end{bmatrix}$$

So the control matrix, $F = R^{-1}A_{12}^T\hat{P}$, is

$$F = \begin{bmatrix} -1.1431 & -1.2873 & -2.940 \\ -4.7961 & -3.4252 & -2.095 \end{bmatrix}$$

and the closed-loop eigenvalues of $(A_{11} - A_{12}F)$ are -2.4934 and $-3.1744 \pm 0.2119j$.

After transforming back to the full state space we get

$$C = \begin{bmatrix} -1.4131 & -1.1712 & 2.1119 & -2.1119 & -1 \\ -4.7962 & -3.9034 & -1.3722 & -0.0420 & 0 \end{bmatrix}$$

For the second example, consider the robot arm discussed in Chapter 2. The matrices for the reduced order (n - m) system were obtained in Chapter 3, section 3.4 and are as follows

$$A_{11} = \begin{bmatrix} 0 & 0 \\ 0 & 0 \end{bmatrix} \qquad A_{12} = \begin{bmatrix} -0.3906 & -0.9206 \\ 0.9026 & -0.3906 \end{bmatrix}$$

Choose $\theta = 30^{\circ}$ and $\alpha = -2$. The Hermitian positive definite solution of the continuous matrix Riccati equation is

$$P = \begin{bmatrix} 3.7321 & 0 \\ 0 & 3.7321 \end{bmatrix}$$

So the control matrix $F = R^{-1}A_{12}^{T}\hat{P}$ is

$$F = \begin{bmatrix} 1.4578 & -3.4356 \\ 3.4356 & 1.4578 \end{bmatrix}$$

and the closed-loop eigenvalues of $(A_{11} - A_{12}F)$ are -3.7231 and -3.7231. After transforming back to the full system, the sliding hyperplane matrix, C, is found to be

$$C = \begin{bmatrix} -1.4578 & -0.3906 & 3.4356 & 0.9206 \\ -3.4356 & -0.9206 & -1.4578 & -0.3906 \end{bmatrix}$$

Consider the method for placing the closed-loop eigenvalues in a region bounded by the intersection of two sectors, which has been outlined in section 4.3.

Choosing $\alpha = -4$, $\theta = 30^{\circ}$, $\beta = -2$ and $\phi = 45^{\circ}$ results in the following Hermitian positive definite solution of the continuous matrix Riccati equation

$$P = \begin{bmatrix} 1.7726 & 0.0906-0.2557j & 0.1777-0.2531j \\ 0.0906+0.2357j & 0.0908 & 0.0600+0.0130j \\ 0.1777+0.2531j & 0.0600-0.0130j & 0.2131 \end{bmatrix}$$

The control matrix, $F = R^{-1}A_{12}^{T}\hat{P}$, with $\hat{P}$ as defined in equation (4.3.33) is given by

$$F = \begin{bmatrix} -1.9018 & 1.4720 & -7.5854 \\ -27.6827 & -8.6487 & -8.3575 \end{bmatrix}$$

and the (n-m) closed-loop eigenvalues of the reduced order equivalent system, $(A_{11}-A_{12}F)$, are -6.9475 and $-4.8436 \pm 0.0691j$, which are within the required sector. After transforming back to the full state, the sliding hyperplane matrix is found to be

$$C = \begin{bmatrix} -1.9018 & -4.3228 & 4.5287 & -4.5287 & -1 \\ -27.6827 & -12.0251 & -0.8527 & -0.5615 & 0 \end{bmatrix}$$

4.5 Effects of Alpha and Theta on the Eigenvalues

The choice of α and θ is restricted to some degree because we shall see that there are some values for which the eigenvalues do not lie in the required region. There is clearly a connection between the root locus plot of the reduced order system, and the feasible regions for the eigenvalues.

The following maximum θ values for various α values have been determined for the five state example, assuming that both R and Q are set to the identity matrix of the appropriate dimensions.

Table 4.5.1 Limiting α and θ values for the 5 state system

α	10	5	2	1	0	-0.5	-1	-2
θ°	88	87	85	83	78	72	62	60

α	-3	-4	-5	-6	-7	-8	-9	-10
θ°	47	49	50	51	52	53	53	54

α	-20	-30	-40	-50	-100	-1000	-1×10^5
θ°	56	56	57	57	58	59	59

Comparing these results with the root locus plot (Fig 4.4) for varying $\tilde{r}$ (R = $\tilde{r}$I, and Q = I), it can be seen that for α values to the right of all the root locus points, the maximum θ value can be predicted as follows :

i) draw a line through α and the locus point with the largest imaginary part.

ii) Calculate the angle between this line and the imaginary axis.

Some of these lines have been drawn in on Fig 4.4, and they show the appropriate θ values for α values of 0, -0.5, -1, -2, and -3. However, once the α value is smaller than about -1.2, in other words it is no longer to the right of all the root locus points, the maximum θ value is no longer easily predicted.

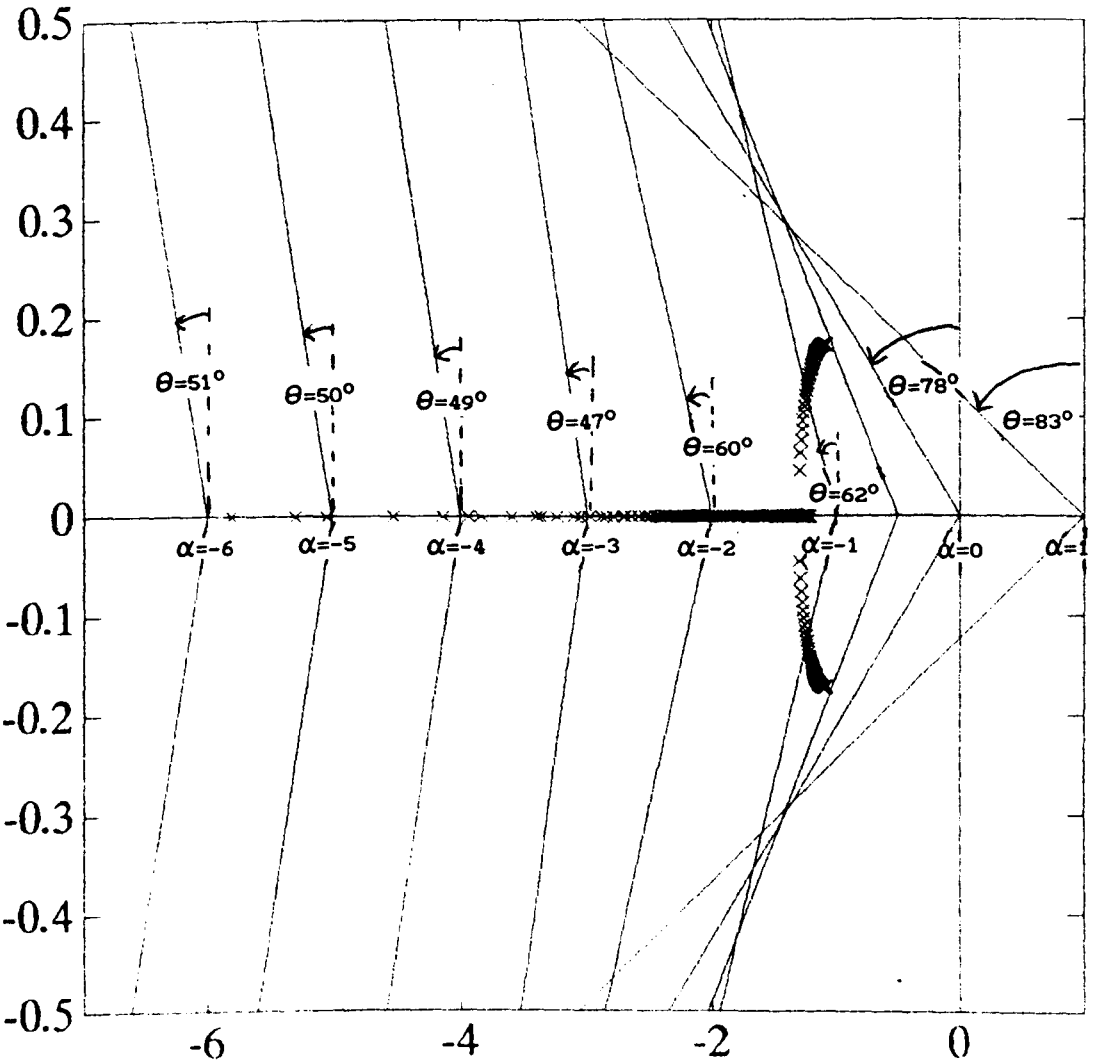

Fig 4.4 Root locus plot for the reduced order system of the five state system

If we consider the root locus plot for the full state space, we can see from Fig 4.5 that it contains more complex values than the plot for the reduced order equivalent system (Fig 4.4). The two arcs of complex values which appear in the plot for the reduced order system (Fig 4.4) are present, and there is also a third arc, which crosses the x-axis, and a ring shape. Again, some lines for various α and θ combinations have been drawn in, and despite the increased complexity of the plot, the same problem of predicting the limiting α and θ values can be seen here. Once the α value is within the ring shape, or to the left of it, there is no obvious way of predicting the limiting θ value.

It can be seen from Table 4.5.1 that the θ value reaches a limiting value of 59° for α values smaller than or equal to -1000. It can also be seen that the maximum θ value decreases as α becomes more negative, until some minimum value is reached, and then it increases again until it reaches this steady state value. There is no obvious way of predicting the *minimum* value of θ, since it occurs for a value of α which is smaller than the smallest α value for which the limits can be predicted, in other words α lies either within or to the left of the ring shape.

If the R matrix is altered from the identity matrix to some other positive definite matrix, it may be possible to place the eigenvalues in a wider range of regions. It may be possible to alter the limiting values of α and θ, and it might be possible to predict these new limits, and this will be discussed in Chapter 6.

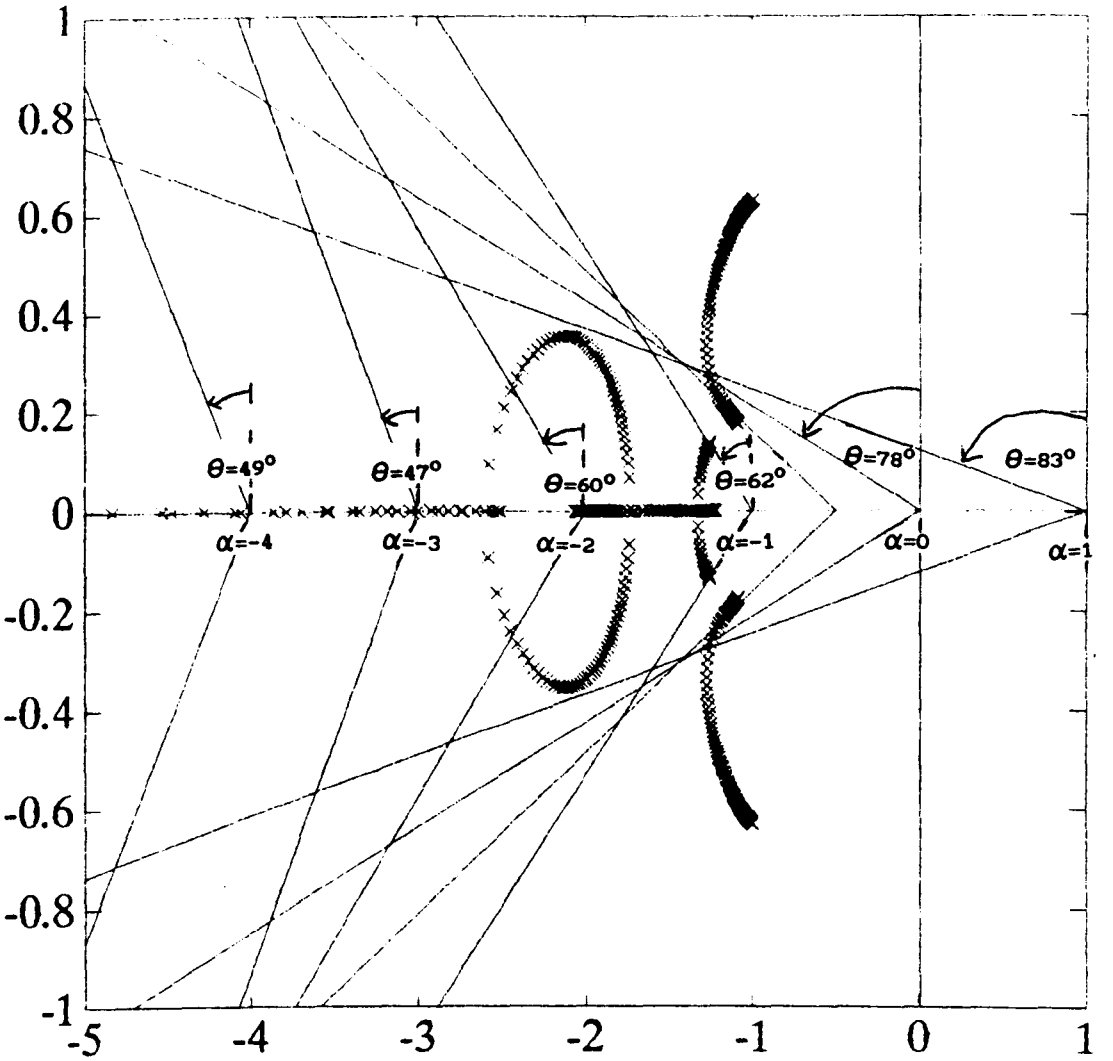

Fig 4.5 Root locus plot for the full five state system

Let us now investigate the limiting values of α and θ for the robot arm discussed in Chapter 2.

Table 4.5.2 Limiting α and θ values for the robot arm

α	10	5	2	1	0	-0.5	-1	-2
θ°	90	90	90	90	90	90	90	67

α	-3	-4	-5	-6	-7	-8	-9	-10
θ°	63	62	61	60	60	60	60	60

α	-20	-30	-40	-50	-100	-1000	-1×10^8
θ°	60	60	60	60	60	60	60

Consider the root locus plot for the reduced order system for the robot arm (Fig 4.6). In this case, all the eigenvalues are real, so it will be more difficult to predict the limiting α and θ values for this example. From the results in Table 4.5.2 it can be seen that for α values ≥ -1 there is no bound on the θ value, apart from the initial restriction that $\theta \leq 90^\circ$. From the root locus plot (Fig 4.6), it can be seen that the largest eigenvalue is -1. Between $\alpha = -2$ and $\alpha = -6$, the θ limit drops to 60° and remains there for all α values < -6. A root locus plot of the full system, Fig 4.7, also has only real eigenvalues.

If the R matrix is altered from the identity matrix to some other positive definite matrix, it may be possible to place the closed-loop eigenvalues of the system in a wider range of sectors. It may then be possible to predict the limiting θ values in some way, and this will be investigated in Chapter 6.

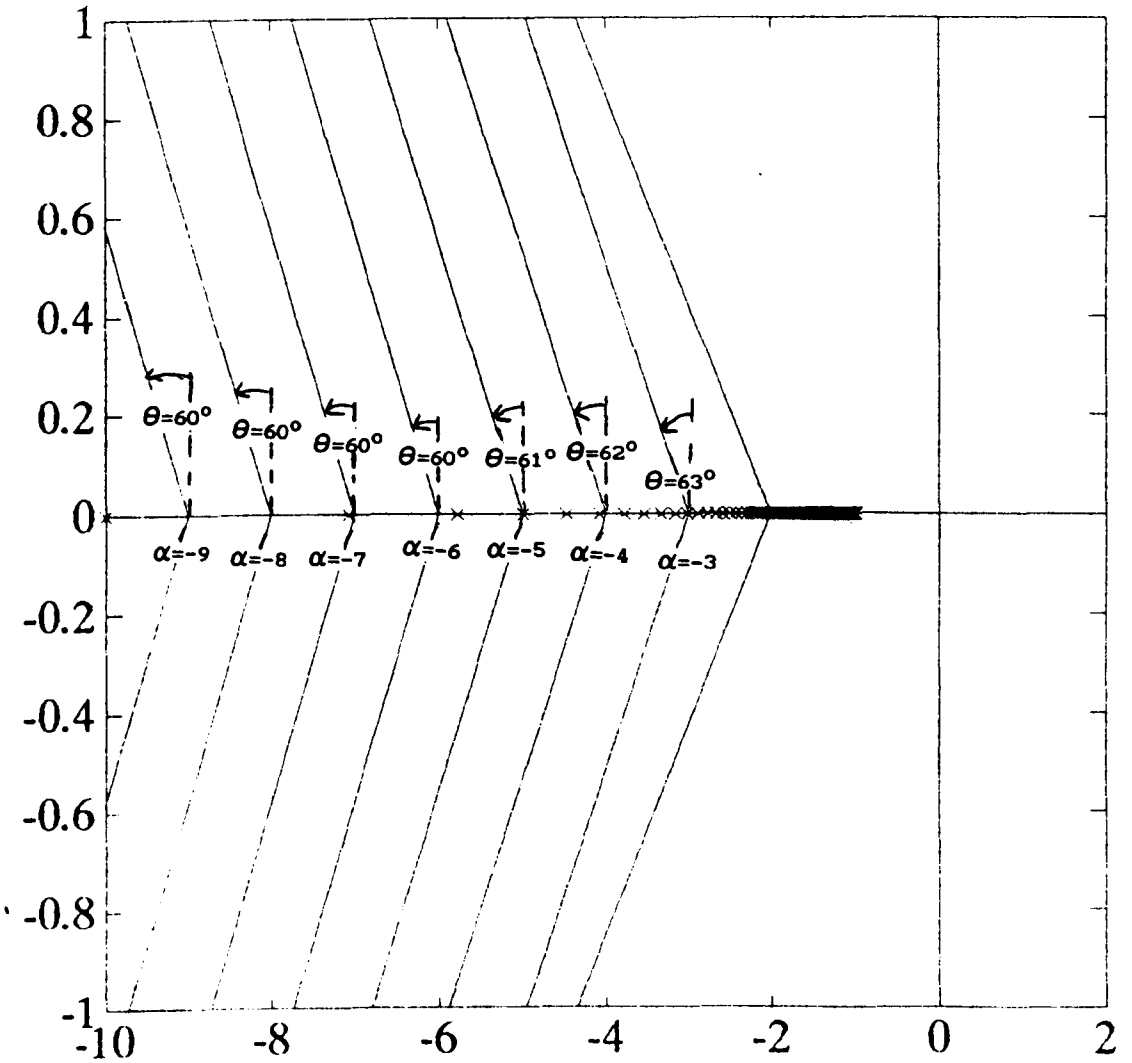

Fig 4.6 Root locus plot for the reduced order system of the robot arm

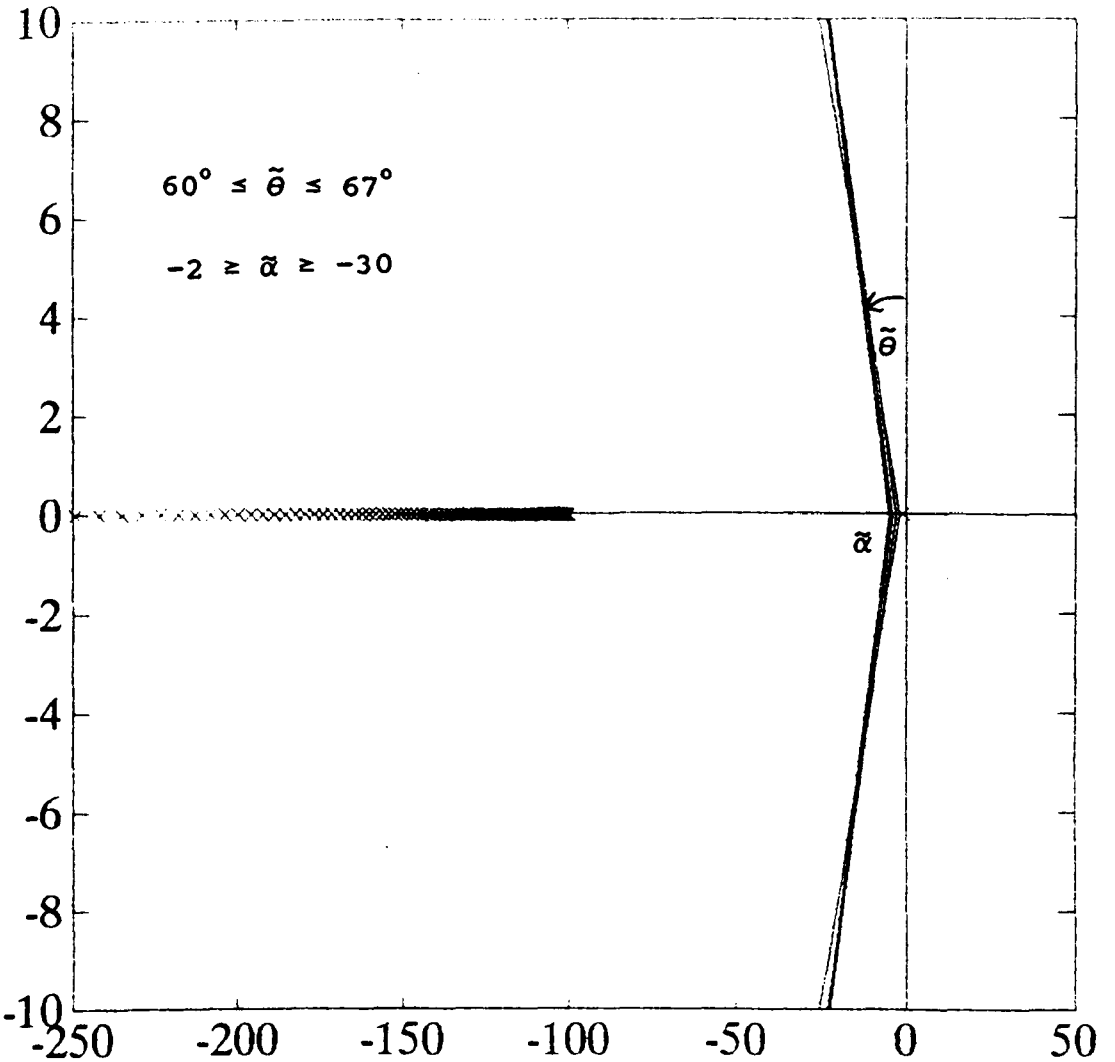

Fig 4.7 Root locus plot for the full Robot arm system

4.6 Discussion

It has been shown that it is possible to place the closed-loop eigenvalues of a system of the form $\dot{x} = Ax + Bu$ in a sector bounded by a straight line at an angle θ to the imaginary axis, crossing the real axis at α, and its reflection in the real axis. It is also possible to place the eigenvalues of the reduced order equivalent system in this sector, and hence it is appropriate to use this method to choose the sliding hyperplanes of a Variable Structure Control System. The specification of a region of the left-hand half-plane in this way is more flexible than the region specifications discussed in Chapter 3, since this sector stretches to negative infinity at its left-hand end. It is also clear that it is much easier to specify a region in this manner than to have to select exact eigenvalues in the left-hand half-plane. The method is straightforward to use, and the choice of a real control matrix, obtained from the complex Hermitian P matrix gives satisfactory results for the numerical examples considered here.

This method has also successfully been extended to give a solution to the problem of placing the closed-loop eigenvalues in a region bounded by two intersecting sectors (Fig 4.3). There is, however, a part of the chosen region in which the eigenvalues will not be placed, the shaded region in Fig 4.3, but they will be within the required region. Again, this technique can be extended to assign the sliding hyperplanes of a Variable Structure Control System.

The limiting values of α and θ have been considered for the region bounded by a single sector, and it can be seen that there is a maximum θ value of ~ 60° for both examples, when α is smaller than a certain value. From the numerical results presented in Section 4.5, for two very different systems, it would appear that the following conclusions can be suggested :

1) If the root locus plot is purely real and α is greater than the largest root locus value then there is no restriction on θ apart from the 90° restriction imposed initially.
2) If the root locus has complex values and α is greater than the real part of the the largest complex pair, then the limiting θ value may be obtained from the root locus plot by calculating the angle between the imaginary axis and the line joining the real axis crossing point, α, and the largest complex eigenvalue.
3) When α is smaller than the majority of the root locus values, the θ value will be approximately 60°.

There is a range of values of α which will fall between conclusions 2 and 3, and for which it is not obvious how to predict the limiting θ value. However, it is useful to be able to predict the limiting θ values for most of the range of α values, and the problem for the values for which θ can not easily be predicted, may be surmounted by selecting smaller θ values.

5. DEPENDENCE OF EIGENVALUE POSITION ON THE R MATRIX DESIGN

5.1 Introduction

The dependence of the solution of a general matrix Riccati equation, continuous or discrete, on the design of the arbitrary matrix R is a property which can possibly be used to position the closed-loop eigenvalues of a system within a chosen region. It would clearly be useful to be able to position the closed-loop eigenvalues of a Variable Structure Control System within the chosen region and to predict which, if any, of them will be complex. It could also be useful to control the scatter of the eigenvalues within the chosen region. Some work has been done on choosing the weighting matrices of the Riccati equation (Harvey & Stein, 1978), Work has also been done on the eigenvalue bounds of the solutions of both the Riccati and Lyapunov equation (Karanam, 1982, Kwon, Youn & Bien, 1985, Komaroff, 1988). The robustness of eigenvalue assignment techniques for non-VSC controllers has also been considered (Burrows & Patton, 1990, a & b).

In section 5.2 the dependence of the solution of the discrete matrix Riccati equation, used in section 3.2 to place the closed-loop eigenvalues of a VSC system in a specified disc, on the design of the arbitrary R matrix, and in the disc size is considered. Section 5.3 contains a similar investigation for the continuous matrix Riccati equation used in section 3.3 to place the closed-loop eigenvalues of a VSC system in a vertical strip. Section 5.4 contains a discussion of the results.

5.2 Design of R for Eigenvalue Positioning within a Disc

Some work on eigenvalue positioning within the disc has been carried out by Furuta and Kim (1987), and this will be briefly considered here. This analysis depends on the eigenvalues of the product B^TPB, which are not easy to predict, and so a further investigation of predicting eigenvalue positioning without using these eigenvalues will also be carried out.

If R is chosen to be diag$\{r_1, r_2, .., r_m\}$ and the linear control has each channel multiplied by a gain $\mathcal{K}$, then it may be written $u = \mathcal{K}Fx$ where $\mathcal{K} = \text{diag}\{k_1\ k_2, \ldots, k_m\}$. The bounds on this gain, $\hat{g}_{min,i}$ and $\hat{g}_{max,i}$ satisfy

$$\hat{g}_{min,i} = \frac{1}{1+a_i} < k_i < \frac{1}{1-a_i} = \hat{g}_{max,i} \qquad i = 1,2,\ldots,m \tag{5.2.1}$$

where

$$a_i = \sqrt{\frac{r^2 r_i}{(r^2 r_i + \lambda_{max})}} \tag{5.2.2}$$

$$\lambda_{max} = \text{Max}\left[\lambda_i (A_{12}^T P A_{12})\right] \tag{5.2.3}$$

where A_{12} is the appropriate part of the partitioned matrix TAT^T (see Section 2.2), λ_i, $i = 1,..,n-m$ are the eigenvalues of $A_{12}^T P A_{12}$ and r is the radius of the disc (Furuta and Kim, 1987).

It can be seen that a_i approaches zero as $r \to 0$, unless $\lambda_{max}=0$, so the difference between the gain bounds, g_D, decreases. This will result in all the eigenvalues of the closed-loop system being assigned to the same point (Furuta & Kim, 1987).

To investigate the difference between the gain bounds for various discs, let us consider again the five state system described in Chapter 3. Choosing α to be -6 + 0j and allowing r, the radius of the disc, to vary, gives the following values of the minimum and maximum gains, equation (5.2.1), the maximum eigenvalue of $A_{12}^T P A_{12}$, λ_m, equation (5.2.3), and $g_D = \hat{g}_{max,i} - \hat{g}_{min,i}$.

Table 5.2.1 Parameter values for α = -6+0j and varying r

r	$\hat{g}_{min,i}$	$\hat{g}_{max,i}$	g_D	λ_m	Eigenvalues of $A_{11}-A_{12}F$
1.0	0.9568	1.0473	0.0905	4.8998×10^2	-5.7565;-5.7997;-5.823
0.5	0.9888	1.0114	0.00226	1.9604×10^3	-5.9390;-5.9499;-5.956
0.25	0.9972	1.0028	0.0056	7.8397×10^3	-5.9848;-5.9875;-5.989
0.1	0.9995	1.0005	0.0010	4.8993×10^3	-5.9976;-5.9980;-5.998

It can be seen from Table 5.2.1 that if the radius is small, then the maximum and minimum values of the gain margin, $\hat{g}_{min,i}$ and $\hat{g}_{max,i}$, both tend to 1, as would be expected, and equation (5.2.1) becomes

$$r \to 0 \qquad k_i \to 1 \tag{5.2.4}$$

If we now consider the effect of altering the R matrix, we can see that equation (5.2.2) does not lead to any conclusive results. If $r_i \to 0$, then the a_i will tend to zero, but if r_i is simply very small, the value of λ_m is not necessarily very large and hence the a_i could be quite large, as can be seen from equation (5.2.2).

Consider the same five state system, and choose a disc specified by α = -6 + 0j and r = 4. The R matrix is allowed to vary in the following way

$$R = R_{fact}I \tag{5.2.5}$$

This leads to the following values of the minimum and maximum values of the gains, $\hat{g}_{min,i}$ and $\hat{g}_{max,i}$, g_D, the closed-loop eigenvalues and λ_m for various values of R_{fact}.

Table 5.2.2 Parameter values for varying R_{fact} values

R_{fact}	$\hat{g}_{min,i}$	$\hat{g}_{max,i}$	g_D	λ_m	Eigenvalues of $A_{11}-A_{12}F$
1.0	0.7152	1.6618	0.9466	47.7516	-3.8808;-4.1879;-4.4259
$1x10^{-1}$	0.7495	1.5020	0.7525	7.1571	-4.2782±0.1649j;-4.8338
$1x10^{-2}$	0.8423	1.2304	0.3881	2.4764	-4.3125;-5.2137;-5.6482
$1x10^{-3}$	0.9356	1.0739	0.1383	1.8896	-4.3036;-5.8634;-5.9543
$1x10^{-4}$	0.9783	1.0227	0.0444	1.8251	-4.3029;-5.9851;-5.9953
$1x10^{-5}$	0.993	1.0071	0.0141	1.8186	-4.3028;-5.9985;-5.9995
$1x10^{-6}$	0.9978	1.0022	0.0044	1.8179	-4.3028;-5.9998;-6.0
$1x10^{-8}$	0.9998	1.0002	0.0004	1.8178	-4.3028;-6.0 ;-6.0

It can be seen from Table 5.2.2 that when R_{fact} is $1x10^{-6}$, g_D is $4.4x10^{-3}$, compared with a value of $1x10^{-3}$ for a disc of radius of 0.1, with R_{fact} equal to 1. Clearly then, the R matrix has to be about 10^5 times smaller than its *nominal* value, I_{n-m}, to have the same effect as decreasing the radius by an order of 2, and this would appear to be due to the effect of λ_m, the largest eigenvalue of $A_{12}^T P A_{12}$. When R_{fact} = 1 and r = 3, it can be seen from Table 5.2.2 that λ_m = 47.7516, and it can be seen from Table

5.2.1 that decreasing the radius from 3 to 0.5 gives an increase in λ_m of 1.9126×10^3. If R_{fact} is decreased from 1 to 1×10^{-8}, it can be seen from Table 5.2.2 that λ_m only changes by 45.9338. A further point to note is that when R_{fact} is small, only two of the closed-loop eigenvalues are close to the centre of the disc, and the third is at a point near to the right-hand edge of the disc.

Thus, by choosing a small value for R_{fact} it is possible to have at least some of the closed-loop eigenvalues close to the centre of the disc, without having to make the radius of the disc particularly small. Since the radius of the disc is not small, the difference between the gain bounds will not be small, which can be advantageous.

Consider the effect on the closed-loop eigenvalue position of a small value for R_{fact} and various values of the radius. Choose $R_{fact} = 1\times10^{-6}$ and $\alpha = -6 + 0j$ with the R matrix defined as in equation (5.2.5).

Table 5.2.3 Eigenvalues for $R_{fact}=1\times10^{-6}$ and varying radii r

r	$\hat{g}_{min,1}$	$\hat{g}_{max,1}$	g_D	λ_m	Eigenvalues of $A_{11}-A_{12}F$
6.0	0.9941	1.0060	1.2×10^{-2}	1.0265	-1.362;-5.9994;-5.9998
5.0	0.9552	1.0048	9.6×10^{-3}	1.0771	-1.905;-5.9996;-5.9999
4.0	0.9956	1.0036	7.1×10^{-3}	1.269	-3.081;-5.9997;-5.9999
3.0	0.9978	1.0022	4.4×10^{-3}	1.8179	-4.303;-5.9998;-6.0
2.0	0.9989	1.0011	2.2×10^{-3}	3.5635	-5.236;-5.9999;-6.0
1.0	0.9997	1.0003	6.0×10^{-4}	13.2804	-5.808;-6.0 ;-6.0
0.5	0.9999	1.0001	2.0×10^{-4}	52.2742	-5.952;-6.0 ;-6.0
0.1	1.0	1.0	0.0	1.3×10^3	-5.998;-6.0 ;-6.0

From the results in Table 5.2.3 it can be seen that if R_{fact} is small, decreasing the magnitude of the radius moves the *off* eigenvalue nearer to the centre of the disc. However, the radius still has to be about the same magnitude for the eigenvalues to be close to the centre whether R_{fact} is 1×10^{-6} or 1.0, so it is clear that the effect of the radius on the closed-loop eigenvalues is the dominant effect.

It is clear from these investigations that when R_{fact} is very small, λ_m is small when r is large, and increases as r decreases. Hence, from the theory outlined earlier, the expression for a_i when R_{fact} is small and the radius of the disc, r, is greater than 1, from equation (5.2.2), is

$$a_i \rightarrow \sqrt{\frac{1}{1 + \frac{1}{r_i}}} \rightarrow 0$$

and so $\hat{g}_{min,i}$ and $\hat{g}_{max,i}$ become

$$\hat{g}_{min,i} \rightarrow 1 \quad \text{and} \quad \hat{g}_{max,i} \rightarrow 1$$

and it can be seen that the difference between the gain bounds, g_D, will tend to zero. The value of λ_m counteracts the effect of a change in the radius to some degree, and this effect is difficult to predict. If the radius of the disc is equal to 1, λ_m is of the order of 10, for small R_{fact}, and the expression for the a_i will once again tend to 1. This is again due to the effect of λ_m, which dominates the expression for a_i when r = 1 and R_{fact} is small. Again, $\hat{g}_{min,i}$ and $\hat{g}_{max,i}$ will tend to 1, and hence $g_D \rightarrow 0$.

If the radius is smaller than 1, then λ_m is of the order of 10^3. If R_{fact} is much larger than r^{-2}, $r^2\bar{r}_i$ will be small, and so the expression for the a_i becomes

$$a_i \rightarrow \sqrt{\frac{0}{\lambda_m}} = 0 \quad \forall \lambda_m$$

In this case, the minimum and maximum gain values will again both be 1, and so the difference in the gain bounds will be zero. Hence, the system is again at the critical point with regard to its stability. It would appear therefore, that the effect of λ_m can lead to critical stability for various combinations of the radius r and the R matrix elements r_i. However, it is not straightforward to predict the size of λ_m from r and r_i.

The effect on the closed-loop eigenvalues of the arbitrary R matrix is harder to predict, partly since the effect of the radius is dominant and partly because it is difficult to predict the effect of R on the solution of the discrete matrix Riccati equation, equation (3.2.8). However, from the results presented so far, it can be seen that it is particular values of R_{fact} which result in complex eigenvalues, rather than particular values of the radius.

It would be useful to be able to choose the R matrix so as to predict the closed-loop eigenvalue positions for a disc with a radius greater than 1 (say).

Consider the same five state system, with $\alpha = -6 + 0j$ and $r = 4$, and vary R_{fact}, with R calculated as outlined in equation (5.2.5).

Table 5.2.4 Eigenvalues for α=-6, r=4 & varying R_{fact}

R_{fact}	det(R)	Eigenvalues of $A_{11}-A_{12}F$
$1x10^{-8}$	$1x10^{-16}$	-3.0806;-6.0 ;-6.0
$1x10^{-7}$	$1x10^{-14}$	-3.0806;-6.0 ;-6.0
$1x10^{-6}$	$1x10^{-12}$	-3.0806;-5.9997;-5.9999
$1x10^{-5}$	$1x10^{-10}$	-3.0807;-5.9973;-5.9992
$1x10^{-4}$	$1x10^{-8}$	-3.0807;-5.9736;-5.9916
$1x10^{-3}$	$1x10^{-6}$	-3.0817;-5.7627;-5.9194
$1x10^{-2}$	$1x10^{-4}$	-3.0925;-4.7351;-5.4004
$5x10^{-2}$	$2.5x10^{-3}$	-3.1792;-3.5853;-4.4849
$8x10^{-2}$	$6.4x10^{-3}$	-3.2467±0.1852j;-4.1920
0.1	$1x10^{-2}$	-3.1875±0.2383j;-4.06
0.2	$4x10^{-2}$	-3.0243±0.2954j;-3.7012
0.5	0.25	-2.8483±0.2685j;-3.37
1.0	1.0	-2.7404±0.2008j;-3.2425
2.0	4.0	-2.6533±0.0570j;-3.1681
3.0	9.0	-2.4773;-2.7458;-3.1425
5.0	25.0	-2.3608;-2.7746;-3.1219
10.0	$1x10^{2}$	-2.2537;-2.7890;-3.1064
$1x10^{2}$	$1x10^{4}$	-2.0809;-2.7990;-3.0925
$1x10^{3}$	$1x10^{6}$	-2.0257;-2.7999;-3.0911
$1x10^{4}$	$1x10^{8}$	-2.0082;-2.8 ;-3.0909
$1x10^{8}$	$1x10^{16}$	-2.0 ;-2.8 ;-3.0909

It can be seen from the results in Table 5.2.4 that as R_{fact} is increased, the closed-loop eigenvalues tend to the limiting values -2, -2.8 & -3.0909, and as R_{fact} is decreased the closed-loop eigenvalues tend to the limiting values of -3.0807, -6 & -6. When R_{fact} is large, one of the eigenvalues is on the right-hand

edge of the disc (which is at -2 in this case), the second eigenvalue is close to the right-hand edge of the disc and the third eigenvalue is about a third of the way between this edge and the centre of the disc, but nearer to the edge. When R_{fact} is small, the position of this third eigenvalue is almost unchanged, but the other two eigenvalues which were on, or near to, the edge of the disc move onto the centre of the disc. It appears, therefore, that the closed-loop eigenvalues are never assigned to the semi-circular region to the left of the disc centre, so in fact they are being assigned to a vertical semi-circle of centre α and radius r.

When R_{fact} lies between the values which position the closed-loop eigenvalues on one or other set of limiting values, the pair of eigenvalues which move within the bounds of the disc take a range of values, both real and complex. It would be helpful if the R_{fact} values associated with the real set of eigenvalues could be picked out from those associated with the complex set of eigenvalues.

For this particular system, complex conjugate pairs of eigenvalues occur for values of R_{fact} between about 2 and 0.08, and the corresponding determinants of the R matrix are between 4 and 0.0064.

It is possible that the determinant of the R matrix could be used to help to predict the closed-loop eigenvalue positions, perhaps in conjunction with the disc radius.

Some results of an initial investigation into the effect of

the determinant of R on the solution are contained in Table 5.2.5. The disc has α = -6 +0j and r = 4, and det(R) is chosen to be 1.

Table 5.2.5 Eigenvalue variations for det(R) = 1

R matrix	Eigenvalues of A_{11}-$A_{12}F$
$\begin{bmatrix} 1 & 0 \\ 0 & 1 \end{bmatrix}$	-2.7404±0.2008j;-3.2425
$\begin{bmatrix} 2 & 1 \\ 1 & 1 \end{bmatrix}$	-2.5267;-2.8282;-3.4568
$\begin{bmatrix} 2 & 0 \\ 0 & 0.5 \end{bmatrix}$	-2.7903±0.1629j;-3.2859
$\begin{bmatrix} 4 & 1 \\ 1 & 0.5 \end{bmatrix}$	-2.6422;-2.8615;-3.5872
$\begin{bmatrix} 4 & 0 \\ 0 & 0.25 \end{bmatrix}$	-2.8346±0.1095j;-3.4606
$\begin{bmatrix} 10 & 0 \\ 0 & 0.1 \end{bmatrix}$	-2.8579±0.0358j;-3.9086
$\begin{bmatrix} 10 & 0.1 \\ 0.1 & 0.101 \end{bmatrix}$	-2.8540±0.0252j;-3.9144
$\begin{bmatrix} 10 & 0.316 \\ 0.316 & 0.11 \end{bmatrix}$	-2.8171;-2.8743;-3.927
$\begin{bmatrix} 12 & 0 \\ 0 & 0.0833 \end{bmatrix}$	-2.8599±0.0139j;-4.0181
$\begin{bmatrix} 12.4 & 0 \\ 0 & 0.081 \end{bmatrix}$	-2.2602±0.0047j;-4.0383
$\begin{bmatrix} 12.5 & 0 \\ 0 & 0.08 \end{bmatrix}$	-2.8559;-2.8647;-4.432
$\begin{bmatrix} 20 & 0 \\ 0 & 0.5 \end{bmatrix}$	-2.8203;-2.9066;-4.3441
$\begin{bmatrix} 50 & 0 \\ 0 & 0.02 \end{bmatrix}$	-2.8066;-2.9259;-4.9346
$\begin{bmatrix} 100 & 0 \\ 0 & 0.01 \end{bmatrix}$	-2.8031;-2.9310;-5.3148

From the results in Table 5.2.5 it can be seen that if R(1,1) ≤ 12, and if the off-diagonal elements are smaller than all of the diagonal elements, then the closed-loop eigenvalues comprise a complex conjugate pair and a real value. As R(1,1) is increased, the real eigenvalue moves towards the centre of the disc, and the complex conjugate pair move closer to the real axis. When R(1,1) > 12, or if the off-diagonal elements are bigger than the diagonal elements, then all the eigenvalues are real.

Consider the same example as that used for Table 5.2.5, but choose the determinant of the R matrix to be 5.

Table 5.2.6 Eigenvalue variations for det(R) = 5

R matrix	Eigenvalues of $A_{11} - A_{12}F$
$\begin{bmatrix} 5 & 0 \\ 0 & 1 \end{bmatrix}$	-2.7±0.0424j;-3.1771
$\begin{bmatrix} 4.5 & 0 \\ 0 & 1.11 \end{bmatrix}$	-2.690±0.0297j;-3.1715
$\begin{bmatrix} 4 & 0 \\ 0 & 1.25 \end{bmatrix}$	-2.6686;-2.6916;-3.1666
$\begin{bmatrix} 4 & \sqrt{3} \\ \sqrt{3} & 2 \end{bmatrix}$	-2.4123;-2.8208;-3.2357
$\begin{bmatrix} 2.5 & 0 \\ 0 & 2 \end{bmatrix}$	-2.5945;-2.6992;-3.1593
$\begin{bmatrix} 7 & 3 \\ 3 & 2 \end{bmatrix}$	-2.4278;-2.8531;-3.3225
$\begin{bmatrix} 9 & 2 \\ 2 & 1 \end{bmatrix}$	-2.5537;-2.8489;-3.3125
$\begin{bmatrix} 10 & 0 \\ 0 & 0.5 \end{bmatrix}$	-2.7685±0.0711j;-3.2567
$\begin{bmatrix} 20 & 0 \\ 0 & 0.25 \end{bmatrix}$	-2.8211±0.0481j;-3.4525

It can be seen from Table 5.2.6, that the results for det(R) = 5 are not conclusive. When R(1,1) ≥ 4.5 and the off diagonal elements are smaller than all of the diagonal elements, then the eigenvalues comprise a complex conjugate pair and a real value. If R(1,1) < 4.5 or if the off diagonal elements are larger than any one of the diagonal elements, the eigenvalues are all real. In this case, two of the eigenvalues are close together and near to the right-hand edge of the disc, and the other one is nearer to the centre of the disc.

It is clear that there is some connection between the determinant and form of the arbitrary R matrix, the position of the eigenvalues within the disc, and the radius and centre of the disc. A series of runs has been carried out for three different discs, and R matrices with determinants of 0.1, 0.5, 1 and 10. The eigenvalues have been plotted in each case and the results are shown in the following figures

Fig 5.1 $r = 4$, $\alpha = -6 + 0j$

Fig 5.2 $r = 4$, $\alpha = -5 + 0j$

Fig 5.3 $r = 4$, $\alpha = -4 + 0j$.

It can be seen from the results for $r = 4$ and $\alpha = -6 + 0j$ (Fig 5.1) that as the determinant of R increases from 0.1 to 10, the complex conjugate pairs of eigenvalues approach the real axis, until, when det(R) = 10, all the eigenvalues are real, and in three clusters. These three clusters are close to the limiting eigenvalues for large values of R_{fact} and det(R).

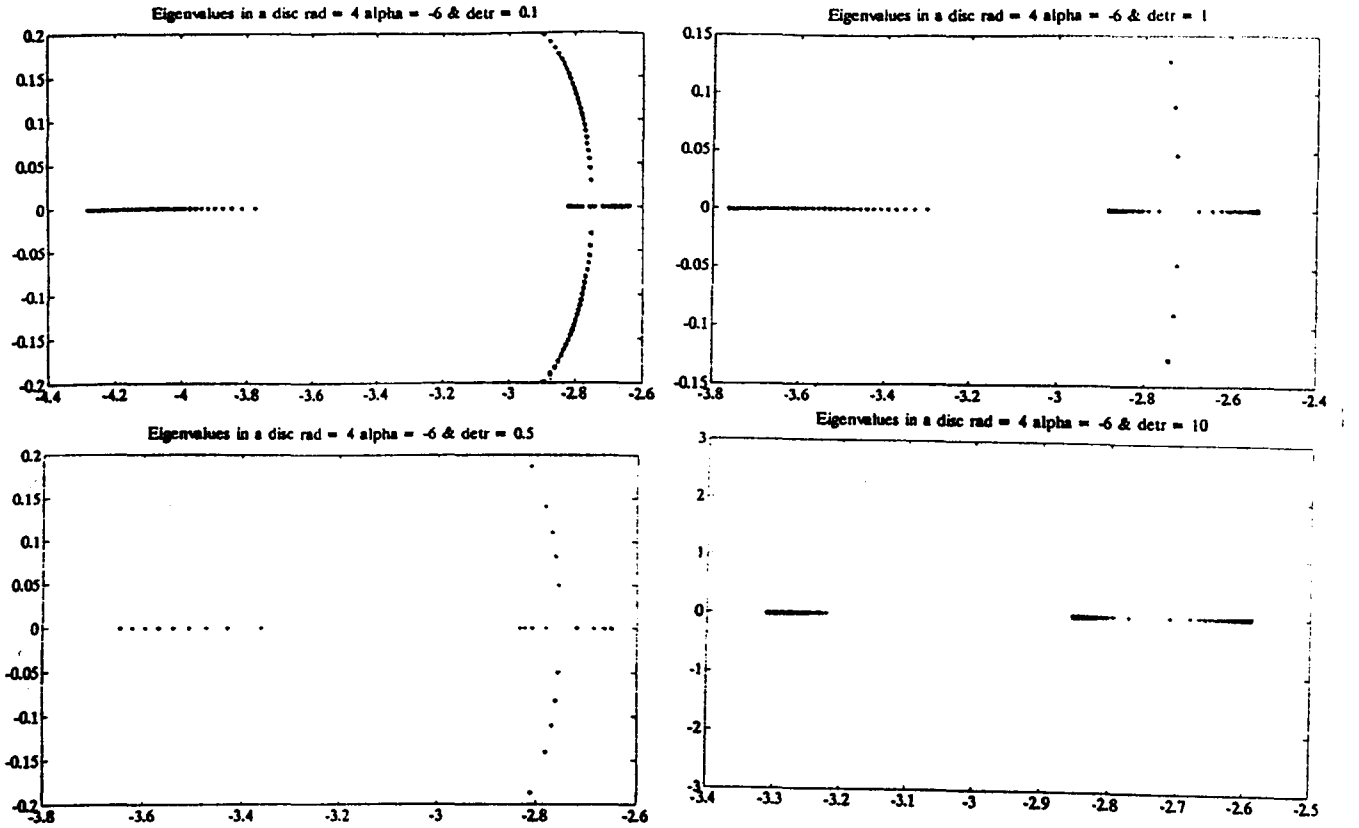

Fig 5.1 Eigenvalue plots for r = 4 and α = -6 + 0j

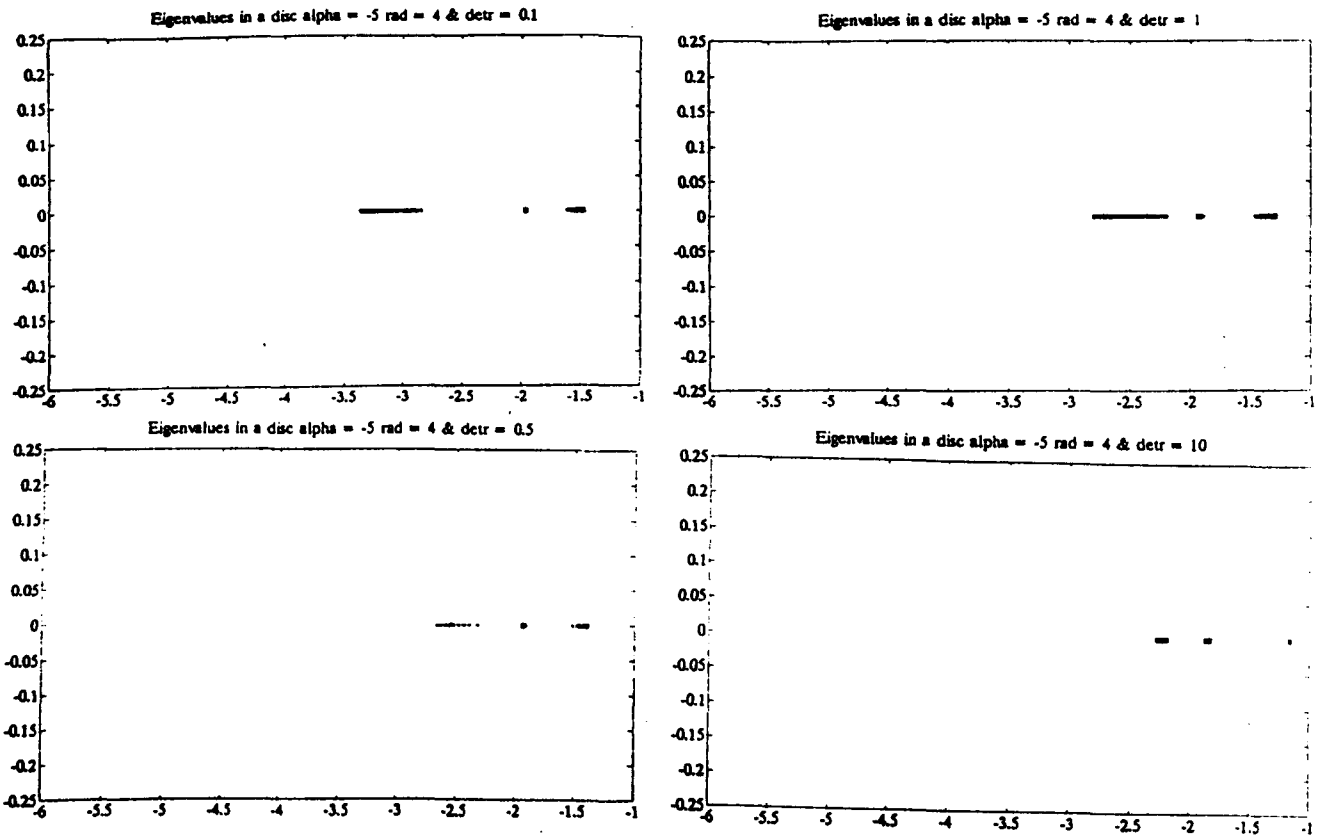

Fig 5.2 Eigenvalue plots for r = 4 and α = -5 + 0j

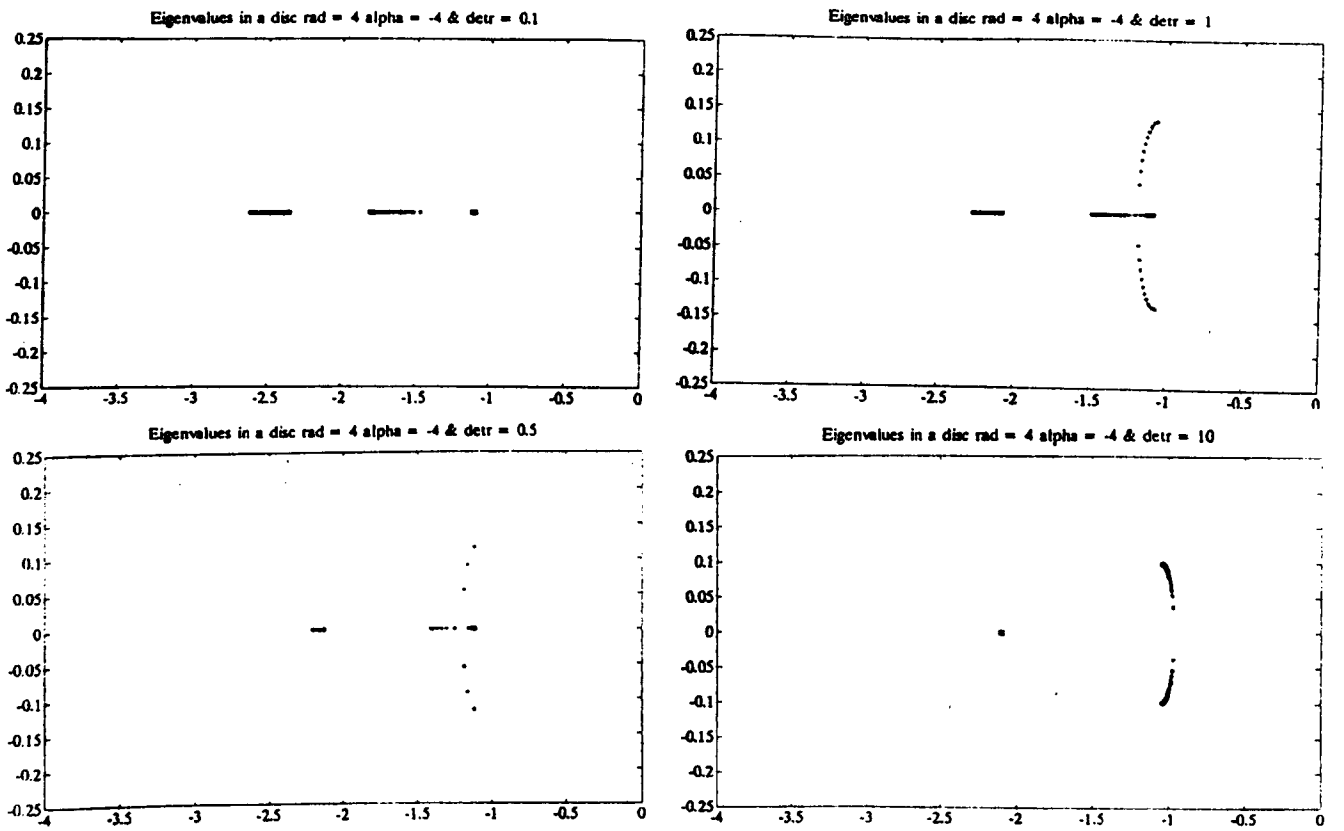

Fig 5.3 Eigenvalue plots for r = 4 and α = -4 + 0j

The results for α = -5 + 0j and r = 4 (Fig 5.2) demonstrate that for all the choices of det(R), the eigenvalues are real and in three clusters. As det(R) increases, the clusters move closer to the limiting eigenvalues for large values of R_{fact} and det(R). The results for α = -4 + 0j and r = 4 (Fig 5.3) demonstrate that when det(R) = 10, the eigenvalues comprise a complex conjugate pair close to -1, and a real value at 2.14, and as det(R) decreases, the complex conjugate pairs tend to the real axis until, at det(R) = 0.1, all the eigenvalues are real.

It is not possible to draw any general conclusions from these results, as a change in the disc centre changes the positioning of the eigenvalues within the disc very dramatically. Some further runs have been carried out for two different values of the disc radius, r = 3 and r = 5. The disc centres have been chosen so that the differences between the disc radius and the disc centre are the same as for the runs for r = 4. The results for these runs are displayed in the following figures

Fig 5.4	r = 5 and α = -7 + 0j	Fig 5.7	r = 3 and α = -5 + 0j
Fig 5.5	r = 5 and α = -6 + 0j	Fig 5.8	r = 3 and α = -4 + 0j
Fig 5.6	r = 5 and α = -5 + 0j	Fig 5.9	r = 3 and α = -3 + 0j

The results for r = 5 and α = -7 + 0j (Fig 5.4) show that when the determinant of R is small, there are a lot of complex conjugate pairs of eigenvalues. As det(R) increases, the number of complex conjugate pairs decreases until, when det(R) = 10, there are only a few complex conjugate pairs of eigenvalues.

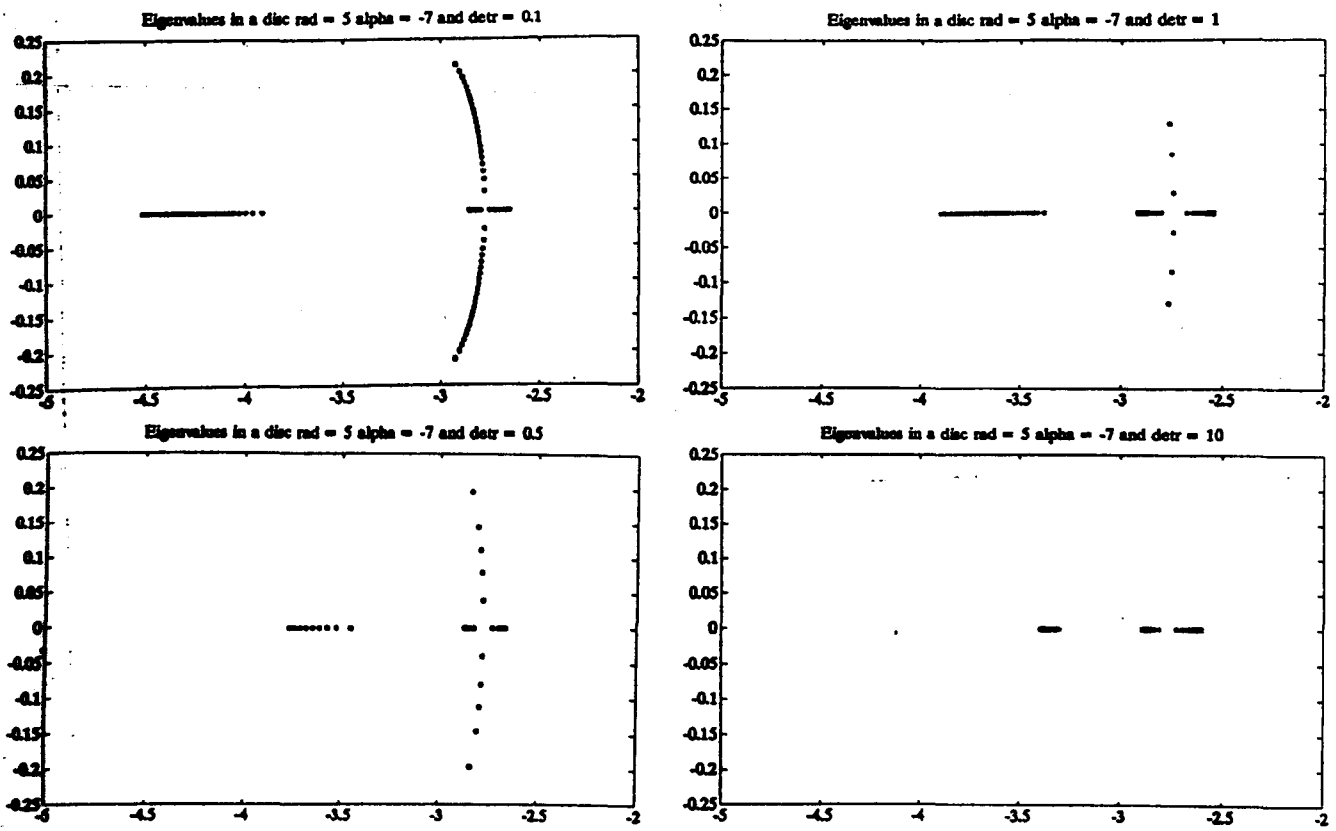

Fig 5.4 Eigenvalue plot for r = 5 and α = -7 + 0j

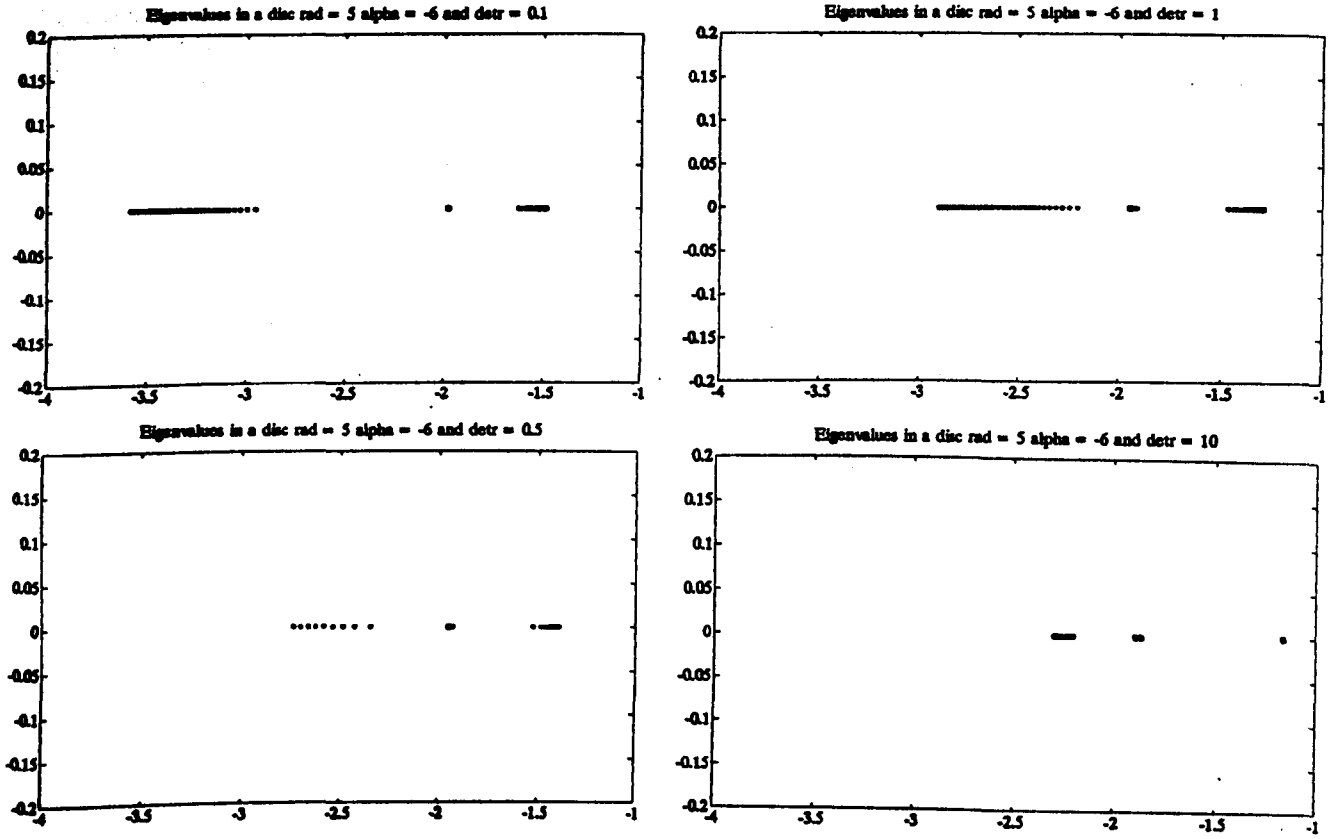

Fig 5.5 Eigenvalue plot for r = 5 and α = -6 + 0j

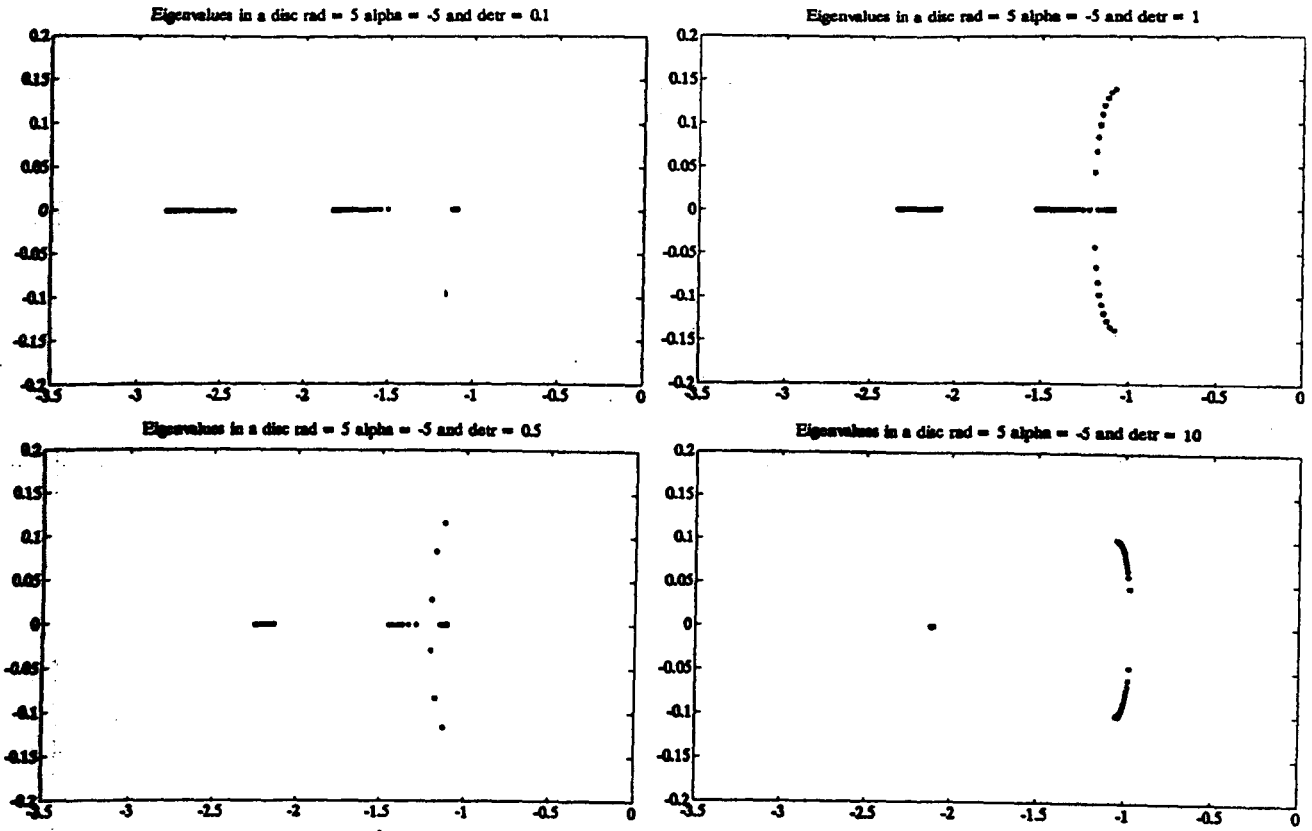

Fig 5.6 Eigenvalue plot for r = 5 and α = -5 + 0j

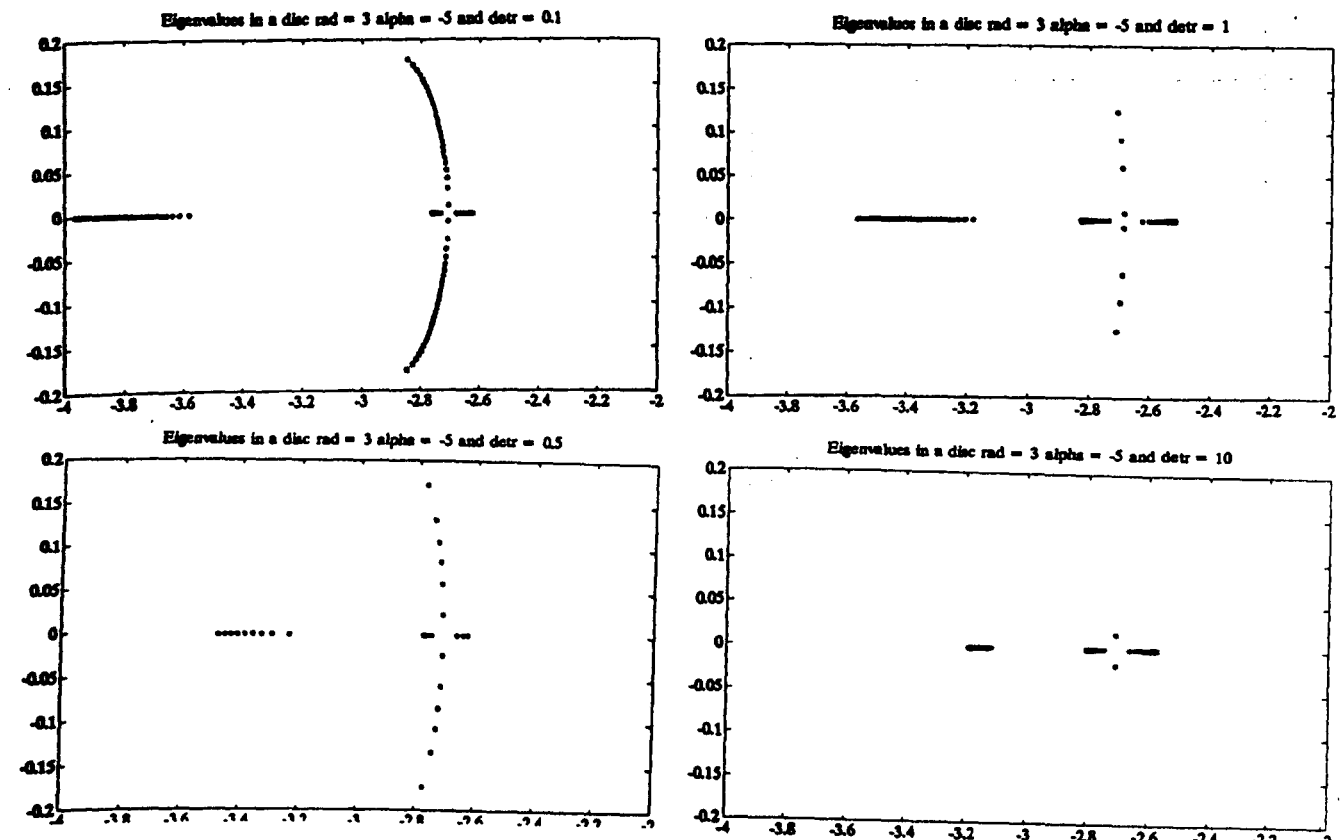

Fig 5.7 Eigenvalue plot for r = 3 and α = -5 + 0j

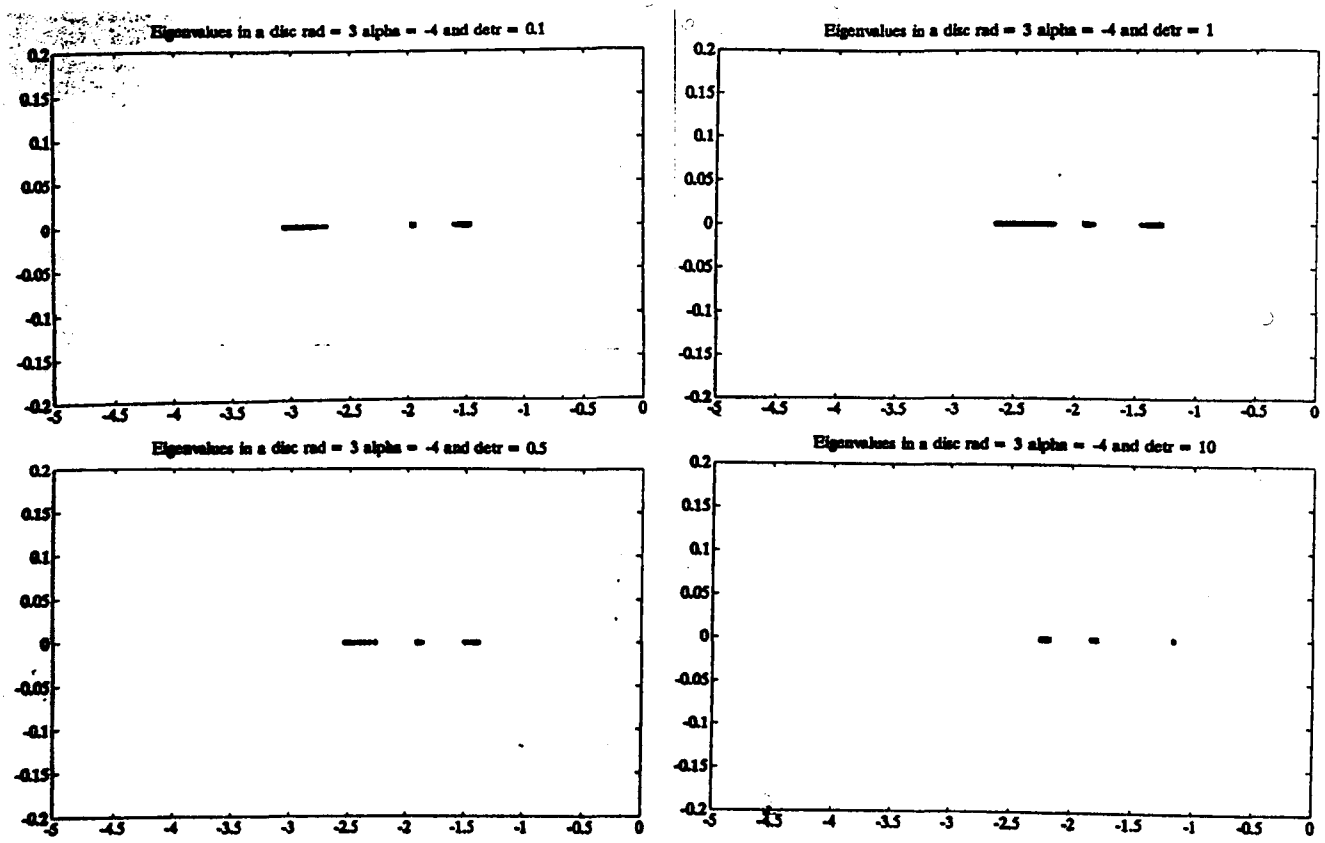

Fig 5.8 Eigenvalue plot for r = 3 and α = -4 + 0j

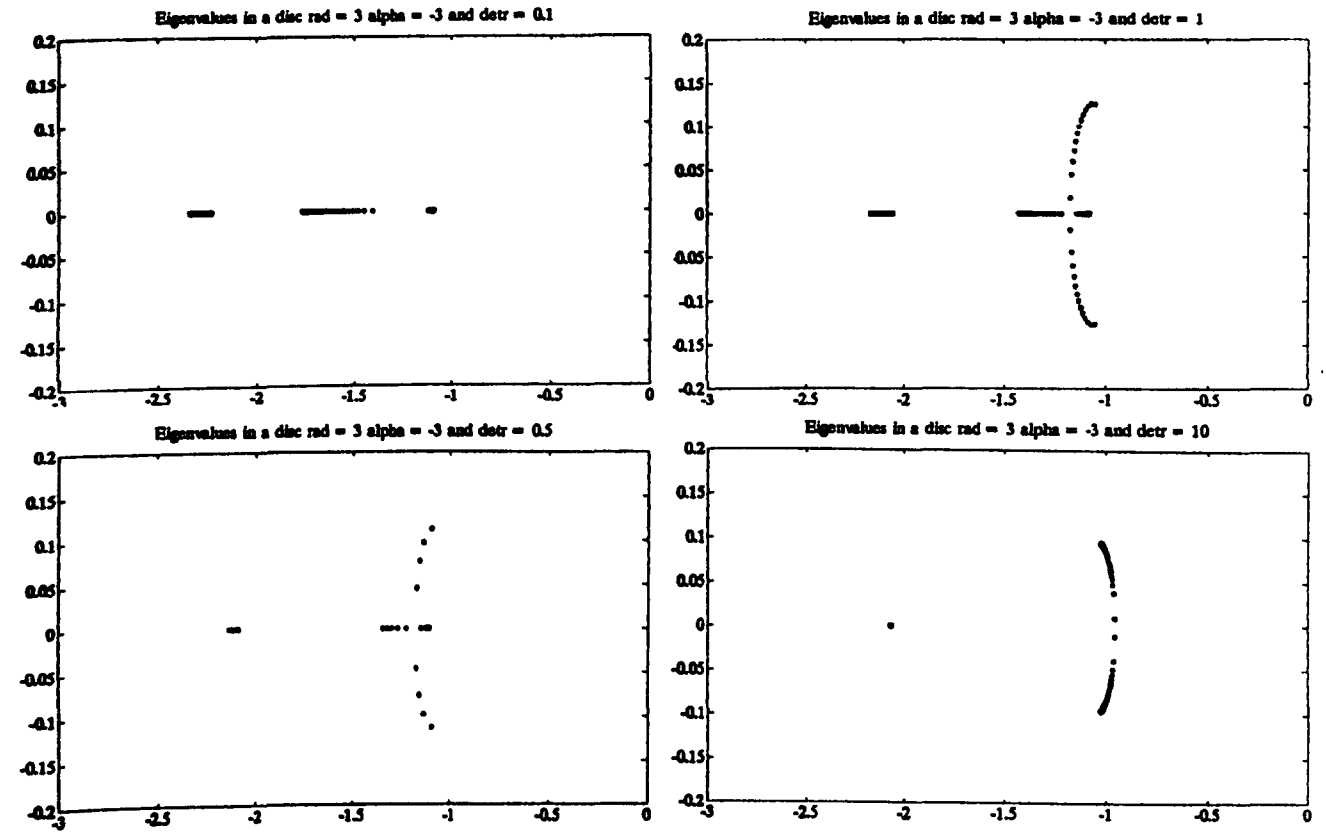

Fig 5.9 Eigenvalue plot for r = 3 and α = -3 + 0j

The results for r = 5 and α = -6 + 0j (Fig 5.5) show that the eigenvalues are real for all choices of the determinant, and as the determinant increases, they move towards the right-hand edge of the disc. When r = 5 and α = -5 + 0j (Fig 5.6), the eigenvalues are all real when the determinant is small. As the determinant increases complex conjugate pairs of eigenvalues approach the real axis, until when det(R) = 10, the eigenvalues comprise one real value and one complex conjugate pair. The results for r = 3 show the same characteristics for the three α values as those for r = 5 and r = 4.

The example of the robot arm, described earlier, has also been investigated for various discs. It was found from these investigations that for all choices of the R matrix, the eigenvalues were real. The results for two discs are shown in the following figures

Fig 5.10 r = 4 and α = -4 + 0j

Fig 5.11 r = 3 and α = -4 + 0j

The results in both of these figures show that when the determinant of R is small, one of the eigenvalues is very close to (or on) the centre of the disc, and the other one is near to the right-hand edge of the disc. When the determinant of R is large, one of the eigenvalues is near to the right-hand edge of the disc, and the other one is on (or almost on) this edge. This pattern was found for the five state example.

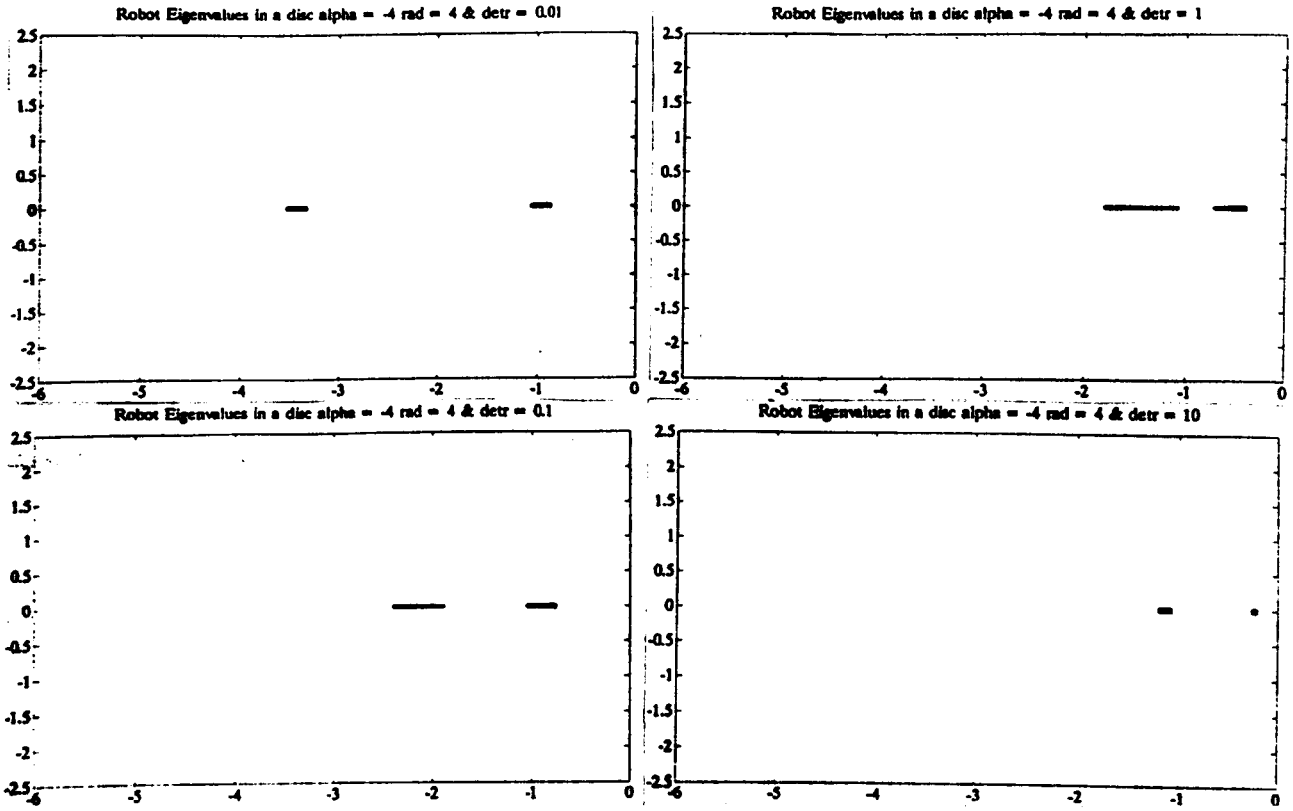

Fig 5.10 Eigenvalue plot for the robot arm

r = 4 and α = −4 + 0j

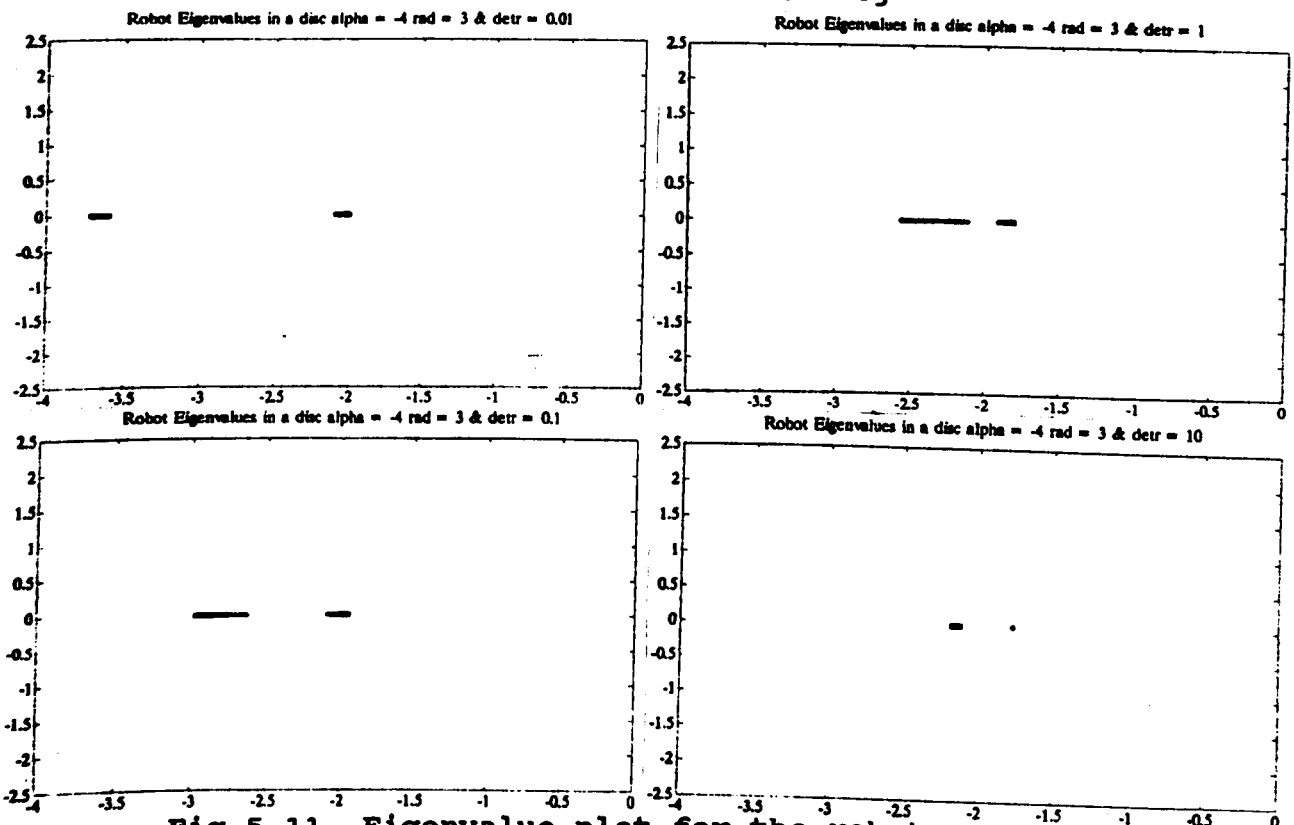

Fig 5.11 Eigenvalue plot for the robot arm

r = 3 and α = −4 + 0j

It would seem that if the root locus plot of the system has all real eigenvalues, then regardless of the choice of the R matrix, or the disc, the eigenvalues will always be real.

It would appear from these results that if $r = |\alpha|$, then an R matrix with a large determinant gives real and complex conjugate pairs of eigenvalues, and an R matrix with a small determinant gives purely real eigenvalues. If $|\alpha| - r = 1$, then the eigenvalues will be purely real for any choice of R matrix. Finally, if $|\alpha| - r > 1$, then an R matrix with a small determinant gives real and complex conjugate pairs of eigenvalues, and an R matrix with a large determinant gives mostly real eigenvalues.

5.3 Design of R for Eigenvalue Positioning within a Strip

An investigation into the effect of changes in the arbitrary R matrix on the solution of the continuous matrix Riccati equation given in equation (3.3.3), and hence on the position of the closed-loop eigenvalues, will now be performed.

Consider once more the five state system discussed in previous chapters, and its third order equivalent system. If h_1 is chosen to be 1, then the real eigenvalue of $A_{11} + h_1 I$ with the largest magnitude is $\lambda = -2$. Since h_2 has to have a magnitude larger than the magnitude of λ, choose h_2 to be 3. The vertical strip then crosses the real axis at the points -3 and -1.

Using the Macfarlane-Potter-Fath method outlined in Chapter 3, section 3.3, to solve the continuous matrix Riccati equation with a null Q matrix, given in equation (3.3.6), and varying the R matrix as before gives the following results

Table 5.3.1 Eigenvalues for varying R_{fact}

R_{fact}	Eigenvalues of $A_{11} - A_{12}F$	det(R)
1.0	-1.0;-2.0;-3.0	1.0
2.0	-1.0;-2.0;-3.0	4.0
3.0	-1.0;-2.0;-3.0	9.0
0.5	-1.0;-2.0;-3.0	0.25
0.1	-1.0;-2.0;-3.0	0.01

It can be seen from the results in Table 5.3.1 that the closed-loop eigenvalues of the reduced order equivalent system, $A_{11}-A_{12}F$, remain unchanged for the range of R_{fact} values investigated.

It would therefore appear that for any choice of the arbitrary R matrix which is a multiple of an identity matrix of the appropriate size, the positions of the eigenvalues within the strip remain unchanged. This would suggest that the control matrix, F, is unaffected by changes in the R matrix, and that the solution of the continuous matrix Riccati equation, P, is altering in proportion to the R matrix.

The solution to the continuous matrix Riccati equation outlined in equation (3.3.6), P, and the corresponding control matrix outlined in equation (3.3.7), F, will now be obtained.

The R_{fact} values are those given in Table 5.3.1, and the resulting P and F matrices are as follows

Table 5.3.2 P and F matrices for various R_{fact} values

R_{fact}	P matrix	F matrix
1.0	$\begin{pmatrix} 0 & 0 & 0 \\ 0 & 0.666 & -0.666 \\ 0 & -0.666 & 0.666 \end{pmatrix}$	$\begin{pmatrix} 0 & -1.6666 & 1.6666 \\ 0 & 1.1785 & -1.1785 \end{pmatrix}$
2.0	$\begin{pmatrix} 0 & 0 & 0 \\ 0 & 1.333 & -1.333 \\ 0 & -1.333 & 1.333 \end{pmatrix}$	$\begin{pmatrix} 0 & -1.6666 & 1.6666 \\ 0 & 1.1785 & -1.1785 \end{pmatrix}$
3.0	$\begin{pmatrix} 0 & 0 & 0 \\ 0 & 2.0 & -2.0 \\ 0 & -2.0 & 2.0 \end{pmatrix}$	$\begin{pmatrix} 0 & -1.6666 & 1.6666 \\ 0 & 1.1785 & -1.1785 \end{pmatrix}$
0.5	$\begin{pmatrix} 0 & 0 & 0 \\ 0 & 0.333 & -0.333 \\ 0 & -0.333 & 0.333 \end{pmatrix}$	$\begin{pmatrix} 0 & -1.6666 & 1.6666 \\ 0 & 1.1785 & -1.1785 \end{pmatrix}$
0.1	$\begin{pmatrix} 0 & 0 & 0 \\ 0 & 0.066 & -0.066 \\ 0 & -0.066 & 0.066 \end{pmatrix}$	$\begin{pmatrix} 0 & -1.6666 & 1.6666 \\ 0 & 1.1785 & -1.1785 \end{pmatrix}$

It can be seen from Table 5.3.2 that all the control matrices are identical, as would be expected, since the eigenvalues of $A_{11} - A_{12}F$ are identical in each case. It can also be seen that the P matrices are all multiples of the solution of the Riccati equation for $R_{fact} = 1$.

This result will now be proved for the reduced order equivalent system of any system of the form of equation (2.2.2). When R_{fact} is chosen to be 1, R is an identity matrix of the appropriate dimensions.

Suppose that the solution of the continuous matrix Riccati equation when R = I is $\tilde{P}$, then

$R_{fact} = 2 \qquad R = 2I \qquad P = 2\tilde{P}$

$R_{fact} = 3 \qquad R = 3I \qquad P = 3\tilde{P}$

$R_{fact} = 0.5 \qquad R = 0.5I \qquad P = 0.5\tilde{P}$

$R_{fact} = 0.1 \qquad R = 0.1I \qquad P = 0.1\tilde{P}$

Consider the continuous matrix Riccati equation with a zero right-hand side, equation (3.3.6)

$$PA_{12}R^{-1}A_{12}^{T}P - \hat{A}^{T}P - P\hat{A} = 0 \qquad (5.3.1)$$

where $\hat{A}$ and the control matrix, F, are given by

$$\hat{A} = A_{11} + h_1 I \qquad (5.3.2)$$

$$F = \mu R^{-1}A_{12}^{T}P \qquad (5.3.3)$$

Let $R = R_1$ and $P = P_1$, and then equation (5.3.1) becomes

$$P_1A_{12}R_1^{-1}A_{12}^{T}P_1 - \hat{A}^{T}P_1 - P_1\hat{A} = 0 \qquad (5.3.4)$$

Now choose the arbitrary matrix, R, to be of the form $r = \alpha R_1$, where α is any positive real number. Let us suppose that the solution to the matrix Riccati equation is P_2.
Then equation (5.3.1.) becomes

$$\frac{1}{\alpha}\left(P_2A_{12}R_1^{-1}A_{12}^{T}P_2\right) - \hat{A}^{T}P_2 - P_2\hat{A} = 0 \qquad (5.3.5)$$

Substituting $P_2 = \alpha P_1$ into equation (5.3.5) gives

$$\frac{1}{\alpha}\,(\alpha P_1 A_{12} R_1^{-1} A_{12}^T \alpha P_1) - \hat{A}^T \alpha P_1 - \alpha P_1 \hat{A} = 0 \qquad (5.3.6)$$

Equation (5.3.6) may be rearranged to give

$$\alpha P_1 A_{12} R_1^{-1} A_{12}^T P_1 - \alpha \hat{A}^T P_1 - \alpha P_1 \hat{A} = 0 \qquad (5.3.7)$$

Clearly, if equation (5.3.7) is divided by the scalar α, it is identical to equation (5.3.4).

Hence, if an arbitrary matrix R gives rise to a solution P of equation (5.3.1) then an arbitrary matrix $R_1 = \alpha r$ will give rise to a solution matrix $P_1 = \alpha P$ for all positive real scalars α.

Consider equation (5.3.3) for the control matrix, when $R = R_1$ and $P = P_1$.

Let the control matrix be F_1, given by

$$F_1 = \mu R_1^{-1} A_{12}^T P_1 \qquad (5.3.8)$$

Let $R_2 = \alpha R_1$, and then the corresponding solution P_2 will be equal to αP_1, and the control matrix will be given by

$$F_2 = \mu R_2^{-1} A_{12}^T P_2 \qquad (5.3.9)$$

Substituting for R_2 and P_2 in equation (5.3.9) gives

$$F_2 = \frac{\mu}{\alpha}\, R_1^{-1} A_{12}^T \alpha P_1 \qquad (5.3.10)$$

Clearly, since α is a scalar, the right-hand side of equation (5.3.10) is identical to the right-hand side of equation (5.3.8) and hence $F_1 = F_2$.

It has therefore been proved the solution matrix of the continuous Riccati equation (3.3.6) with R replaced by αR will be αP, where α is a positive real scalar, and hence the control matrix will remain unchanged. This results holds for all systems of the form of the standard regulator problem given in equation (2.2.2). The solution of this method of placing all the closed-loop eigenvalues of the reduced order equivalent system of a Variable Structure Control system, and hence (n-m) of the closed-loop eigenvalues of the full order VSC system, within an infinite vertical strip in the left-hand half-plane is therefore unaffected by positive scalar multiple changes in the arbitrary positive definite symmetric R matrix.

The effect of a change to the R matrix which is not obtained by multiplying an identity matrix of the appropriate dimensions by a positive real scalar will now be investigated.

Consider the same five state example which was used before, which has a third order equivalent system. Suppose that the required vertical strip crosses the real axis at the points -3 and -1, so that $h_1 = 1$ and $h_2 = 3$, since the magnitude of the smallest eigenvalue is 2.

Allowing the R matrix to vary by a different factor in each element gives the following results.

Table 5.3.3 Eigenvalues for various R matrices

R matrix	Eigenvalues of $A_{11}-A_{12}F$	P matrix	F matrix
$\begin{bmatrix}1 & 0\\0 & 1\end{bmatrix}$	-1;-2;-3	$\begin{bmatrix}0 & 0 & 0\\0 & 0.66 & -0.66\\0 & -0.66 & 0.66\end{bmatrix}$	$\begin{bmatrix}0 & -1.666 & 1.666\\0 & 1.179 & -1.179\end{bmatrix}$
$\begin{bmatrix}2 & 0\\0 & 1\end{bmatrix}$	-1;-2;-3	$\begin{bmatrix}0 & 0 & 0\\0 & 1.0 & -1.0\\0 & -1.0 & 1.0\end{bmatrix}$	$\begin{bmatrix}0 & -1.250 & 1.250\\0 & 1.768 & -1.768\end{bmatrix}$
$\begin{bmatrix}2 & 0\\0 & 0.5\end{bmatrix}$	-1;-2;-3	$\begin{bmatrix}0 & 0 & 0\\0 & 0.66 & -0.66\\0 & -0.66 & 0.66\end{bmatrix}$	$\begin{bmatrix}0 & -0.833 & 0.833\\0 & 2.357 & -2.357\end{bmatrix}$
$\begin{bmatrix}5 & 0\\0 & 1\end{bmatrix}$	-1;-2;-3	$\begin{bmatrix}0 & 0 & 0\\0 & 1.43 & -1.43\\0 & -1.43 & 1.43\end{bmatrix}$	$\begin{bmatrix}0 & -0.714 & 0.714\\0 & 2.525 & -2.525\end{bmatrix}$
$\begin{bmatrix}10 & 0\\0 & 1\end{bmatrix}$	-1;-2;-3	$\begin{bmatrix}0 & 0 & 0\\0 & 1.21 & -1.21\\0 & -1.21 & 1.21\end{bmatrix}$	$\begin{bmatrix}0 & -0.576 & 0.576\\0 & 2.722 & -2.722\end{bmatrix}$
$\begin{bmatrix}0.1 & 0.01\\0.01 & 0.1\end{bmatrix}$	-1;-2;-3	$\begin{bmatrix}0 & 0 & 0\\0 & 0.06 & -0.06\\0 & -0.06 & 0.06\end{bmatrix}$	$\begin{bmatrix}0 & -1.631 & 1.631\\0 & 1.229 & -1.229\end{bmatrix}$

It can be seen from Table 5.3.3 that the closed-loop eigenvalues of the reduced order equivalent system $A_{11} - A_{12}F$ remain unchanged for all the R matrices used. In this case, the control matrices are not the same, but they are equivalent to one another, since each one can be obtained from any of the others by elementary transformations (Hohn, 1958). It can be argued that, provided the control matrices are equivalent to one another, the eigenvalues of $A_{11} - A_{12}F$ will remain the same.

Thus, the solution of this method of placing the closed-loop eigenvalues of the reduced order equivalent system of a Variable Structure Control system within a vertical strip in the left-hand half plane is unaffected by the choice of the arbitrary R matrix.

Consider the robot arm system discussed in previous chapters, and its second order equivalent system. If h_1 is chosen to be 1 then the real eigenvalue of $A_{11} + h_1 I$ with the largest magnitude is $\lambda = -1$. Since h_2 has to have a magnitude greater than that of λ, choose h_2 to be 3. The vertical strip then crosses the real axis at the points -3 and -1. Using the Macfarlane-Potter-Fath method outlined in Chapter 3, section 3.3, to solve the continuous matrix Riccati equation with a null Q matrix, and varying the R matrix, gives the following results

Table 5.3.4 Eigenvalues for varying R matrices

R matrix	E-values	P matrix	F matrix
I	-2 ; -2	2I	$\begin{pmatrix} -0.781 & 1.841 \\ -1.841 & -0.781 \end{pmatrix}$
2I	-2 ; -2	4I	$\begin{pmatrix} -0.781 & 1.841 \\ -1.841 & -0.781 \end{pmatrix}$
3I	-2 ; -2	6I	$\begin{pmatrix} -0.781 & 1.841 \\ -1.841 & -0.781 \end{pmatrix}$
0.5I	-2 ; -2	I	$\begin{pmatrix} -0.781 & 1.841 \\ -1.841 & -0.781 \end{pmatrix}$
0.1I	-2 ; -2	0.2I	$\begin{pmatrix} -0.781 & 1.841 \\ -1.841 & -0.781 \end{pmatrix}$
$\begin{pmatrix} 1 & 0 \\ 0 & 0.5 \end{pmatrix}$	-2 ; -2	$\begin{pmatrix} 1.1526 & -0.3596 \\ -0.3596 & 1.8476 \end{pmatrix}$	$\begin{pmatrix} -0.781 & 1.841 \\ -1.841 & -0.781 \end{pmatrix}$
$\begin{pmatrix} 100 & 0 \\ 0 & 0.01 \end{pmatrix}$	-2 ; -2	$\begin{pmatrix} 30.532 & 71.9083 \\ -71.9083 & 169.4880 \end{pmatrix}$	$\begin{pmatrix} -0.781 & 1.841 \\ -1.841 & -0.781 \end{pmatrix}$

It can be seen from Table 5.3.4 that the relationship between the R, P and F matrices outlined in equations (5.3.1) to (5.3.10) holds, namely

$$R_1 = \alpha R \quad \Rightarrow \quad P_1 = \alpha P \quad \text{and} \quad F_1 = F \tag{5.3.11}$$

which would be expected, since these equations hold for all A_{11} and A_{12} matrices, and hence all full order systems of the form

$$\dot{x} = Ax + Bu \tag{5.3.12}$$

However, it can be seen from the results in Table 5.3.4 that even if R_1 is not a scalar multiple of R, F_1 is still equal to F, and this result will now be considered. For the robot arm example, recall from Chapter 3 that the reduced order system matrix A_{11} is the null matrix, and this will have an effect on the solution of the Riccati equation (3.3.6). Substituting $A_{11} = 0$ into equation (3.3.6) gives

$$PA_{12}R^{-1}A_{12}^{T}P - (h_1 I)^{*}P - P(h_1 I) = 0 \tag{5.3.13}$$

Since h_1 is a real scalar, equation (5.3.13) may be rearranged to give

$$PA_{12}R^{-1}A_{12}^{T}P - 2h_1 P = 0 \tag{5.3.14}$$

Post-multiplying both sides of equation (5.3.14) by P^{-1} gives

$$PA_{12}R^{-1}A_{12}^{T} - 2h_1 = 0 \tag{5.3.15}$$

Since $A_{12}R^{-1}A_{12}^T$ is always a square matrix, as A_{12} is $(n-m)\times m$ and r is $m\times m$, and assuming it is non-singular, equation (5.3.15) may be rearranged to give

$$P = 2h_1\left[A_{12}R^{-1}A_{12}^T\right]^{-1} \tag{5.3.16}$$

The control matrix F is then given by

$$F = 2\mu h_1 R^{-1}A_{12}^T\left[A_{12}R^{-1}A_{12}^T\right]^{-1} \tag{5.3.17}$$

It can be seen from equation (5.3.17) that in the particular case when A_{11} is zero, the F matrix is independent of the solution P of the matrix Riccati equation (3.3.6). This is illustrated in the results in Table 5.3.4 for the R matrices which are not a scalar multiple of the identity matrix. If A_{12} is a square matrix, then equation (5.3.17) may be further simplified to give

$$F = 2\mu h_1 A_{12}^{-1} \tag{5.3.18}$$

As an example, consider the case when $R = \begin{bmatrix}1 & 0\\ 0 & 0.5\end{bmatrix}$, and hence $R^{-1} = \begin{bmatrix}1 & 0\\ 0 & 2\end{bmatrix}$.

From equation (5.3.16), since h_1 was chosen to be 1, P is given by

$$P = 2\left[\begin{bmatrix}-0.3906 & -0.9206\\ 0.9206 & -0.3906\end{bmatrix}\begin{bmatrix}1 & 0\\ 0 & 2\end{bmatrix}\begin{bmatrix}-0.3906 & 0.9206\\ -0.9206 & -0.3906\end{bmatrix}\right]^{-1} \tag{5.3.19}$$

Multiplying out the bracketed expression in equation (5.3.19) gives

$$P = 2\begin{bmatrix} 1.8476 & 0.3596 \\ 0.3596 & 1.1526 \end{bmatrix}^{-1} \qquad (5.3.20)$$

Since the determinant of the matrix to be inverted in equation (5.3.20) is equal to 2, P becomes

$$P = \begin{bmatrix} 1.1526 & -0.3596 \\ -0.3596 & 1.8476 \end{bmatrix} \qquad (5.3.21)$$

It can be seen that the P matrix obtained in equation (5.3.21) is identical to that obtained earlier, and displayed in Table 5.3.4.

Since, in this example the matrix A_{12} is square, F may be obtained from equation (5.3.18).

$$F = 2\mu h_1 A_{12}^{-1} = 2\begin{bmatrix} -0.3906 & -0.9206 \\ 0.9206 & -0.3906 \end{bmatrix}^{-1} \qquad (\mu = 1) \qquad (5.3.22)$$

So the control matrix, F, becomes

$$F = \begin{bmatrix} -0.781 & 1.841 \\ -1.841 & -0.781 \end{bmatrix} \qquad (5.3.22)$$

It is clear that the F matrix given in equation (5.3.22) is identical to the F matrix for the appropriate R matrix given in Table 5.3.4, and will be the same for all choices of the arbitrary R matrix.

It may be concluded, therefore, that for a general system of the form $\dot{x} = Ax + Bu$, in the particular case when its reduced order equivalent system matrix A_{11} is zero, the solution of the continuous matrix Riccati equation given in equation (3.3.6), P, will be given by equation (5.3.16) and that the control matrix, F, will be independent of the solution matrix P and will be given by equation (5.3.17). In addition, if the reduced order equivalent system matrix A_{12} is a square matrix, in other words, if $n-m = m$, then the control matrix, F, is only dependent on the right-hand strip limit h_1, the matrix A_{12} and μ, as can be seen from equation (5.3.18)

5.4 Discussion

It has been shown that the positioning of the closed-loop eigenvalues of a system within a specified disc in the left-hand half-plane depend more on the determinant of the arbitrary R matrix than on its structure, and also depend on the choice of the disc centre and radius. Owing to the complexity of the solution of the discrete matrix Riccati equation, it is not easy to determine the exact relationship between the R matrix, the disc centre and radius, and the positioning of the eigenvalues. However, from the investigations contained in this chapter, it would appear that there are some generalizations which can be made about the relationship between eigenvalue positioning and the choice of the R matrix and the disc parameters, for a fixed arbitrary positive definite symmetric Q matrix.

From the numerical results obtained from two very different systems, the following conclusions are suggested :

1) If the root locus plot of the system comprises only real eigenvalues, then regardless of the choice of R matrix and disc parameters, the eigenvalues will always be placed along the real axis, within the disc.

2) If the root locus plot has complex values, and the radius and the modulus of the centre of the disc are equal, then an R matrix with a small determinant will lead to real eigenvalues within the disc, and an R matrix with a large determinant will lead to real and complex eigenvalues.

3) If the root locus plot has complex eigenvalues, and the difference in magnitude between the radius and the centre of the disc is equal to 1, then the eigenvalues will be real for all choices of the R matrix. An R matrix with a large determinant will place the eigenvalues close to the right-hand edge of the disc.

4) If the root locus plot has complex eigenvalues, and the difference in magnitude between the radius and the centre of the disc is greater than 1, then an R matrix with a small determinant will lead to complex and real eigenvalues within the disc, and an R matrix with a large determinant will lead to all real eigenvalues.

It is therefore possible to choose an R matrix with an appropriate determinant, depending on the choice of disc, to ensure that the eigenvalues are all real or a mixture of real and complex conjugate pairs.

The investigation into the effect of the arbitrary R matrix on the positioning of the eigenvalues within a vertical strip crossing the real axis at the points $-h_1$ and $-h_2$ leads to the following conclusions, which have been demonstrated for all systems in the form of equation (2.2.2) :

1) If the arbitrary R matrix is multiplied by a positive real scalar, then the solution of the continuous matrix Riccati equation will be multiplied by the same scalar, and the control matrix, F, and the closed-loop eigenvalues will remain unchanged.

2) If the R matrix is not a multiple of the identity matrix, the solution matrices of the continuous matrix Riccati equation are scalar multiples of each other, the control matrices are equivalent to one another, and the eigenvalues are unchanged.

3) If the reduced order system matrix A_{11} is zero, then the control matrix is independent of the solution of the continuous matrix Riccati equation. If the reduced order system matrix A_{12} is a square matrix, then the control matrix is independent of the arbitrary R matrix, and so only depends on h_1, A_{12} and μ.

It has therefore been proved that eigenvalue placement within a vertical strip is independent of any change in the arbitrary R matrix. In the particular case when A_{11} is zero, and A_{12} is square ($n-m = m$), the control matrix is independent of both the solution of the continuous matrix Riccati equation, and the arbitrary matrix R.

6. DEPENDENCE OF EIGENVALUE POSITIONING WITHIN A SECTOR ON THE R MATRIX DESIGN

6.1 Introduction

The dependence of the positioning of the closed-loop eigenvalues within the sector described in Chapter 4 on the design of the R matrix will now be considered. This will involve some investigations into the effect of the arbitrary R matrix on the solution of a complex continuous matrix Riccati equation with a non-zero arbitrary matrix Q. This work follows on, to some degree, from the investigation carried out in Chapter 5, Section 5.3 on the effect of the R matrix on the solution of a real continuous matrix Riccati equation with a zero Q matrix. The robustness property may be more useful in the case of the sector than in the cases of the disc and the strip discussed in the previous chapter, since it might be possible to place the eigenvalues in sectors outside those described by the limiting θ and α values discussed in Chapter 4. It would also be useful to be able to predict the position of the eigenvalues within the sector, and in particular, to predict whether they will be real or complex.

The placing of the eigenvalues in wider range of sectors than was shown to be possible in Chapter 4, Section 4.5, is considered in section 6.2. Section 6.3 contains the investigations into the possibility of predicting the positioning of the eigenvalues within the sector, and Section 6.4 contains a discussion of the results.

6.2 Effect of the R Matrix on the Limiting Alpha & Theta Values

The effect of the arbitrary R matrix on the solution of the continuous matrix Riccati equation given in equation (4.2.30), and hence on the limiting α and θ values discussed in Chapter 4, section 4.5 will be considered.

Consider once more the five state VSC example, outlined in section 3.4, when $\alpha = -2$ and $\theta = 65^{\circ}$, bearing in mind that the maximum θ value for $\alpha = -2$ was previously found to be 60° (see section 4.5). The R matrix is varied as follows

$$R = R_{fact}I \tag{6.2.1}$$

Table 6.2.1 Eigenvalues for $\theta = 65^{\circ}$, $\alpha = -2$ & varying R_{fact}

R_{fact}	Closed-loop Eigenvalues
1.0	-1.9991 ± 0.2091j ; -2.8783
2.0	-1.8216 ± 0.2596j ; -2.7662
3.0	-1.7419 ± 0.2589j ; -2.7175
4.0	-1.6442 ± 0.2518j ; -2.6888
5.0	-1.6617 ± 0.2437j ; -2.6694
0.9	-2.0314 ± 0.1894j ; -2.8995
0.8	-2.0694 ± 0.1590j ; -2.9248
0.7	-2.1148 ± 0.1033j ; -2.9559
0.6	-2.0697 ; -2.2714 ; -2.9953
0.5	-2.0383 ; -2.4440 ; -3.0478
0.333	-2.0411 ; -2.7878 ; -3.1985
0.25	-2.0616 ; -3.0264 ; -3.3561
0.2	-2.0826 ; -2.1961 ; -3.5311
0.1	-2.1600 ; -3.6740 ; -4.4009

It can be seen from the results displayed in Table 6.2.1, that as R_{fact} is increased the real eigenvalue, which is within the required sector, moves towards α, the right-hand limit of the sector. For a suitably large value of R_{fact}, this eigenvalue may possibly move beyond α, and out of the required sector.

The real part of the complex eigenvalues, which are outside the sector for R_{fact} values greater than or equal to 1, move closer to the origin as R_{fact} increases, and away from the origin and hence into the sector as R_{fact} decreases. The imaginary parts of the complex pairs of eigenvalues are outside the required sector for all the α values displayed in Table 6.2.1, and their magnitude increases as R_{fact} increases, until it reaches some maximum value, and then it decreases again. As R_{fact} decreases, the imaginary parts move nearer to the real axis, but are always outside the required sector. If R_{fact} is smaller than or equal to 0.6, the eigenvalues are all real, and all lie within the required sector, and as R_{fact} decreases beyond 0.6, the eigenvalues move along the real axis, towards α. It can be seen from these results that a suitable choice of value for R_{fact} will increase the maximum value of θ from 60^{o} to 65^{o}. It is possible, therefore, that if R_{fact} is made suitably small, the restrictions on the choice of α and θ could be relaxed.

Using MATLAB, a routine has been written which alters the R matrix by multiplying it by a scalar until the eigenvalues lie in the required sector. Consider once more the five state example, and the case when $\alpha = -2$, and let θ hold a range of values greater than its previous maximum value of 60^{o}. The R matrix is altered according to equation (6.2.1) and the R_{fact} values which result in the eigenvalues lying in the required sector are contained in Table 6.2.2.

The closed-loop eigenvalues of the reduced order equivalent system $A_{11} - A_{12}F$ and the appropriate θ values are also displayed in Table 6.2.2.

Table 6.2.2 Comparison of R_{fact}, θ & eigenvalues for $\alpha = -2$

θ°	R_{fact}	Closed-loop Eigenvalues
55	1	-2.1105 ; -2.6100 ; -2.7800
60	1	-2.1602 ± 0.0762j ; -2.8686
65	0.6	-2.0697 ; -2.2714 ; -2.9953
70	0.5	-2.0149 ; -2.1687 ; -3.0575
75	0.05	-2.0093 ; -4.2078 ; -5.5167
80	0.01	-2.0407 ; -6.9188 ; -10.9108
81	0.01	-2.0204 ; -6.9120 ; -10.8893
82	0.01	-2.0004 ; -6.9071 ; -10.8677
83	0.007	-2.0025 ; -7.8734 ; -12.7947
84	0.005	-2.0011 ; -8.9593 ; -14.9597
85	0.003	-2.0050 ; -11.0065 ; -19.0494
86	0.002	-2.0012 ; -13.0500 ; -23.1282
87	0.001	-2.0028 ; -17.6713 ; -32.3649
88	4×10^{-4}	-2.0029 ; -26.8507 ; -50.7169
89	1×10^{-4}	-2.0011 ; -51.8421 ; -100.6919
89.5	2×10^{-5}	-2.0013 ; -113.6408 ; -224.2860
89.9	1×10^{-6}	-2.0000 ; -100.7000 ; -501.8000
89.95	2×10^{-7}	-2.0000 ; -1119.9000 ; -2236.7000

It can be seen from the results displayed in Table 6.2.2 that by choosing a suitable value for R_{fact}, the limiting value of θ for $\alpha = -2$ can be increased from 60° to 89.95°. However, it is clear that as R_{fact} becomes very small, and θ moves closer to 90°, two of the eigenvalues move further away from α in the negative real direction, and the other eigenvalue moves very close to α. This results in the spread of the eigenvalues being considerable, as can be seen from the results displayed in Table 6.2.2 for $R_{fact} = 2\times10^{-7}$.

Consider the α values and their corresponding limiting θ values displayed in section 4.5, Table 4.5.1. For these α values, the R matrix has been altered as described in equation (6.2.1), and the new limiting θ values of the various α values are displayed in Table 6.2.3, along with both the old and the new closed-loop eigenvalues.

Table 6.2.3 New limiting θ values for various α values

α	θ_o°	Eigenvalues for θ_o	R_{fact}	θ_n°	Eigenvalues for θ_n
10	88	-1.139±0.22j;-2.383	3×10^{-1}	90	-1.648;-2.013;-3.242
5	87	-1.177±0.23j;-2.420	3×10^{-1}	90	-1.648;-2.013;-3.242
2	85	-1.210±0.24j;-2.440	3×10^{-1}	90	-1.648;-2.013;-3.242
1	83	-1.225±0.24j;-2.436	3×10^{-1}	90	-1.648;-2.013;-3.242
0	78	-1.257±0.24j;-2.424	3×10^{-1}	90	-1.648;-2.013;-3.242
-0.5	72	-1.306±0.25j;-2.423	3×10^{-1}	90	-1.648;-2.013;-3.242
-1	62	-1.470±0.25j;-2.467	3×10^{-1}	90	-1.648;-2.013;-3.242
-2	60	-2.160±0.08j;-2.869	2×10^{-11}	89	$-2;-1.1\times10^{5};-2.2\times10^{5}$
-3	47	-3.037;-4.220±0.33j	6×10^{-6}	67	-3;-22.738;-42.413
-4	49	-4.012;-5.472±0.31j	1×10^{-7}	64	-4;-1583.9;-3164.4
-5	50	-5.062;-6.224±0.25j	2×10^{-6}	62	-5;-356.880;-709.109
-6	51	-6.092;-7.920±0.14j	2×10^{-7}	61	-6;-1129.1;-2239.3
-7	52	-7.085;-8.864;-9.25	2×10^{-7}	61	-7;-1122.4;-2239.8
-8	53	-8.033;-9.82;-10.46	6×10^{-6}	61	-8;-209.02;-412.53
-9	53	-9.14;-10.99;-11.77	3×10^{-7}	61	-9;-918.24;-1830.52
-10	54	-10.02;-11.9;-12.85	7×10^{-8}	60	-10;-1895.7;-3784.9
-20	56	-20.03;-22.4;-24.28	1×10^{-5}	60	-20;-169.34;-326.71
-30	56	-30.69;-33.6;-35.98	1×10^{-6}	60	-30;-516.14;-1015.44
-40	57	-40.33;-43.6;-46.50	5×10^{-7}	60	-40;-728.30;-1434.69
-50	57	-50.84;-57.8;-54.49	2×10^{-7}	60	-50;-1144.2;-2261.54
-100	58	-100.9;-106;-110.83	1×10^{-8}	60	$-100;-5051.2;-1\times10^{4}$
-1000	59	-1014.2;-1030;-1045	1×10^{-12}	60	$-1000;-5\times10^{5};-1\times10^{6}$
-1×10^{5}	59	$-1\times10^{5};-1\times10^{5};-1\times10^{5}$	1×10^{-20}	60	$-1\times10^{5};-2\times10^{9};-3\times10^{9}$

It can be seen from Table 6.2.3 that for $\alpha \geq -1$, the limiting value of θ is 90° for a suitable choice of R_{fact}, and for $\alpha < -1$, the limiting value of θ drops to 60°, which appears to be the limiting value of θ for all small α values.

Consider the robot arm example outlined in section 2.4, and its α values and corresponding θ values displayed in section 4.5, Table 4.5.2. The R matrix is altered as described in earlier, and the new limiting θ values for the α values smaller than -1 are displayed in Table 6.2.4, along with the old and new closed-loop eigenvalues. It is unnecessary to consider the cases when $\alpha \geq -1$, since the limiting θ value is 90° for these values when R = I.

Table 6.2.4 New limiting θ values for the robot arm

α	θ_o°	Eigenvalues for θ_o	R_{fact}	θ_n°	Eigenvalues for θ_n
-2	67	-2.0506; -2.0506	1/4	90	-2 ; -2
-3	63	-3.0567; -3.0567	1/9	90	-3 ; -3
-4	62	-4.0054; -4.0054	1/16	90	-4 ; -4
-5	61	-5.0463; -5.0463	1/25	90	-5 ; -5
-6	60	-6.1623; -6.1623	1/36	90	-6 ; -6
-7	60	-7.1401; -7.1401	1/49	90	-7 ; -7
-8	60	-8.1231; -8.1231	1/64	90	-8 ; -8
-9	60	-9.1098; -9.1098	1/91	90	-9 ; -9
-10	60	-10.0990;-10.0990	1×10^{-2}	90	-10 ; -10
-20	60	-20.0499;-20.0499	2.5×10^{-3}	90	-20 ; -20
-30	60	-30.0333;-30.0333	1.1×10^{-3}	90	-30 ; -30
-40	60	-40.0250;-40.0250	6.25×10^{-4}	90	-40 ; -40
-50	60	-50.0200;-50.0200	4×10^{-4}	90	-50 ; -50
-100	60	-1.0×10^{2};-1.0×10^{2}	1×10^{-4}	90	-100 ; -100
-1000	60	-1.0×10^{3};-1.0×10^{3}	1×10^{-6}	90	-1000 ;-1000
-1×10^{5}	60	-1.0×10^{5};-1.0×10^{5}	1×10^{-10}	90	-1×10^{5};-1×10^{5}

It can be seen from the results displayed in Table 6.2.4, that for all choices of α, the limiting θ value may be increased to 90°, by a suitable choice of the arbitrary matrix R. It can also be seen that the appropriate choice of R_{fact} for the eigenvalues to be on the right-hand point of the sector is $1/\alpha^2$ in each case.

The results noted from the investigations of these two systems will now be verified for the reduced order equivalent system of any system of the form of equation (2.2.2). When θ is equal to 90°, $e^{j\theta}$ and $e^{-j\theta}$ become j and -j respectively, so substituting for them in equation (4.2.29) gives

$$j(A_{11} - \alpha I)^{*}P - jP(A_{11} - \alpha I) - PA_{12}R^{-1}A_{12}^{T}P = -Q \qquad (6.2.2)$$

Equation (6.2.2) may be expanded to give

$$(-jA_{11})^{*}P - \alpha jP + P(-jA_{11}) + \alpha jP - PA_{12}R^{-1}A_{12}^{T}P = -Q \qquad (6.2.3)$$

The α terms in equation (6.2.3) cancel, to give

$$(-jA_{11})^{*}P + P(-jA_{11}) - PA_{12}R^{-1}A_{12}^{T}P = -Q \qquad (6.2.4)$$

Equation (6.2.4) is clearly a standard form of a continuous complex matrix Riccati equation which is independent of α for all matrices A_{11} and A_{12}. Thus, if θ = 90°, the Riccati equation has the same solution for all values of α, provided that the R matrix is chosen to be the same in each case.

Clearly, for the closed-loop eigenvalues to lie in the required region, the α value must be smaller than all the real negative eigenvalues of $A_{11} - A_{12}F$, where $F = R^{-1}A_{12}^{T}P$. This result holds for all A_{11} and A_{12} matrices, and it is illustrated in the results in Table 6.2.3, and in the results for the robot arm in Table 4.5.2. When $\theta = 90^{\circ}$, the eigenvalues of $A_{11} - A_{12}F$ for this example are -1.648, -2.013 and -3.242 and so the limiting θ value will be 90° for $\alpha \geq -1.648$. When $\alpha = -2$, only one of the eigenvalues of $A_{11} - A_{12}F$ is larger than α and so a small R matrix will give a limiting θ value of 89°, for the five state example. When $\alpha = -3$, two of the eigenvalues of $A_{11} - A_{12}F$ are larger than α and so the limiting θ value is only 67°, for the five state example. When $\alpha < -3$, all three eigenvalues of $A_{11} - A_{12}F$ are larger than α, and the limiting θ value drops quickly to its steady state value of 60°, for the five state example. The robot arm example will have a limit of 90° for all α values, provided that $R_{fact} = 1/\alpha^{2}$.

In general, the limiting value of θ will be 90°, for a suitable choice of the arbitrary R matrix, providing the following condition described above, holds

$$\alpha \geq \max\left[\text{Real}\left\{\lambda_i(A_{11} - A_{12}F)\right\}\right] , \quad i = 1, \ldots, n-m \qquad (6.2.5)$$

where $\text{Real}\{\lambda_i\}$ denotes the real eigenvalues.

When α does not satisfy the condition given in equation (6.2.5), then the limiting θ value will drop back to 60°.

For the robot arm, the reduced order equivalent system matrix A_{11} is zero, and the reduced order equivalent system matrix A_{12} is orthogonal ($A_{12}^{-1} = A_{12}^{T}$), and so it is a special case of the above theory.

Substituting $A_{11} = 0$ into equation (6.2.4) gives

$$-PA_{12}R^{-1}A_{12}^{T}P = -Q \qquad (6.2.6)$$

If $Q = I_{n-m}$ and $R = R_{fact}I_{m}$, then equation (6.2.6) becomes

$$P^{2} = R_{fact}A_{12}A_{12}^{T} \qquad (6.2.7)$$

Since A_{12} is orthogonal, the expression for P becomes

$$P = \sqrt{R_{fact}}\, I \qquad (6.2.8)$$

The control matrix, $F = -R^{-1}A_{12}^{T}P$, is therefore given by

$$F = \frac{-1}{\sqrt{R_{fact}}} A_{12}^{T} \qquad (6.2.9)$$

and the closed-loop reduced order system is given by

$$A_{11} - A_{12}F = \frac{1}{\sqrt{R_{fact}}} I \qquad (6.2.10)$$

The closed-loop eigenvalues are therefore a double root at

$$\lambda = \frac{1}{\sqrt{R_{fact}}} \qquad (6.2.11)$$

If the eigenvalues are required to be $\leq \alpha$, then, from equation (6.2.11), R_{fact} must be chosen to be

$$R_{fact} \leq 1/\alpha^2 \qquad (6.2.12)$$

This result has thus been proved for all systems where the reduced order equivalent system matrices comprise a null matrix A_{11}, and an orthogonal matrix A_{12}. The results for the robot arm in Table 6.2.4 clearly illustrate this result.

In these examples it can be seen that for a suitable choice of the arbitrary matrix, R, the limiting values of θ can be increased, and so the closed-loop eigenvalues of the reduced order equivalent system of a VSC system can be placed in a wider range of regions, including the region which is part of the negative real axis. If the condition in equation (6.2.5) holds then the limiting value of θ will be 90°, otherwise it will fall in stages, until it reaches 60°.

In the particular case where the matrices of the reduced order equivalent system comprise a null matrix A_{11} and an orthogonal matrix A_{12}, the limiting θ value will be 90° for all choices of α, provided R_{fact} satisfies equation (6.2.12). In this case, the solution of the continuous matrix Riccati equation, P, may be found from equation (6.2.8).

6.3 Effect of the R Matrix on Eigenvalue Positioning

The theory of the dependence of the positioning of eigenvalues within a disc on the design of the R matrix will now be investigated for the case of a specified sector in the left-hand half-plane.

For the initial investigation, the five state example was again considered, and the values of α and θ were chosen to be $\alpha = -2$ and $\theta = 30^{\circ}$. The R matrix was altered according to equation (6.2.1), and the resulting eigenvalues are displayed below.

Table 6.3.1 Eigenvalues for $\theta = 30^{\circ}$ and $\alpha = -2$

R_{fact}	Closed-loop Eigenvalues
1	-2.4934 ; -3.1744 ± 0.2119j
2	-2.3253 ; -3.0810 ± 0.2382j
3	-2.2466 ; -3.0457 ± 0.2396j
4	-2.1985 ; -3.0265 ± 0.2386j
5	-2.7122 ; -3.0143 ± 0.2374j
1/2	-2.7122 ; -3.2364 ; -3.4288
1/3	-2.8693 ; -3.1693 ; -3.7682
1/4	-2.9925 ; -3.1624 ; -4.0228
1/5	-3.0761 ; -3.1880 ; -4.2455

It can be seen from the results displayed in Table (6.3.1) that when $R_{fact} \geq 1$, the closed-loop eigenvalues comprise a real value and a complex conjugate pair. When $R_{fact} < 1$, the eigenvalues are all real, and move further away from α as R_{fact} decreases. It would clearly be useful if this result held for all sectors, but it must be noted that for this particular choice of α and θ, the eigenvalues lie within the sector without having to alter the R matrix.

Consider the same example , but let $\theta = 65^\circ$ and $\alpha = -2$, and recall from the previous section that R_{fact} must be 0.6 or smaller for the eigenvalues to lie in the required region. The results for this investigation are shown below.

Table 6.3.2 Eigenvalues for $\theta = 65^\circ$ and $\alpha = -2$

R	Eigenvalues of $A_{11} - A_{12}F$	within sector
1I	-1.9991 ± 0.2090j ; -2.8783	no
0.9I	-2.0314 ± 0.1894j ; -2.8995	no
0.7I	-2.1147 ± 0.1033j ; -2.9559	no
0.6I	-2.0697 ; -2.7140 ; -2.9953	yes
$\begin{pmatrix} 0.6 & 0.5 \\ 0.5 & 0.6 \end{pmatrix}$	-1.9760 ; -2.5869 ; -4.3098	no
$\begin{pmatrix} 0.6 & 0.1 \\ 0.1 & 0.6 \end{pmatrix}$	-2.0525 ; -2.4632 ; -2.8536	yes
0.2I	-2.0826 ; -3.1962 ; -3.5311	yes
0.01I	-2.3740 ; -6.9730 ;-11.2354	yes

It can be seen from the results displayed in Table 6.3.2, that when R_{fact} is greater than 0.6, the eigenvalues comprise a real eigenvalue, which is within the required sector, and a complex conjugate pair of eigenvalues, which are outside the required sector. When R_{fact} is less than or equal to 0.6, the eigenvalues are all real, and are all within the required sector. If the R matrix has some non-zero off-diagonal terms, then the eigenvalues are still real, but are outside the required sector if the off-diagonal terms are very close to the diagonal terms.

These results suggest that if R_{fact} has to be smaller than 1 for the eigenvalues to lie within the required sector, then the eigenvalues will lie in the sector and be purely real. If R_{fact}

can be equal to, or larger than 1, then if R has off-diagonal terms very close to the diagonal terms, the eigenvalues will lie in the sector and be purely real. If the R matrix is a diagonal one, then the eigenvalues will lie in the sector and comprise at least one complex conjugate pair. It also appears that a matrix with off-diagonal terms close to the diagonal terms will place the eigenvalues in the required sector, where a diagonal matrix of the same magnitude will not. Conversely, if a diagonal matrix results in the eigenvalues being just inside the sector, then the introduction of off-diagonal terms of a similar magnitude will push some of the eigenvalues back out of the sector.

To investigate these suppositions, some runs have been carried out for two sectors with the R matrix being altered using two different methods. The first method is to alter R_{fact} from 10 to 1 in steps of 0.5, with $R = R_{fact}I$, and the second method is to alter the leading diagonal in the same way as in the first method, but to choose the off-diagonal terms so that the determinant of R is equal to 0.5. The results for these runs are displayed in the following figures :

Fig 6.1 $\alpha = -2$ $\theta = 30^{\circ}$ $\det(R) = 0.5$

Fig 6.2 $\alpha = -2$ $\theta = 30^{\circ}$ $R = R_{fact}I$

Fig 6.3 $\alpha = -6$ $\theta = 25^{\circ}$ $\det(R) = 0.5$

Fig 6.4 $\alpha = -6$ $\theta = 25^{\circ}$ $R = R_{fact}I$

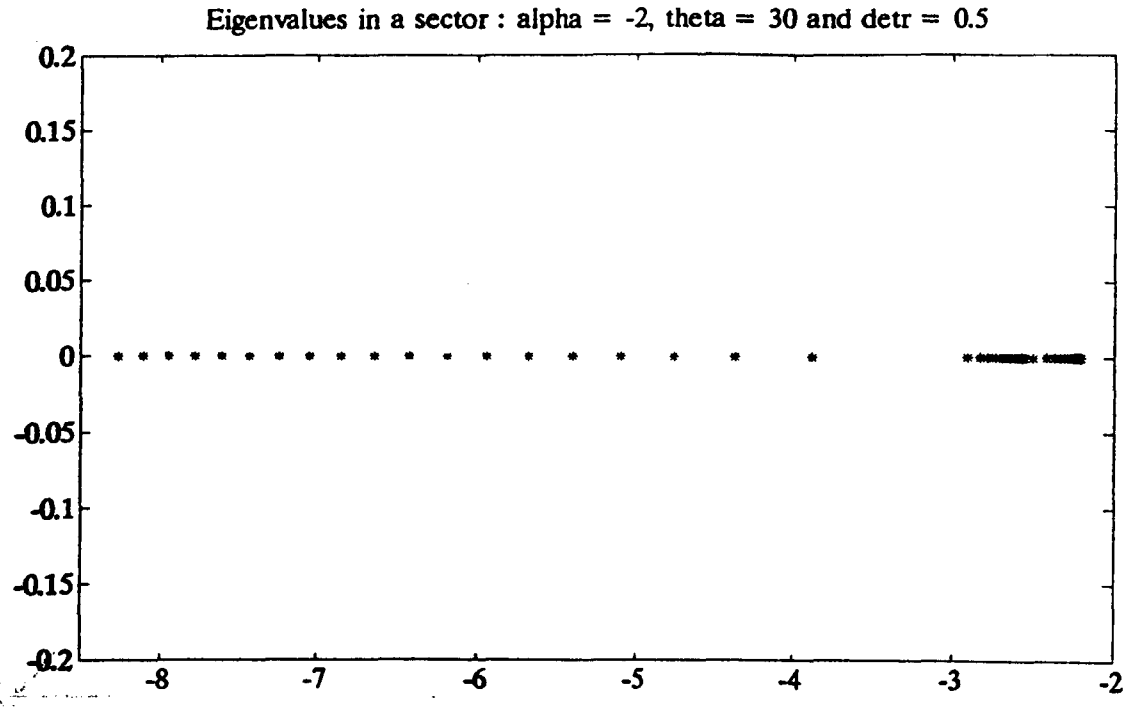

Fig 6.1 Eigenvalues for $\alpha = -2$, $\theta = 30^{\circ}$ and det(R) = 0.5

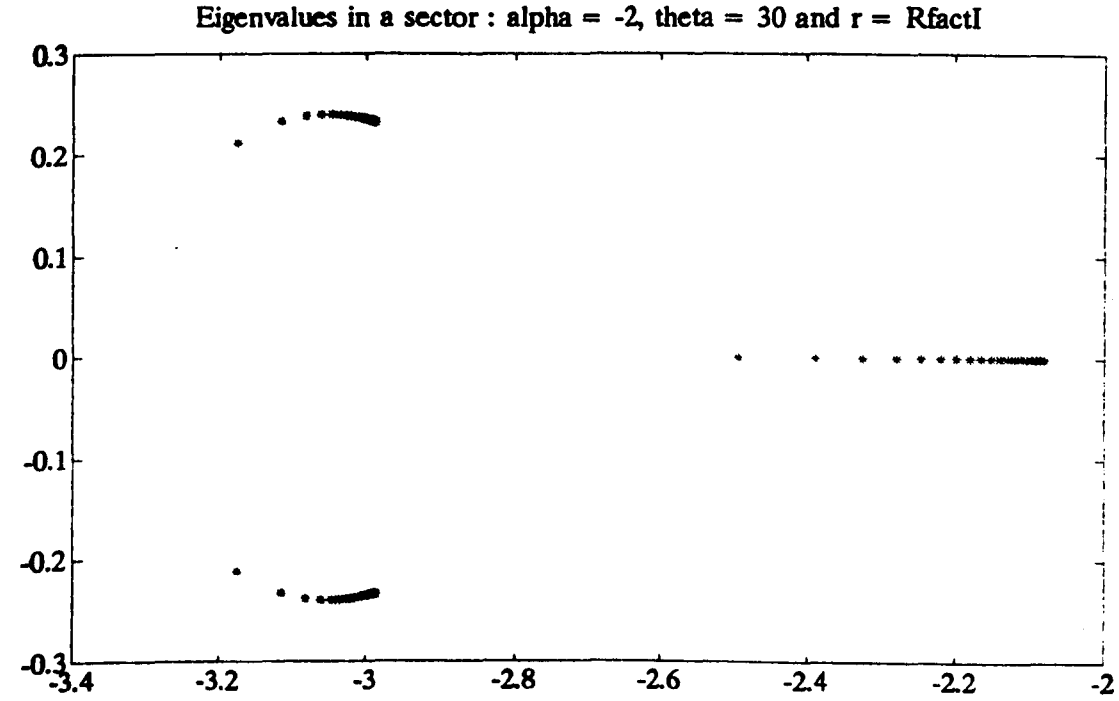

Fig 6.2 Eigenvalues for $\alpha = -2$, $\theta = 30^{\circ}$ and $R = R_{fact}I$

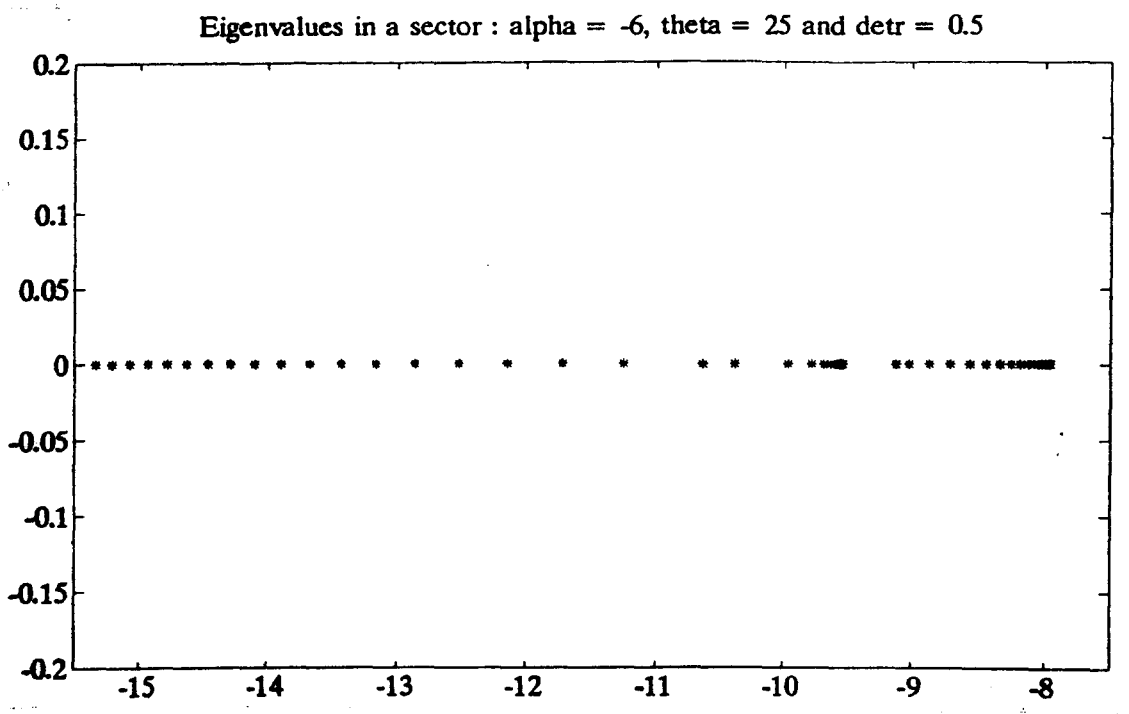

Fig 6.3 Eigenvalues for $\alpha = -6$, $\theta = 25^{\circ}$ and det(R) = 0.5

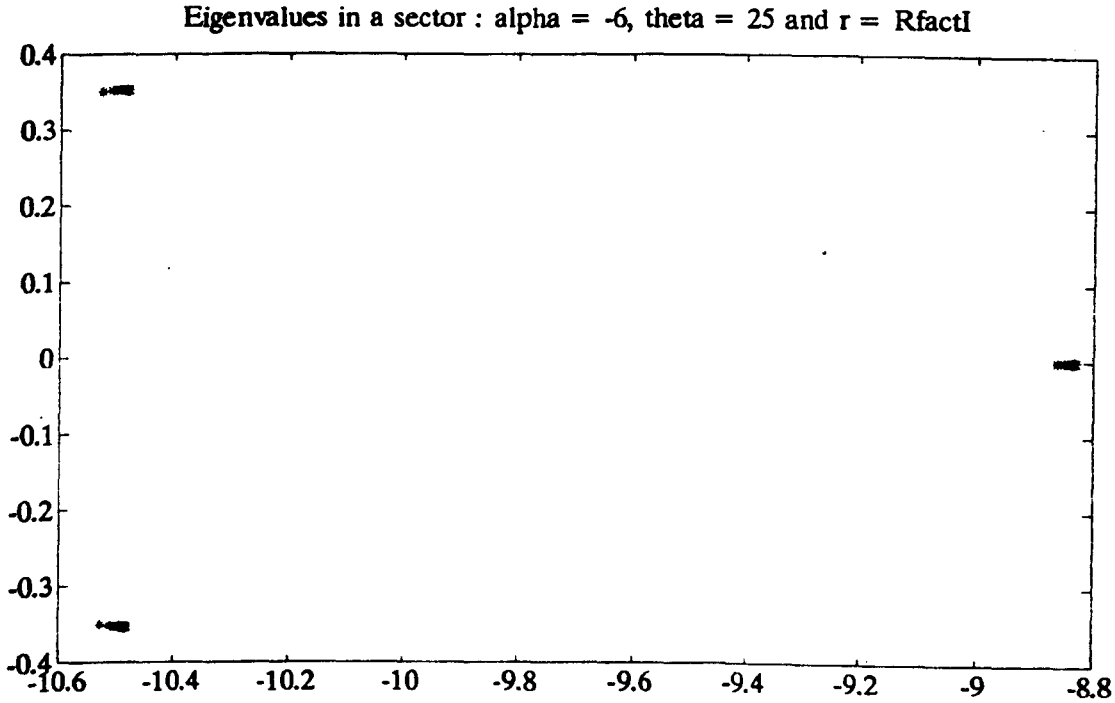

Fig 6.4 Eigenvalues for $\alpha = -6$, $\theta = 25^{\circ}$ and R = $R_{fact}I$

It can be seen from figures 6.1 and 6.2, that introducing non-zero off-diagonal terms to the R matrix, so that its determinant is equal to 0.5 places all the eigenvalues on the real axis. When the off-diagonal terms are zero, the eigenvalues comprise a real value and a complex conjugate pair. These results are repeated for the second sector, as can be seen from figures 6.3 and 6.4. This result will only hold if the eigenvalues are within the required sector for the diagonal R matrix.

An investigation into the largest diagonal R matrix, and the largest non-diagonal matrix required to place the eigenvalues within the required sector has been carried out for various sectors. The results are displayed below.

Table 6.3.3 Largest R matrices for placement within the sector

α	θ°	R_{fact}	Eigenvalues	R_{ii}	R_{ij}	Eigenvalues
0	80	0.7	-1.39±0.24j;-2.56	1×10^8	9.99×10^8	-1.20;-1.90;-3.63
-1	65	0.8	-1.54±0.24j;-2.52	1×10^8	9.99×10^8	-1.29;-1.94;-3.86
-2	75	0.05	-2.01;-4.21;-5.52	-	-	-
-3	60	0.05	-3.01;-5.05;-6.41	-	-	-
-4	55	0.07	-4.03;-6.00;-6.70	0.02	0.0199	-4.02;-4.84;-34.1
-5	58	0.01	-5.08;-9.11;-13.2	-	-	-
-10	56	0.01	-10.2;-14.1;-17.2	0.1	0.099	-10.7;-11.4;-38.1

It can be seen from the results displayed in Table 6.3.3 that for some sectors, it is possible to use a very large R matrix, provided its determinant is small, and still have the eigenvalues within the required region. For other sectors, the largest R matrix which places the eigenvalues within the sector is that of the form $R = R_{fact}I$.

It is clearly possible to have some control over the form of the eigenvalues, in other words whether they are real or complex, depending on the sector chosen. In general, if R_{fact} has to be smaller than 1, with the R matrix given by $R_{fact}I$, for the closed-loop eigenvalues to be within the required sector, then the eigenvalues will be real. If the leading diagonal elements of R are ≥ 1, with the off-diagonal elements close to the leading diagonal elements, and the closed-loop eigenvalues are within the required sector, then they will also be real. If a matrix of the form $R_{fact}I$, where R_{fact} is a positive scalar, places the closed-loop eigenvalues within the required sector then some of the eigenvalues will be complex. If the R matrix has to be very small, in other words R_{fact} must be small, to place the eigenvalues within the required sector, then there is little scope for moving them around within the sector.

In the particular case when the reduced order system matrices comprise a null matrix A_{11} and an orthogonal matrix A_{12} (for example, the robot arm system), the closed-loop eigenvalues are given by equation (6.2.11). It is clear from this equation that the eigenvalues will always be real, since the arbitrary matrix, R, from the continuous matrix Riccati equation, must be positive definite, and hence the scalar R_{fact} cannot be either negative or zero.

6.4 Discussion

It can be seen, therefore, that the closed-loop eigenvalues of a VSC system may be placed in a wider range of sectors than was previously supposed (section 4.5), provided that the arbitrary R matrix from the continuous matrix Riccati equation is chosen appropriately. Some general rules have been verified, for systems of the form given in equation (2.2.2), and they are as follows :

1) If α is $\geq$ the largest real closed-loop eigenvalue of the reduced order equivalent system, then the limiting θ value will be 90°, for a suitable (small) choice of the R matrix.
2) If α is $<$ the largest real closed-loop eigenvalue of the reduced order equivalent system, then the limiting θ value drops to 60°, for a suitable choice of the R matrix.
3) For the particular case when the system matrices of the reduced order equivalent system comprise a null matrix A_{11} and an orthogonal matrix A_{12}, provided that the R matrix is chosen to be I/α^2, the limiting θ value will be 90°, for all choices of α.

The above conditions may be successfully applied to the reduced order equivalent systems of all systems of the general form given in equation (2.2.2). It is therefore possible to ensure that the closed loop eigenvalues lie within the required sector, provided that the sector chosen satisfies these conditions.

The positioning of the eigenvalues within the required sector has also been considered, and some control over their form, real or complex, is available. The following general conditions have been deduced

1) If the R matrix has to be smaller than the identity matrix for the eigenvalues to be within the required sector, then the eigenvalues will all be real.
2) If an R matrix which is larger than the identity matrix will place the eigenvalues within the required sector, then the eigenvalues will be real and complex if R is a scalar multiple of the identity matrix, and purely real if the R matrix has off-diagonal elements very close to the leading diagonal elements.
3) In the particular case when the system matrices of the reduced order equivalent system comprise a null matrix A_{11} and an orthogonal matrix A_{12}, the eigenvalues will always be real.

It is clearly possible to force the eigenvalues to be either all real, or a mixture of real values and complex conjugate pairs for some sectors in the left-hand half-plane. The properties above, coupled with the conditions on the R matrix for the eigenvalues to be in the required sector, enable the eigenvalue forms to be predicted, and in some cases influenced.

7. MINIMIZATION OF THE LINEAR CONTROL

7.1 Introduction

In this chapter, the effect of "minimizing" the linear part of the control is investigated. The technique of finding an optimal control which minimizes the performance index of a system, is well-known (see for example, Anderson and Moore, 1969 & 1971, Grimble and Johnson, 1988). Work has also been done on optimal eigenstructure assignment (see for example Fahmy and O'Reilly, 1982, Kautsky, Nichols and Van Dooren, 1985, Burrows and Patton, 1990, a & b). Little work appears to have been done regarding minimizing the control effort of a VSC system. It is clearly more efficient to use the smallest effective control possible, bearing in mind other design considerations such as the choice of the closed-loop eigenvalues. The choice of both the the sliding hyperplanes and the m remaining eigenvalues for the linear feedback system affect the form of the linear control. If the sliding mode eigenvalues are being chosen explicitly, then there is no flexibility for minimizing the linear part of the control, except by suitable choice of the m remaining eigenvalues. If, however, the sliding mode eigenvalues are simply required to be in a particular region of the left-hand half-plane then there is clearly scope for positioning the eigenvalues within the chosen region and minimizing the linear part of the control. It is therefore possible to combine one of the eigenvalue assignment methods outlined in Chapters 3 and 4 with a minimization of the linear part of the control, and this will now be considered. It

is not possible to predict the effect of this minimization on the resulting control, or on the performance. The effects of both the sliding mode eigenvalues and the m remaining eigenvalues on the control magnitude, and on the performance will be investigated in this chapter.

Section 7.2 contains an outline of the theory of controller design, once the sliding hyperplanes have been chosen, and the C matrix calculated, and these results are used in later sections. Section 7.3 contains an investigation of the effect of minimizing the 2-norm of the linear part of the control, using the robot arm simulation outlined in Chapter 2. Section 7.4 contains an investigation into the effect of minimizing the condition number of the closed-loop matrix for the linear part of the control, again using the robot arm simulation. Section 7.5 contains a brief discussion of the results.

7.2 Controller Design Theory

Once the sliding hyperplane matrix, C, has been chosen, using one of the methods outlined in previous chapters, the state feedback control function $u : \mathcal{R}^n \rightarrow \mathcal{R}^m$ must be selected. The function of u is to drive the state x into the null space of C, and then to maintain it within this subspace. In general, the variable structure control law consists of two parts, a linear part u^L and a non-linear part u^N, and these are added together to form the control u.

$$u = u^L + u^N \tag{7.2.1}$$

The linear control, u^L, is a state feedback controller of the form

$$u^L(x) = Lx \tag{7.2.2}$$

The nonlinear control, u^N, incorporates the discontinuous elements of the control law, and has several possible forms which have been discussed elsewhere (Zinober, 1991, Young, 1977, Ryan, 1983). Here, the unit vector method, (Ryan & Corless, 1984) will be considered, which works on the principle of rapid motion onto a subspace within the state space, followed by slower transient motion within the subspace, which approaches the state space origin asymptotically. The individual controls are continuous, except on the final intersection of the hyperplanes, $\mathcal{N}(C)$, where all the controls are discontinuous together. The design technique ensures that the motion is always towards the final target, the null space of C, $\mathcal{N}(C)$. The control structure has the form

$$u(x) = Lx + \frac{\rho}{\|Mx\|} Nx \tag{7.2.3}$$

where the null spaces of N, M and C are coincident.

$$\mathcal{N}(N) = \mathcal{N}(M) = \mathcal{N}(C) \tag{7.2.4}$$

Recall the transformed state y, outlined in Chapter 2, which is of the form $y = Tx$, and the transformed system

$$\dot{y} = TAT^T y + TBu \qquad \text{with} \qquad CT^T y = 0 \tag{7.2.5}$$

Consider a second transformation, $T_2 : \mathcal{R}^n \rightarrow \mathcal{R}^n$, of the form

$$z = T_2 y \tag{7.2.6}$$

where

$$T_2 = \begin{bmatrix} I_{n-m} & 0 \\ F & I_m \end{bmatrix} \tag{7.2.7}$$

F is the control matrix for the reduced order equivalent system. The inverse of T_2 is given by

$$T_2^{-1} = \begin{bmatrix} I_{n-m} & 0 \\ -F & I_m \end{bmatrix} \tag{7.2.8}$$

Partition z into $z_1 \in \mathcal{R}^{n-m}$ and $z_2 \in \mathcal{R}^m$, so that $z^T = [z_1^T \; z_2^T]$. Equation (7.2.6) may then be similarly partitioned to give the system equations of the second transformation

$$z_1 = y_1 \tag{7.2.9a}$$

$$z_2 = Fy_1 + y_2 \tag{7.2.9b}$$

The transformed system equations are therefore

$$\begin{aligned} y_1 &= z_1 \quad \rightarrow \quad \dot{y}_1 = \dot{z}_1 \\ y_2 &= z_2 - Fz_1 \quad \rightarrow \quad \dot{y}_2 = \dot{z}_2 - F\dot{z}_1 \end{aligned} \tag{7.2.10}$$

Recall from Chapter 2 that the partitioned system equations of the reduced order system resulting from the first transformation, T are

$$\dot{y}_1 = A_{11} + A_{12}y_2 \tag{7.2.11}$$

$$\dot{y}_2 = A_{21}y_1 + A_{22}y_2 + B_2u \tag{7.2.12}$$

Substituting for y_1 and y_2 from equation (7.2.10) into equation (7.2.11) and rearranging gives

$$\dot{z}_1 = (A_{11} - A_{12}F)z_1 + A_{12}z_2 \qquad (7.2.13)$$

Substituting for y_1 and y_2 from equation (7.2.10) into equation (7.2.12) gives

$$\dot{z}_2 - F\dot{z}_1 = A_{21}z_1 + A_{22}z_2 - A_{22}Fz_1 + B_2u \qquad (7.2.14)$$

Substituting for $\dot{z}_1$ from equation (7.2.13) into equation (7.2.14) and rearranging gives

$$\dot{z}_2 = (A_{21}-A_{22}F+FA_{11}-FA_{12}F)z_1 + (A_{22}+FA_{12})z_2 + B_2u \qquad (7.2.15)$$

Equations (7.2.13) and (7.2.15) may be simplified by using the following substitutions

$$\Sigma = A_{11} - A_{12}F$$

$$\Psi = A_{22} + FA_{12}$$

$$\chi = A_{21} - A_{22}F + FA_{11} - FA_{12}F = A_{21} - A_{22}F + F\Sigma$$

Substituting for these expressions in equations (7.2.13) and (7.2.15) gives

$$\dot{z}_1 = \Sigma z_1 + A_{12}z_2 \qquad (7.2.16)$$

$$\dot{z}_2 = \chi z_1 + \Psi z_2 + B_2u \qquad (7.2.17)$$

In order to obtain the sliding mode, z_2 and $\dot{z}_2$ must be forced to zero. If $\dot{z}_2$ is zero, equation (7.2.17) becomes

$$B_2u = -\chi z_1 - \Psi z_2 \qquad (7.2.18)$$

Now, recalling that B_2 is an m×m non-singular matrix, define the linear part of the control to be

$$u^L(z) = -B_2^{-1}\left[\chi z_1 + (\Psi - \Psi_*) z_2\right] \qquad (7.2.19)$$

where Ψ_* is any m×m matrix with left-hand half-plane eigenvalues.

Given a real spectrum $\left\{\zeta_i : \text{Real}(\zeta_i) < 0,\ i = 1,\ldots,m\right\}$, generally known as the range space eigenvalues, Ψ_* may be set to $\text{diag}\left\{\zeta_i : i = 1,\ldots,m\right\}$.

Transforming equation (7.2.19) back to the original x space, recalling that $z = T_2 y$ and $y = Tx$, gives

$$L = -B_2^{-1}\left[\chi \quad (\Psi - \Psi_*)\right] T_2 T \qquad (7.2.20)$$

The linear part of the control, u^L, will drive the state component z_2 to zero asymptotically, since substituting for u from equation (7.2.19) into equation (7.2.17) gives $\dot{z}_2 = -\Psi_* z_2$. The non-linear part of the control, u^N, must be designed so as to attain $\mathcal{N}(C)$ in finite time. The non-linear control is discontinuous when $z_2 = 0$, and continuous elsewhere. Let P_D be the unique positive definite solution of the Lyapunov equation

$$P_D\Psi_* + \Psi_*^T P_D + I_m = 0 \qquad (7.2.21)$$

Then $P_D z_2 = 0$ if and only if $z_2 = 0$.

The linear control can be chosen to be

$$u^N(z) = \frac{-\rho}{\left|P_D z_2\right|} B_2^{-1} P_D z_2 \qquad (z_2 \neq 0) \tag{7.2.22}$$

where $\rho > 0$ is a scalar parameter selected by the designer to be sufficiently large.

When $z_2 = 0$, u^N is undefined, so it may be arbitrarily defined to be any function satisfying $\left|u^N\right| \leq \rho$. The control $u = u^L + u^N$ is then given by

$$u = -B_2^{-1}\left[\chi z_1 + (\Psi - \Psi_*) z_2\right] - \frac{\rho}{\left|P_D z_2\right|} B_2^{-1} P_D z_2 \tag{7.2.23}$$

This control will drive an arbitrary initial state z° to the sliding subspace in time τ, given by

$$\tau \leq \frac{1}{\rho}\sqrt{\frac{\langle z_2^\circ, P_D z_2^\circ\rangle}{\sigma_{min}(P_D)}} \tag{7.2.24}$$

where $\sigma_{min}(P_D)$ denotes the minimum eigenvalue of P_D and $\langle .,. \rangle$ denotes the Euclidean inner product on $\Re^m$. Transforming the nonlinear control into x space gives

$$N = -B_2^{-1}\begin{bmatrix} 0 & P_D \end{bmatrix} T_2 T \tag{7.2.25}$$

$$M = \begin{bmatrix} 0 & P_D \end{bmatrix} T_2 T \tag{7.2.26}$$

Therefore, the control in x space is given by equation (7.2.3).

To minimize the control effort required to drive the state onto the subspace, it is clearly necessary to "minimize" the linear part of the control in some way, and two possibilities will now be considered. The linear part of the control, L, depends on the choice of the control matrix, F, as can be seen from equation (7.2.20). It is clear, therefore, that there are restrictions on the design on the linear part of the control, imposed by the design of the control matrix F and the range space eigenvalues.

If the sliding mode eigenvalues are being explicitly chosen, then there is clearly no scope for minimizing the linear part of the control by a suitable choice of the control matrix, since it has therefore been fixed. The sliding mode eigenvalue placement methods in Chapters 3 and 4 offer some degree of flexibility in the F matrix, and hence in the choice of L, since they only require the eigenvalues to be within a particular region of the left-hand half-plane. A method for the minimization of the linear part of the control will therefore be investigated for these methods. A similar method could be applied to exact sliding mode eigenvalue placement techniques, provided that there were tolerances on the required positions of the closed-loop eigenvalues. The choice of the range space eigenvalues has an effect on both the linear part and the non-linear part of the control, and so a suitable choice could lead to a minimization of the linear part of the control.

7.3 Minimization of the 2-norm of L

The 2-norm of a matrix may be defined to be the maximum value of the ratio between the norm of the product of the matrix with a vector, and the norm of the vector. This shows the amount by which the transformation can magnify the Euclidean norm of the vector. The 2-norm of the linear control gives the magnification of the distance of any vector from the origin, by the controller. Since the function of the linear control is to drive the state to the origin, it seems appropriate to try to minimize this magnification. It is not feasible to minimize the 2-norm of L, and hence the linear control effort, at each time step, and so the 2-norm of the control matrix L will be minimized by a suitable choice of the closed-loop eigenvalues of the reduced order equivalent system. A suitable choice of the range space eigenvalues will decrease the value of the 2-norm of L. Some work has been done eigenstructure assignment for a low norm linear feedback control law (Burrows and Patton, 1990, a & b).

Consider first the effect of minimizing the 2-norm of the linear part of the control, L, on the control effort. The 2-norm of L is defined to be

$$\|L\|_2 = \max_{x \neq 0} \frac{\|Lx\|}{\|x\|} = \sqrt{\lambda_{max}[L^T L]} \qquad (7.3.1)$$

where λ_{max} is the maximum eigenvalue of $[L^T L]$.

In the first instance, this investigation was carried out using the optimization package in MATLAB, and in particular the routine "attgoal" (Grace, 1990). This is a very general routine which attempts to minimize the objectives returned by a user-given function, using a sequential quadratic programming method. The goal values are given by the user, along with weighting values for the goals. The initial value of a design variable k must be chosen, along with its bounds. k is varied by the routine to try to achieve the goals, and can be a scalar or a matrix.

For our investigation we require the 2-norm of L to be minimized whilst the closed-loop eigenvalues remain in the sector (section 4.2). The variable k will be used to alter the R matrix as follows

$$newr = k*R \tag{7.3.2}$$

where k is a positive scalar, and R is fixed by the designer.

For the sector, the goal is to minimize $\|L\|_2$ whilst placing all the closed-loop eigenvalues of the reduced order equivalent system within a sector specified by α and θ (section 4.2). Since the requirement for the eigenvalues to be within the required sector is a rigid one, a switch variable, reg_pen, is set up, and is given the value 1 if the eigenvalues are within the required sector, and 10 otherwise. The weighting value for reg_pen must be zero, since all of the closed-loop eigenvalues must be within the required sector, even if the value of $\|L\|_2$ is not minimized.

Consider again the five state example, and choose $\alpha = -2$, $\theta = 30^{\circ}$, and the range space eigenvalues, ζ_m, to be [-2.5,-5]. Using the eigenvalue placement technique outlined in section 4.2, with $Q = I_{n-m}$ and $R = I_m$, gives the closed-loop eigenvalues of $A_{11} - A_{12}F$ as -2.4934 and -3.1744 ± 0.2119j, which are within the required sector, so reg_pen = 1. The initial value of $\|L\|_2$ is 19.499 and the initial value of k is 1.

The following results are obtained after 202 steps, with the closed-loop eigenvalues within the required sector :

$\|L\|_2 = 14.0072$ k = 27.1509

Closed-loop eigenvalues : -2 and -2.9643 ± 0.2272j

It is clear that the closed-loop eigenvalues are within the required sector, and that $\|L\|_2$ is smaller than it was for k = 1, but the minimum has not been reached after 202 steps, and the computational time is excessive.

As as a second example, using the same five state system, choose $\alpha = -2$ and $\theta = 65^{\circ}$, with the same range space eigenvalues. Using the same eigenvalue placement technique as for the previous case, with $Q = I_{n-m}$ and $R = I_m$, gives the closed-loop eigenvalues of $A_{11} - A_{12}F$ as -2.8783 and -1.9991 ± 0.2091. These eigenvalues are clearly not all in the sector, so reg_pen = 10. The initial value of $\|L\|_2$ is 11.4911, and this will probably increase since the eigenvalues are not all in the sector. k is chosen to be 1.

The following results were obtained after 202 steps, with some of the closed-loop eigenvalues outside the required sector :

$\|L\|_2 = 11.4911 \quad k = 1$

Closed-loop eigenvalues : -2.8783 and -1.9991 ± 0.2091j

It is clear that after 202 steps, there is no change in k and two of the eigenvalues are still outside the required sector.

There are clearly problems with using this very general optimization package with a discontinuous variable such as reg_pen. The main difficulty is that the eigenvalues are either within the required sector, or outside it, and attgoal seems to find it difficult to cope with a variable which switches between two values, as reg_pen does, rather than continuously iterating with each step. This results in the program oscillating between two k values and being unable to find an acceptable answer. Alternatively, k may be moved in the *wrong* direction, since the program is unable to tell which direction is correct from reg_pen.

To overcome this problem, a more specific MATLAB routine has been written, which can cope with the variable reg_pen switching between two values, and will not search in the wrong direction for a large number of steps. This routine uses an iterative one-variable search to find the R matrix which will minimize the 2-norm of L.

The R matrix is altered as outlined in equation (7.3.2) by a positive scalar, R_{fact}, which is increased or decreased, until :

1) the minimum of $\|L\|_2$ is obtained.
2) the "computational steady state" of min$\|L\|_2$ is obtained.
3) the smallest possible value of $\|L\|_2$ is obtained, whilst still having the closed-loop eigenvalues within the required sector.

The "computational steady state" of the minimum is defined as a value which changes marginally ($< 1\times10^{-6}$) for a step change in R_{fact}

Table 7.3.1 contains the results for various sectors with the value of $\|L\|_2$ for $R_{fact} = 1$, $\left(\|L\|_2\right)_o$ and the value of reg_pen for $k = 1$, $\bar{rp}_o$ given for comparison. The ζ_i are the range space eigenvalues, $\left(\|L\|_2\right)_{min}$ is the minimum $\|L\|_2$ value, and δs is the number of steps taken to reach the minimum. rp represents the final value of reg_pen, and an indication is given of whether the minimum value has been reached.

Table 7.3.1 Minimum $\|L\|_2$ values for various sectors

θ°	α	rp_o	$\left(\|L\|_2\right)_o$	ζ_i	$\left(\|L\|_2\right)_{min}$	δs	rp	R_{fact}	Minimum reached
30	-2	1	12.9599	-2.5;-3.5	9.4352	14	1	25	Y
60	-2	1	8.4912	-2.5;-3.5	8.4912	22	1	1	Y
65	-2	10	7.7137	-2.5;-3.5	8.7343	27	1	0.6	Y
35	-4	1	175.1379	-4.0;-8.0	169.4164	22	1	110	Y
60	-4	10	77.4880	-4.0;-8.0	224.3618	42	1	0.01	Y
20	-6	1	617.3135	-4.0;-8.0	614.2129	16	1	40	Y
55	-6	10	244.0771	-4.0;-8.0	328.0779	39	1	0.04	Y

It can be seen from the results displayed in Table 7.3.1 that in all cases a minimum value of $\|L\|_2$ is reached, and the closed-loop eigenvalues of the reduced order equivalent system are within the required sector. Three of the cases listed in Table 7.3.1 initially have eigenvalues outside the required sector ($rp_o = 10$), and it can be seen that the method used finds the smallest value of $\|L\|_2$ for which the eigenvalues are within the required the sector.

This specialized routine is clearly successful for the particular problem of minimizing a system containing a discontinuous variable, and the number of steps required is not too large, even in the cases where the eigenvalues are initially outside the required sector.

It can be seen from the results in Table 7.3.1 that for some sectors, $\theta = 30^\circ$ and $\alpha = -2$ for example, it is possible to alter the value of $\|L\|_2$ by a reasonable amount (~ 25%), and for other sectors, $\theta = 35^\circ$ and $\alpha = -4$ for example, the value of $\|L\|_2$ is not altered very much (< 4%). In the case of $\theta = 60^\circ$ and $\alpha = -2$, for example, the minimum value of $\|L\|_2$ occurs when $R = I_m$. There is clearly a lot of variation in the value of $\|L\|_2$ for the various sectors, and a lot of difference in its minimum value, and so the effect on the linear part of the control will vary depending on which sector is being considered.

It can also be seen from the results in Table 7.3.1 that as R_{fact} increases, the value of $\|L\|_2$ decreases. It was observed from the results obtained in section 6.2 that as R_{fact} decreases, the eigenvalues move away from the origin, and further into the sector. It is therefore clear that there is a trade-off between the value of R_{fact} which gives the minimum value of $\|L\|_2$, and the value of R_{fact} which results in the eigenvalues being in the required sector. If the eigenvalues lie well within the required sector when $R = I_m$, and hence $R_{fact} = 1$, then there is clearly scope for increasing the size of R_{fact} without pushing the eigenvalues out of the sector, and so $\|L\|_2$ may be minimized. If, however, the eigenvalues are only just in the sector when $R_{fact} = 1$, or if R_{fact} had to be decreased to push the eigenvalues into the required sector, then there is clearly very little scope for altering R_{fact}, and hence very little scope for minimizing $\|L\|_2$ by choice of the control matrix.

The method for placing the closed-loop eigenvalues of the reduced order equivalent system in a disc may also be adapted for the minimization of $\|L\|_2$. This method, outlined in section 3.2, was found to place the closed-loop eigenvalues within the required disc for all positive choices of R_{fact}, as can be seen from the robustness results presented in section 5.2.

The minimization of $\|L\|_2$ whilst placing the closed-loop eigenvalues within various discs will now be investigated.

The results for the various discs, of radius r and centre α, are given in Table 7.3.2.

Table 7.3.2 Minimum $\|L\|_2$ values for various discs

α	r	$\left(\|L\|_2\right)_o$	ζ_1	$\left(\|L\|_2\right)_{min}$	δs	R_{fact}	Min/st-st reached
-6	4	14.7742	-2;-4	10.1634	70	195310	Y
-6	2	138.0144	-4;-8	136.7579	17	45	Y
-6	6	5.0419	-1;-6	4.6391	22	110	Y
-4	1	43.2668	-1;-6	42.3589	20	60	Y
-4	4	5.0050	-1;-6	4.6390	22	110	Y
-3	1	11.5615	-2;-4	8.6177	70	195310	Y

It can be seen from the results displayed in Table 7.3.2, that $\|L\|_2$ is minimized within a reasonable number of steps for the various combinations of α and r. It can also be seen that if the difference between α and r is the same then, regardless of their actual values, the values of $\|L\|_2$ for $R_{fact} = 1$, and the minimum of $\|L\|_2$ are very similar. It was noted in section 5.2 that, as R_{fact} is increased, some, or all of the closed-loop eigenvalues are moved towards the right-hand edge of the disc. It can be seen from the results in Table 7.3.2, that as R_{fact} increases, the value of $\|L\|_2$ decreases, until either a minimum or a "computational steady state" value is reached. There is no problem, with this method, of the closed-loop eigenvalues moving out of the required disc, for large values of the scalar R_{fact}. The closed-loop eigenvalues will always lie in the required disc, for any positive definite choice of the matrix R.

It is also possible to minimize $\|L\|_2$ by choosing appropriate values for the range space eigenvalues. The effect of this minimization method will be harder to predict, since the choice of the range space eigenvalues also affects the non-linear part of the control, as can be seen from equation (7.2.22). A MATLAB routine which linearly alters the range space eigenvalues until the minimum of $\|L\|_2$ is reached has been written. There is clearly a restriction on the choice of the range space eigenvalues, since they must be negative.

The results for the five state system for various sectors are displayed below, with the initial value of ζ_1 being [-1 -10] in each case.

Table 7.3.3 Minimum $\|L\|_2$ values for different choices of ζ_1

θ°	α	$\left(\|L\|_2\right)_o$	ζ_1	$\left(\|L\|_2\right)_{min}$	δs
30	-2	41.6831	-0.92;-2	6.8334	17
60	-2	27.0482	-0.92;-2	4.6394	17
35	-4	222.4532	-0.92;-2	33.4322	17
20	-6	786.9282	-0.92;-2	120.0821	17
40	-6	532.7077	-0.92;-2	80.8720	17

It can be seen from the results displayed in Table 7.3.3 that the minimization of $\|L\|_2$ is affected much more by the choice of the range space eigenvalues, than by the choice of the sliding mode eigenvalues. In each case, the value of $\|L\|_2$ is altered by about 80% which is a bigger difference than was obtained by altering the control matrix, and also gives consistent results

which are independent of the sector chosen. It is possible that a combination of these results for choices of control matrix and range space eigenvalues will give good performance results, and this will now be investigated.

It has been shown, therefore, that the value of $\|L\|_2$ may be minimized by a suitable choice of the value R_{fact}, whilst still having the closed-loop eigenvalues of the reduced order equivalent system within the required sector or disc. It has also been shown that the value of $\|L\|_2$ may be minimized by a suitable choice of the range space eigenvalues. However, it is difficult to assess the effect of the minimization of $\|L\|_2$ on the performance of a system, since the choice of the control matrix, F, and the choice of the range space eigenvalues affect the components of the linear part of the control, and the choice of the range space eigenvalues affects the non-linear part of the control, as can be seen from equation (7.2.22). It is clearly not easy to predict, in general, the effect of altering the non-linear part of the control on a system. The effect must be considered for each particular example separately.

The numerical example which will now be considered is the model-following example of the robot arm, described in Chapter 2. This example has been chosen since it will be possible to see the effect of minimizing $\|L\|_2$ on the θ_r and ϕ_r errors of the robot arm, as well as on the components of the control.

Firstly, a suitable choice of a sector must be made, so that the minimum value of $\|L\|_2$ differs as much as possible from its value when $R_{fact} = 1$, to enable the differences in the results to show up clearly.

The system matrices, the transformation matrix, T, and the matrices of the reduced order equivalent system for the robot arm are obtained in section 3.4, and the simulation of the performance of the robot arm is discussed in section 2.4.

Consider various sectors for the closed-loop eigenvalues of the reduced order equivalent system of the robot arm system to lie within. The results of the investigation into the sector which gives the biggest change in the value of $\|L\|_2$ are displayed in Table 7.3.4. The variables displayed in this table are the same as those displayed in Table 7.3.1, and the range space eigenvalues are initially set to [-1 -10].

Table 7.3.4 Minimum $\|L\|_2$ values for various sectors

α	θ°	rp_o	$\left(\|L\|_2\right)_o$	$\left(\|L\|_2\right)_{min}$	δs	rp	R_{fact}	minimum reached
-2	30	1	0.3805	0.3556	28	1	260	Y
-2	40	1	0.3460	0.3186	29	1	285	Y
-2	60	1	0.2592	0.2225	33	1	685	Y
-4	30	1	0.6968	0.6835	19	1	55	Y
-6	30	1	1.0241	1.0152	17	1	45	Y
-1	30	1	0.2391	0.1993	35	1	935	Y
-1	60	1	0.1896	0.1409	39	1	1435	Y
-1	10	1	0.2596	0.2198	34	1	810	Y
-0.5	30	1	0.1817	0.1314	39	1	1435	Y

It can be seen from the results displayed in Table 7.3.4 that the biggest percentage difference between the value of $\|L\|_2$ when $R_{fact} = 1$, and its minimum value, occurs when $\alpha = -0.5$ and $\theta = 30°$. The robot arm simulation will be run for this sector with both the nominal value of $\|L\|_2$ and its minimized value.

The simulation will also be run for the minimization of $\|L\|_2$ by choice of the range space eigenvalues, for comparison.

The minimization of $\|L\|_2$ by choice of the range space eigenvalues will now be investigated for the robot arm. Again, the sector giving the biggest difference between the initial and minimized values of $\|L\|_2$ is required. The initial choice of the range space eigenvalues is [-1 -10].

Table 7.3.5 Minimum $\|L\|_2$ values for different choices of ζ_1

$\theta°$	α	$\left(\|L\|_2\right)_o$	ζ_1	δs	$\left(\|L\|_2\right)_{min}$
30	-2	0.3805	-0.92;-2	17	0.0902
40	-2	0.3460	-0.92;-2	17	0.0823
60	-2	0.2592	-0.92;-2	17	0.0621
30	-4	0.6968	-0.92;-2	17	0.1624
30	-6	1.0241	-0.92;-2	17	0.2367
30	-1	0.2391	-0.92;-2	17	0.0547
60	-1	0.1896	-0.92;-2	17	0.0445
10	-1	0.2569	-0.92;-2	17	0.0616
30	-0.5	0.1817	-0.92;-2	17	0.0435

It can be seen from the results displayed in Table 7.3.5 that the percentage differences between the initial value of $\|L\|_2$ and the minimum value of $\|L\|_2$ are the same for all of the sectors

investigated. Again, the minimization of $\|L\|_2$ by the appropriate choice of the range space eigenvalues, appears to be more effective than the minimization by choice of the sliding mode eigenvalues. This method of minimizing $\|L\|_2$ is also more consistent, since the results do not depend on the choice of sector. The robot arm simulation will therefore be run for the sector defined by $\alpha = -0.5$ and $\theta = 30^\circ$, for ease of comparison with the minimization by choice of sliding mode eigenvalues method.

The results of the simulation runs for the three examples, for θ_r error, ϕ_r error, u1 and u2 are displayed in figures 7.1 to 7.6, with the parameters as follows :

Fig 7.1 & 7.2	Plots for ζ_i = [-1 -10] and $\|L\|_2$ not minimized
Fig 7.3 & 7.4	Plots for $\|L\|_2$ minimized by sliding mode design
Fig 7.5 & 7.6	Plots for $\|L\|_2$ minimized by range space design

The errors in all these cases are larger than for the run in Chapter 2, which is due, in part, to coupling effects between the angles. The simulation run in section 2.4 used partial eigenvector assignment to remove this coupling effect, which resulted in very small errors. The eigenvector assignment has not been included for these investigations, since it would mask the effects of the minimizations.

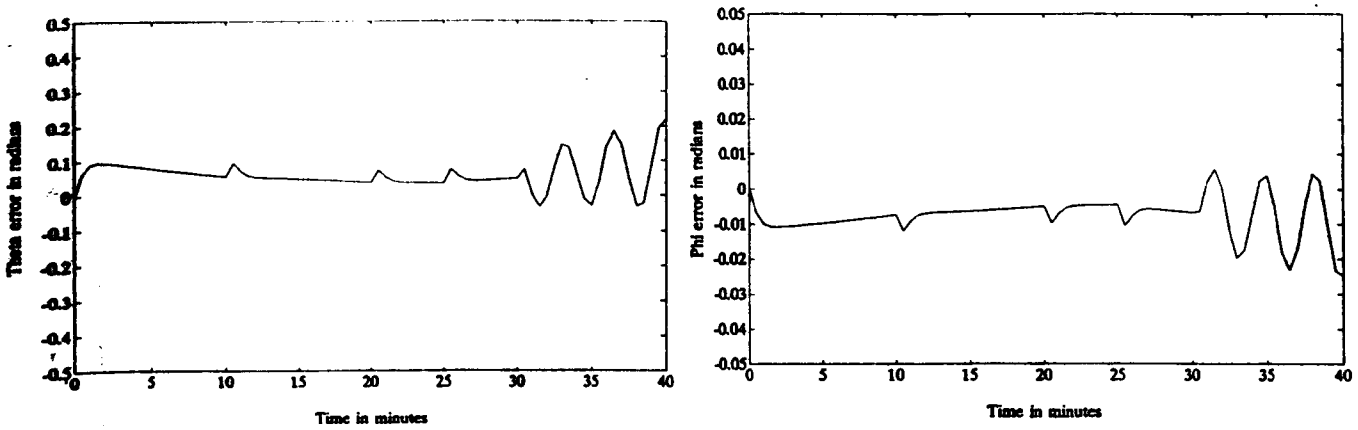

Fig 7.1 θ_r errors and ϕ_r errors for nominal $\|L\|_2$ for a sector with α = -0.5, θ = 30° and ζ_1 = [-1 -10]

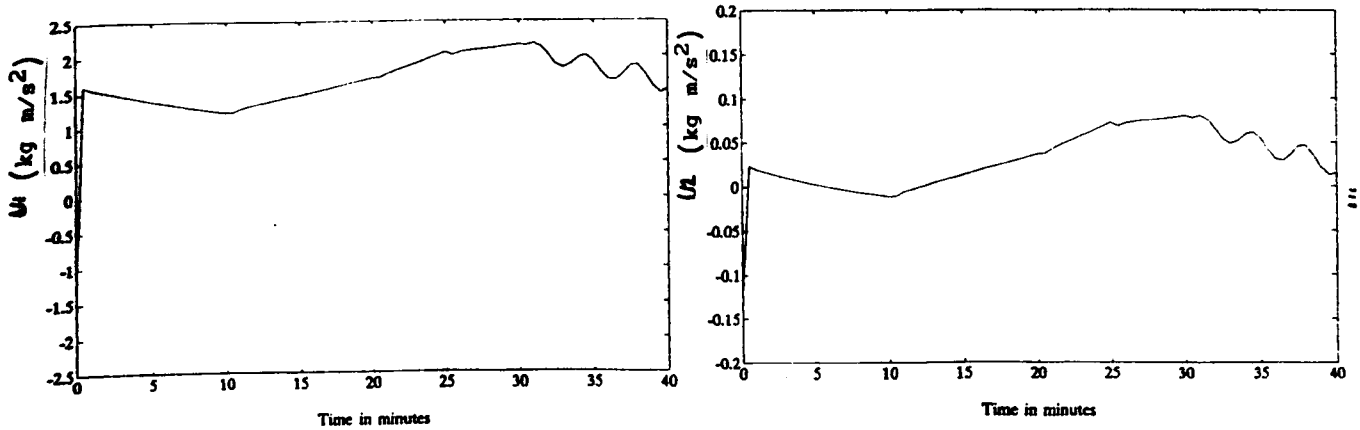

Fig 7.2 Control components for nominal $\|L\|_2$ for a sector with α = -0.5, θ = 30° and ζ_1 = [-1 -10]

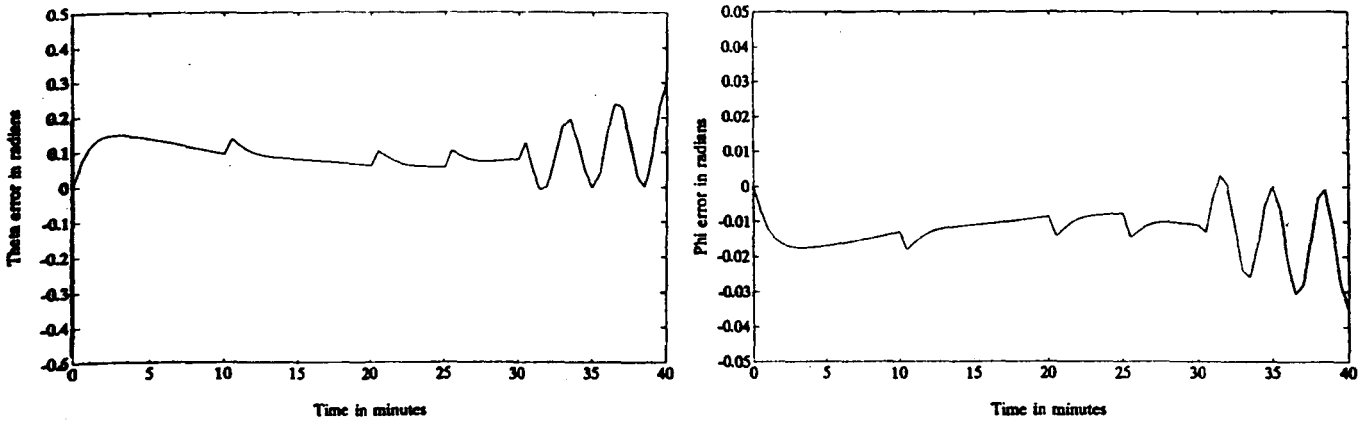

Fig 7.3 θ_r and ϕ_r errors for $\|L\|_2$ minimized by sliding mode design, α = -0.5, θ = 30° and ζ_i = [-1 -10]

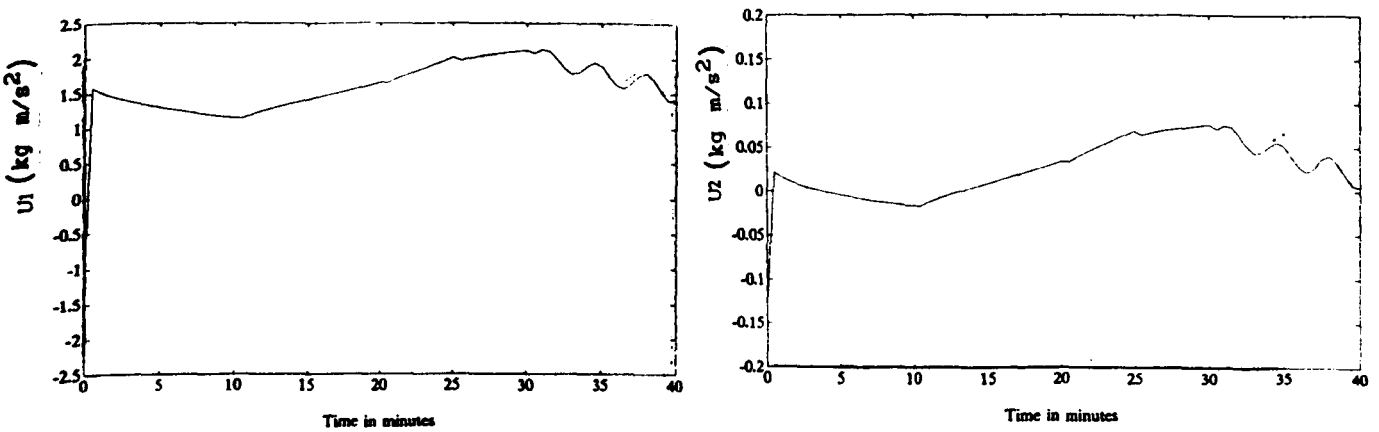

Fig 7.4 Control components for $\|L\|_2$ minimized by sliding mode design, α = -0.5, θ = 30° and ζ_i = [-1 -10]

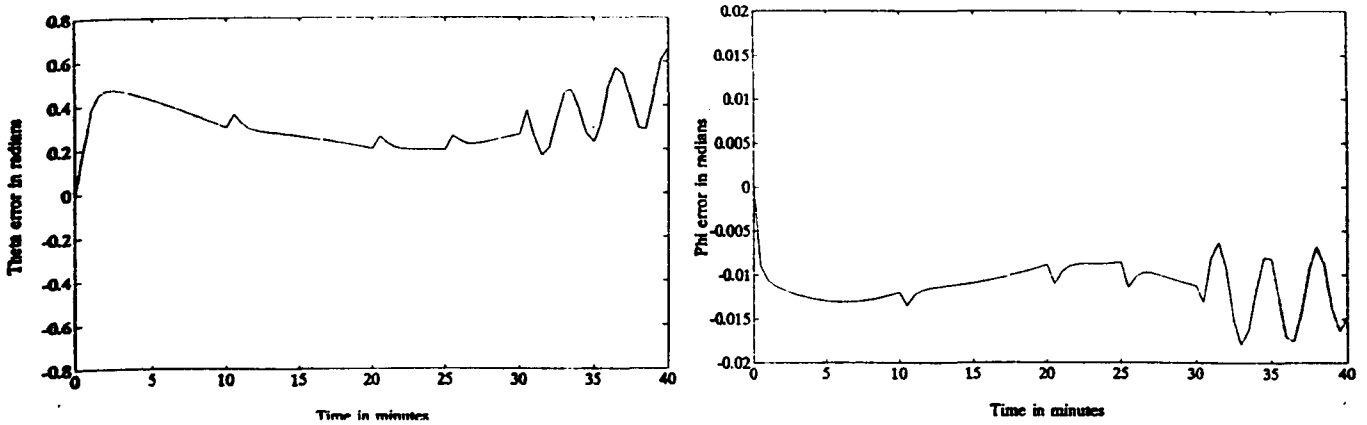

Fig 7.5 θ_r and ϕ_r errors for $\|L\|_2$ minimized by range space design, α = -0.5, θ = 30° and ζ_1 = [-0.92 -2]

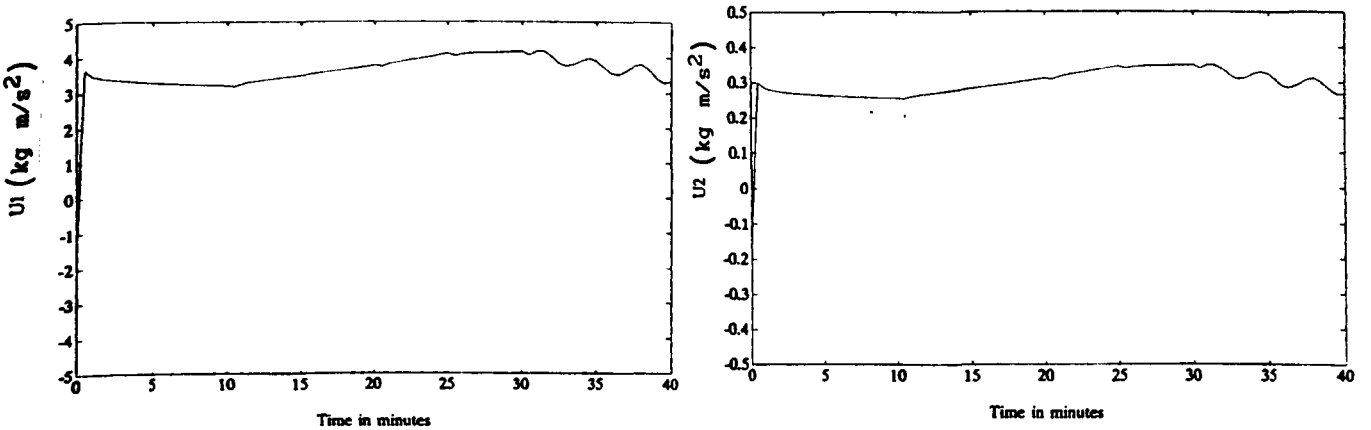

Fig 7.6 Control components for $\|L\|_2$ minimized by range space design, α = -0.5, θ = 30° and ζ_1 = [-0.92 -2]

It can be seen from figures 7.1 and 7.3 that when $\|L\|_2$ is minimized by choice of the sliding mode eigenvalues, the θ_r and ϕ_r error plots are very similar in shape, but those for the minimized value of $\|L\|_2$ are larger than those for its nominal value. The error plots for θ_r and ϕ_r for the minimization of $\|L\|_2$ by choice of the range space eigenvalues (Fig 7.5) are again the same shape, but are larger again. The angle error plots for all three cases have spikes when the robot arm changes direction, and the worst spikes occur at the changes of direction during the sinusoidal part of the trajectory. The steady state and worst case errors are as follows :

Fig 7.1	$\theta_r = 12.6^\circ$	(worst case)	$\theta_r = 2.86^\circ$	(steady state)
	$\phi_r = 1.43^\circ$		$\phi_r = 0.29^\circ$	
Fig 7.3	$\theta_r = 17.2^\circ$		$\theta_r = 5.73^\circ$	
	$\phi_r = 2.01^\circ$		$\phi_r = 0.46^\circ$	
Fig 7.5	$\theta_r = 37.2^\circ$		$\theta_r = 17.2^\circ$	
	$\phi_r = 0.89^\circ$		$\phi_r = 0.57^\circ$	

It can be seen from figures 7.2 and 7.4 that the control effort is slightly smaller when $\|L\|_2$ has been minimized by choosing appropriate sliding mode eigenvalues. If $\|L\|_2$ has been minimized by choosing appropriate range space eigenvalues, it can be seen from figure 7.6 that the control effort is increased by about 50% compared with the other two results.

The control plots are all very similar in shape, smooth waves about a constant value and these values are as follows :

Fig 7.2	u1 : 1.5	u2 : 0.025
Fig 7.4	u1 : 1.4	u2 : 0.02
Fig 7.6	u1 : 3.3	u2 : 0.28

It is clear from these results, that minimizing $\|L\|_2$ by choosing the appropriate range space eigenvalues leads to both a larger control effort, and larger errors in the angles than either minimizing $\|L\|_2$ by choosing appropriate sliding mode eigenvalues, or not minimizing $\|L\|_2$ at all.

It would appear from these results that the effect of the range space eigenvalues is more significant than the effect of the size of $\|L\|_2$. If $\|L\|_2$ is minimized by choosing the appropriate sliding mode eigenvalues, then it appears that choosing the range space eigenvalues to be small (ie large and negative) gives a small decrease in the control effort and a small increase in the angle errors.

Minimizing $\|L\|_2$ by choosing the appropriate range space eigenvalues leads to an increase in both the control effort and the angle errors. It would appear, therefore, that a smaller control effort could be obtained simply by choosing the range space eigenvalues to be large and negative, which would have the effect of maximizing the value of $\|L\|_2$.

The magnitude of the control effort clearly depends on the choice of the range space eigenvalues, and the choice of the sliding hyperplanes, and the size of $\|L\|_2$. It is not obvious from the theory how these interact, and it might be necessary to minimize $\|L\|_2$ by simultaneous choice of the sliding hyperplanes and the range space eigenvalues. There is clearly scope for an investigation into a far more complicated optimization problem than has been considered in this work.

7.4 Minimization of the Condition Number of (A + BL)

Suppose a matrix transformation maps vectors onto a surface $\mathcal{G}$. Then the condition number of the matrix is defined to be the ratio of the largest to the smallest distances from the origin to a point on this surface $\mathcal{G}$, and it will always be ≥ 1. A matrix with a condition number close to 1 is called a well-conditioned matrix. Again, since the linear control drives the state to zero, it is appropriate to try and minimize its condition number, and hence the ratio of distances. The condition number will be minimized during the design process by choice of the sliding mode eigenvalues. Suitable choice of the range space eigenvalues will lead to a decrease in the size of the condition number.

Consider the effect of minimizing the condition number (with respect to the 2-norm) of the closed-loop system for the linear control, (A + BL), on the control effort and the system performance.

The 2-norm condition number of the linear closed-loop system is defined to be

$$\kappa(A + BL) = \left\| (A + BL) \right\|_2 \left\| (A + BL)^{-1} \right\|_2 \qquad (7.4.1)$$

where $\| \ \|_2$ is as defined in equation (7.3.1).

The optimization package in MATLAB (Grace, 1990) was not used to investigate this minimization problem, since the same difficulties experienced when trying to minimize $\|L\|_2$, outlined in the previous section, will clearly arise.

A MATLAB routine for the specific problem of minimizing the condition number of (A + BL), whilst placing the closed-loop eigenvalues of the reduced order equivalent system within the required sector of the left-hand half-plane has been written. The R matrix is altered in the following way

$$newr = R_{fact}R \qquad (7.4.2)$$

where R_{fact} is a positive scalar, and R is the chosen starting matrix, usually set to I_m. The scalar R_{fact} is altered, as appropriate, until :

1) The minimum of the condition number of (A + BL) is reached.
2) A "computational steady state" minimum value is reached.
3) The smallest possible value of the condition number of (A + BL) is obtained, whilst still having the closed-loop eigenvalues within the required sector.

The results for an investigation into minimizing the condition number of (A + BL) for a sector defined by α and θ are contained in Table 7.4.1, with the values of κ(A + BL) for R_{fact} = 1 given for comparison. rp_o and rp are the switch values for R_{fact} = 1 and the minimum value of the condition number of (A + BL), $\left(\kappa(A+BL)\right)_m$, respectively, and will be set to 1 if the eigenvalues are within the required sector, and 10 otherwise.

Table 7.4.1 Minimum κ(A + BL) values for various sectors

θ°	α	rp_o	$\left(\kappa(A+BL)\right)_o$	ζ_i	$\left(\kappa(A+BL)\right)_m$	δs	R_{fact}	rp	minimum
30	-2	1	24.5883	-2.5;-3.5	16.7203	14	25	1	Y
60	-2	1	14.149	-2.5;-3.5	14.1496	22	1	1	Y
65	-2	10	12.5349	-2.5;-3.5	14.5527	27	0.6	1	Y
35	-4	1	510.7013	-4.0;-8.0	490.1365	24	160	1	Y
60	-4	10	193.5621	-4.0;-8.0	717.5465	42	0.01	1	Y
20	-6	1	2021.2	-4.0;-8.0	2001.85	17	45	1	Y
55	-6	10	724.2187	-4.0;-8.0	1039.9	39	0.04	1	Y

It can be seen from the results in Table 7.4.1 that in all cases a minimum, or a steady state value of the minimum, of κ(A + BL) is reached, and the closed-loop eigenvalues of the reduced order equivalent system are within the required sector. Three of the cases listed in Table 7.4.1 initially have eigenvalues outside the required sector (rp_o = 10), and it can be seen that the method used finds the smallest value of κ(A + BL) for which the eigenvalues are within the required the sector.

This specialized routine is again clearly successful for this particular minimization problem, with a discontinuous variable, even in the cases where the eigenvalues are initially outside the required sector.

It can be seen from the results in Table 7.4.1 that for some sectors, $\theta = 30^\circ$ and $\alpha = -2$ for example, it is possible to alter the value of $(\kappa(A + BL)$ by a reasonable amount (~ 33%), and for other sectors, $\theta = 20^\circ$ and $\alpha = -6$ for example, the value of $\kappa(A + BL)$ is not altered very much (< 1%). In the case of $\theta = 60^\circ$ and $\alpha = -2$, for example, the minimum value of $\kappa(A + BL)$ occurs when $R = I_m$, and this is also the point where the minimum of $\|L\|_2$ occurs. There is clearly a lot of variation in the value of $\kappa(A+BL)$ for the various sectors, and a lot of difference in its minimum value for the various sectors. The minimum value of $\kappa(A + BL)$ occurs for the same R_{fact} value as the minimum value of $\|L\|_2$ does, for all of the sectors investigated in Table 7.4.1, except for $\theta = 35^\circ$ and $\alpha = -4$ and $\theta = 20^\circ$ and $\alpha = -6$. The values of $\kappa(A +\_BL)$ for the various sectors are much bigger than the values of $\|L\|_2$, and the differences between the condition number when $R_{fact} = 1$ and the minimum value of the condition number are generally much larger, of the order 10 in some cases.

It can also be seen from the results in Table 7.4.1 that as R_{fact} increases, the value of $\kappa(A + BL)$ decreases. It was observed from the results obtained in section 6.2 that as R_{fact} decreases, the eigenvalues move away from the origin, and further into the sector. It is therefore clear that once again there is a trade-off between the value of R_{fact} which gives the minimum value of $\kappa(A + BL)$, and the value of R_{fact} which results in the eigenvalues being in the required sector. If the eigenvalues lie well within the required sector when $R = I_m$, and hence $R_{fact} = 1$, then

there is clearly scope for increasing the size of R_{fact} without pushing the eigenvalues out of the sector, and so the value of $\kappa(A + BL)$ may be minimized. If, however, the eigenvalues are only just in the sector when $R_{fact} = 1$, or if R_{fact} had to be decreased to push the eigenvalues into the required sector, then there is clearly very little scope for altering R_{fact}, and hence very little scope for minimizing $\kappa(A + BL)$.

The method for placing the closed-loop eigenvalues of the reduced order equivalent system in a disc will adapt itself well to the minimization of $\kappa(A + BL)$, and will now be investigated. The results for the various discs, of radius r and centre α, are given in Table 7.3.2. The other values listed in the table are the same as those for Table 7.4.1, except that in this case there is no need for the variable reg_pen, since the closed-loop eigenvalues are always within the required disc.

Table 7.4.2 Minimum $\kappa(A+BL)$ values for various discs

α	r	$\left(\kappa(A+BL)\right)_o$	ζ_1	$\left(\kappa(A+BL)\right)_m$	δs	R_{fact}	min / st-st reached
-6	4	28.0092	-2;-4	18.0119	73	429690	Y
-6	2	385.7116	-4;-8	381.4360	18	50	Y
-6	6	11.4562	-1;-6	11.4562	22	1	Y
-4	1	94.1963	-1;-6	91.0061	24	160	Y
-4	4	11.5075	-1;-6	11.5075	22	1	Y
-3	1	20.8214	-2;-4	14.9933	70	195310	Y

It can be seen from the results in Table 7.4.2 that $\kappa(A + BL)$ is minimized within a reasonable number of steps for the various combinations of α and r. It can also be seen that if the

difference between the magnitudes of α and r are zero then, the initial values of $\kappa(A + BL)$ are very similar, and the minimum values occur when $R_{fact} = 1$. For this example, except in the case when $\alpha = -3$ and $r = 1$, the minimum of the condition number of $A + BL$ does not occur for the same R_{fact} value as the minimum of $\|L\|_2$ occurs. In the case where $\alpha = -6$ and $r = 2$, for example, the minimum of the condition number occurs one step later than the minimum of the 2-norm. Again, as R_{fact} is increased, the condition number decreases, but since the eigenvalues will always lie in the disc, this does not cause any problems.

It is also possible to minimize $\kappa(A + BL)$ by choosing appropriate values for the range space eigenvalues. The effect of this minimization method will again be harder to predict, for the reasons outlined in the previous section. A MATLAB routine which alters the range space eigenvalues by scalar multiplication, until the minimum of $\kappa(A + BL)$ is reached has been written.

The results for the five state system for various sectors are displayed below, with the initial value of ζ_1 being [-1 -10] in each case.

Table 7.4.3 Minimum $\kappa(A + BL)$ values for different ζ_1

θ°	α	$\left(\kappa(A+BL)\right)_o$	ζ_1	$\left(\kappa(A+BL)\right)_m$	δs
30	-2	90.4474	-0.92;-2	14.6921	17
60	-2	55.9696	-0.92;-2	9.8194	17
35	-4	532.3128	-0.92;-2	72.3342	17
20	-6	2095.2	-0.92;-2	260.3421	17
40	-6	1388.2	-0.92;-2	175.2452	17

It can be seen from the results displayed in Table 7.4.3 that the minimization of $\kappa(A + BL)$ is affected much more by the choice of the range space eigenvalues, than by the choice of the sliding mode eigenvalues. In each case, the value of $\kappa(A + BL)$ is altered by about 80% which is a bigger difference than was obtained by altering the control matrix, and also gives consistent results which are independent of the sector chosen. Again, a combination of these minimization techniques will be considered.

It has been shown, therefore, that the value of $\kappa(A + BL)$ may be minimized by a suitable choice of the value R_{fact}, whilst still having the closed-loop eigenvalues of the reduced order equivalent system within the required sector or disc. It has also been shown that the value of $\kappa(A + BL)$ may be minimized by a suitable choice of the range space eigenvalues. However, as was found in the previous section, it is difficult to assess the effect of the minimization of $\kappa(A + BL)$ in general, due to the effects on both the linear and the non-linear part of the control of these two minimization techniques. The effect on the performance of a system must be considered for each individual case.

The model-following example of the robot arm will again be considered, so that the effects on performance as well as on the control magnitude can be seen. Firstly, a suitable choice of a sector must be made, so that the minimum value of $\kappa(A + BL)$ differs as much as possible from its value for $R_{fact} = 1$, to enable the differences in the results to show up clearly.

Investigating various sectors for the robot arm system, with the values displayed in Table 7.4.4 the same as those displayed in Table 7.4.1, and the range space eigenvalues initially set to [-1 -10], gives the following results

Table 7.4.4 Minimum κ(A+BL) values for various sectors

α	θ°	rp_o	$\left(\kappa(A+BL)\right)_o$	$\left(\kappa(A+BL)\right)_m$	δs	rp	R_{fact}	min / st-st reached
-2	30	1	64.7675	61.2386	27	1	235	Y
-2	40	1	59.8787	56.0377	28	1	260	Y
-2	60	1	47.9311	43.2057	30	1	310	Y
-4	30	1	110.6398	108.7009	19	1	55	Y
-6	30	1	158.6691	157.3581	16	1	40	Y
-1	30	1	45.2984	40.4466	30	1	310	Y
-1	60	1	39.3652	35.9382	20	1	60	Y
-1	10	1	47.6224	42.8779	30	1	310	Y
-0.5	30	1	38.5434	35.9353	8	1	8	Y

It can be seen from the results in Table 7.4.4 that the biggest difference between the initial value of κ(A + BL) and the minimum value of κ(A + BL) occurs when α = -1 and θ = 30°. The robot arm simulation will be run for this sector with both the nominal and minimized values of κ(A + BL).

The simulation will also be run for the minimization of κ(A + BL) by choice of the range space eigenvalues, for comparison.

The minimization of κ(A + BL) by choice of the range space eigenvalues will now be investigated for the robot arm. Again, the sector giving the biggest difference between the initial and minimized values of κ(A + BL) is required.

The initial choice of the range space eigenvalues is [-1 -10].

Table 7.4.5 Minimum $\kappa(A+BL)$ values for different choices of ζ_1

θ°	α	$\left(\kappa(A+BL)\right)_o$	ζ_1	δs	$\left(\kappa(A+BL)\right)_m$
30	-2	64.7675	-0.92;-2	17	16.0361
40	-2	59.8787	-0.92;-2	17	14.8996
60	-2	47.9311	-0.92;-2	17	12.1217
30	-4	110.6398	-0.92;-2	17	26.6973
30	-6	158.6691	-0.92;-2	17	37.8584
30	-1	45.2948	-0.92;-2	17	11.5085
60	-1	39.3652	-0.92;-2	17	10.1290
10	-1	47.6224	-0.92;-2	17	12.0499
30	-0.5	38.5434	-0.92;-2	17	9.9378

It can be seen from the results displayed in Table 7.4.5 that the percentage differences between the initial value of $\kappa(A + BL)$ and its minimum value are the same for all the sectors. Again, the minimization of $\kappa(A + BL)$ by the appropriate choice of the range space eigenvalues, appears to be more effective than the minimization by design of the sliding mode. This method of minimizing $\kappa(A + BL)$ is again more consistent, as was found in the minimization of $\|L\|_2$ case. The robot arm simulation will therefore be run for the sector defined by $\alpha = -1$ and $\theta = 30^\circ$, for comparison with the minimization by design of the sliding mode.

The results of the simulation runs for θ_r and ϕ_r error, u1 and u2 are displayed in figures 7.7 to 7.12, as follows :

Fig 7.7 & 7.8 Plots for ζ_1 = [-1 -10], $\kappa(A+BL)$ not minimized

Fig 7.9 & 7.10 Plots for $\kappa(A+BL)$ minimized; sliding mode design

Fig 7.11 & 7.12 Plots for $\kappa(A+BL)$ minimized; range space design

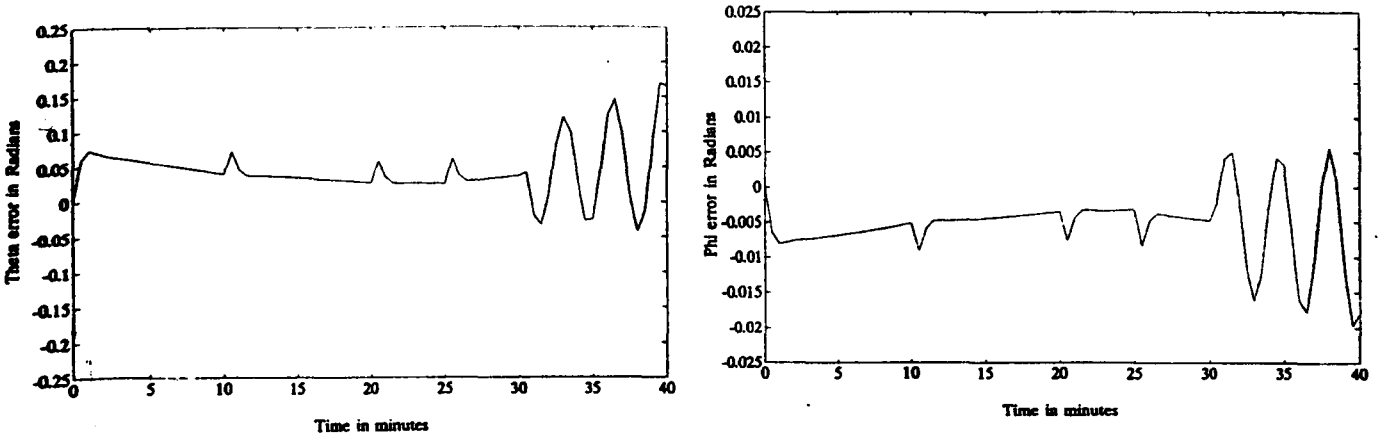

Fig 7.7 θ_r and ϕ_r errors for nominal $K(A + BL)$ for a sector with $\alpha = -1$, $\theta = 30^\circ$ and $\zeta_i = [-1\ -10]$

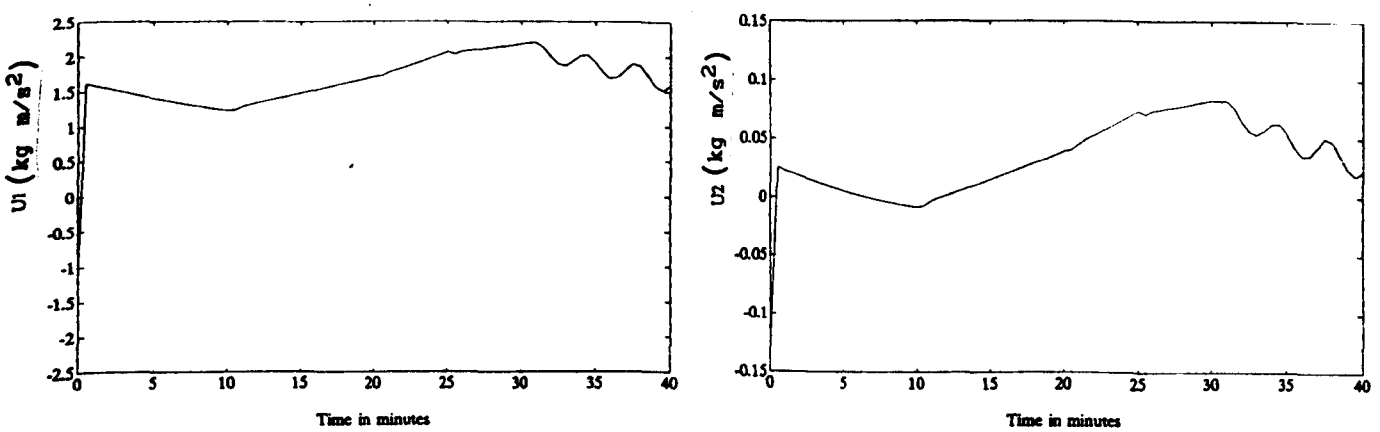

Fig 7.8 Control components for nominal $K(A+BL)$ for a sector with $\alpha = -1$, $\theta = 30^\circ$ and $\zeta_i = [-1\ -10]$

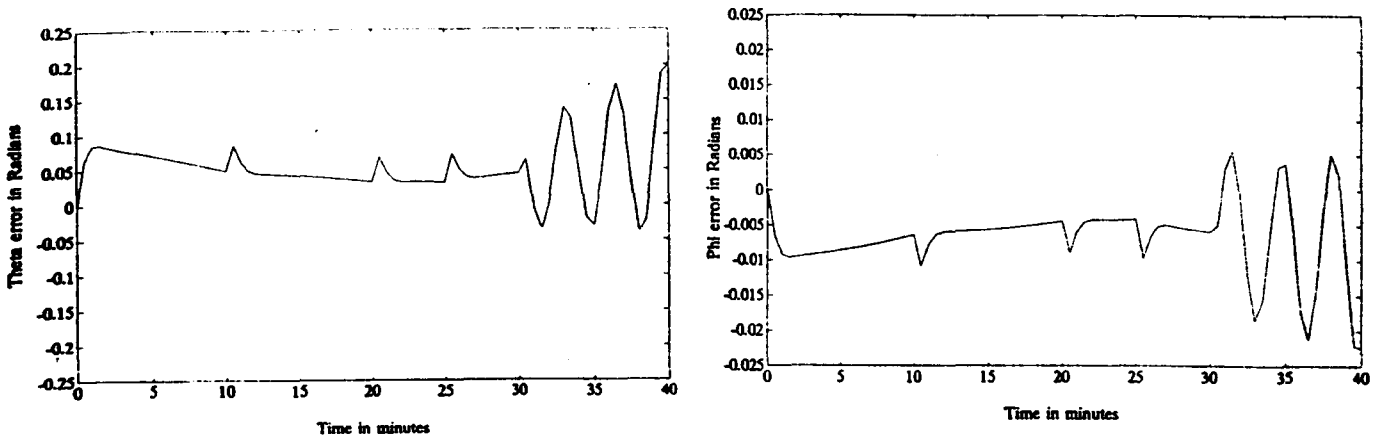

Fig 7.9 θ_r and ϕ_r errors for κ(A+BL) minimized by sliding mode design, α = -1, θ = 30° and ζ_i = [-1 -10]

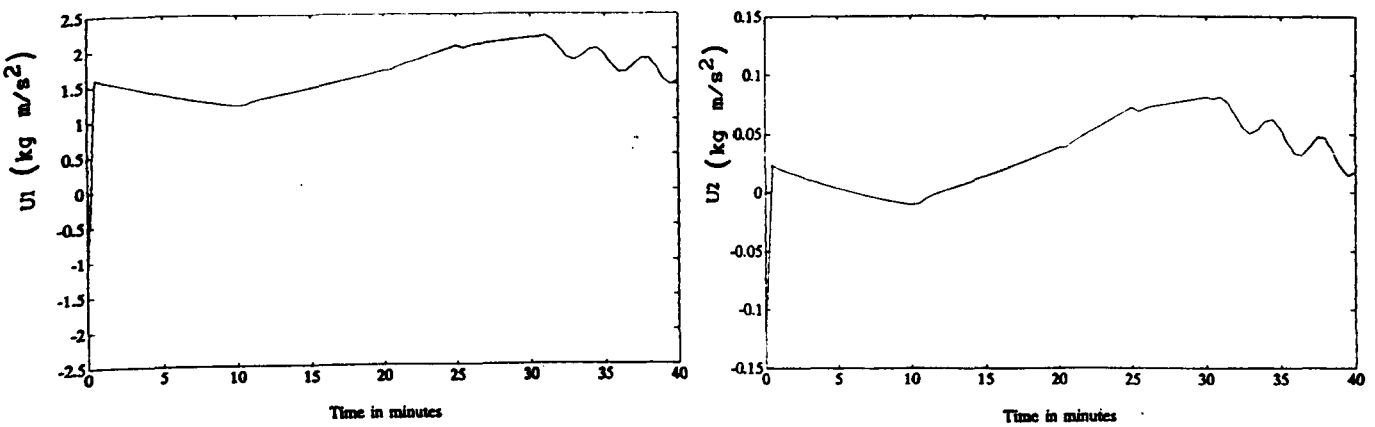

Fig 7.10 Control components for κ(A+BL) minimized by sliding mode design, α = -1, θ = 30° and ζ_i = [-1 -10]

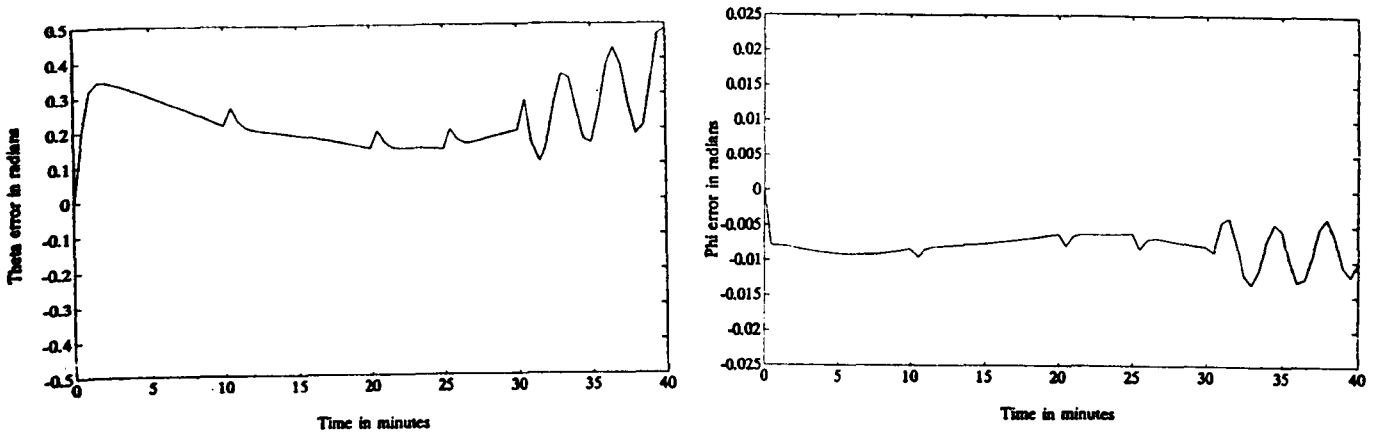

Fig 7.11 θ_r and ϕ_r errors for κ(A+BL) minimized by range space design, α = -1, θ = 30° and ζ_1 = [-0.92 -2]

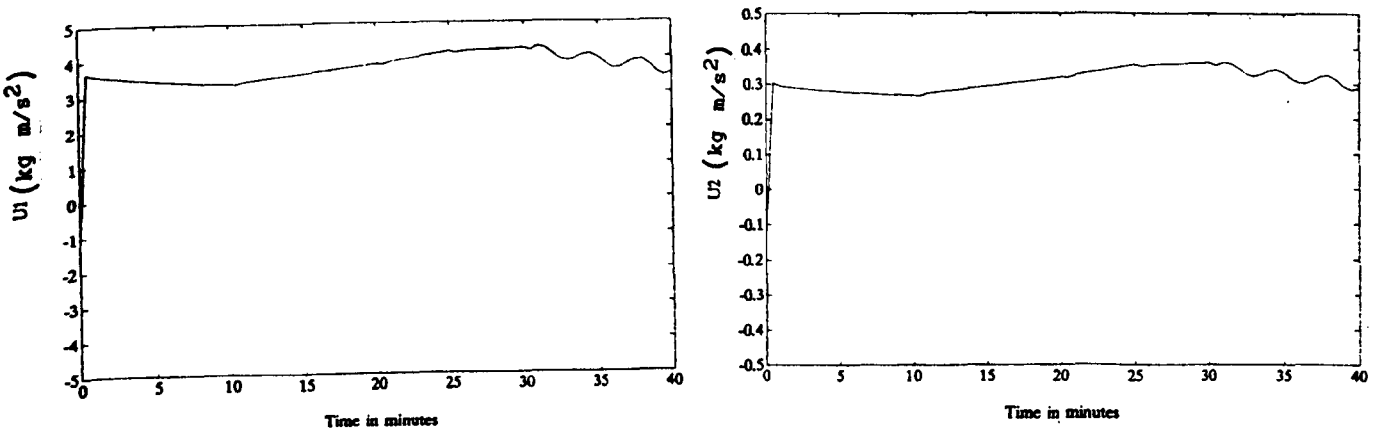

Fig 7.12 Control components for κ(A+BL) minimized by range space design, α = -1, θ = 30° and ζ_1 = [-0.92 -2]

Again, the errors in all these cases are larger than for the simulation run in Chapter 2, due, in part, to coupling effects between the angles, discussed in the previous section.

It can be seen from figures 7.7 and 7.9 that when $\kappa(A + BL)$ is minimized by choice of the sliding mode eigenvalues, the θ_r and ϕ_r error plots are very similar in shape, but those for the minimized value of $\kappa(A + BL)$ are larger than those for its nominal value. The error plots for θ_r and ϕ_r for the minimization of $\kappa(A + BL)$ by choice of the range space eigenvalues (Fig 7.11) are again the same shape, but are larger again, except for the sinusoidal part of the trajectory, when the ϕ_r errors are smaller than those in figures 7.7 and 7.9, by about 30%.

The angle error plots for all three cases have spikes when the robot arm changes direction, and the worst spikes occur at the changes of direction during the sinusoidal part of the trajectory. The steady state and worst case errors are as follows :

Fig 7.7	$\theta_r = 9.74^\circ$	(worst case)	$\theta_r = 2.29^\circ$	(steady state)
	$\phi_r = 1.15^\circ$		$\phi_r = 0.23^\circ$	
Fig 7.9	$\theta_r = 11.5^\circ$		$\theta_r = 2.86^\circ$	
	$\phi_r = 1.29^\circ$		$\phi_r = 0.29^\circ$	
Fig 7.11	$\theta_r = 28.1^\circ$		$\theta_r = 11.5^\circ$	
	$\phi_r = 0.77^\circ$		$\phi_r = 0.40^\circ$	

It can be seen from figures 7.8 and 7.10 that the control effort is indistinguishable for the nominal and minimized by sliding mode design values of $\kappa(A + BL)$. If $\kappa(A + BL)$ has been minimized by choosing appropriate range space eigenvalues, it can be seen from figure 7.12 that the control effort is increased by about 50% compared with the other two results, and varies less, after the first second, than the other two control plots do. The control plots are all very similar in shape, smooth waves about a constant value and these values are as follows :

Fig 7.8	u1 : 1.6	u2 : 0.035
Fig 7.10	u1 : 1.6	u2 : 0.035
Fig 7.12	u1 : 3.5	u2 : 0.3

It is clear from these results, that minimizing $\kappa(A + BL)$ by choosing the appropriate range space eigenvalues leads to both a larger control effort, and larger errors in the angles than either minimizing $\kappa(A + BL)$ by choosing appropriate sliding mode eigenvalues, or not minimizing $\kappa(A + BL)$ at all.

It would appear from these results that the effect of the range space eigenvalues is more significant than the effect of the size of $\kappa(A + BL)$. If $\kappa(A + BL)$ is minimized by choosing the appropriate sliding mode eigenvalues, then it appears that choosing the range space eigenvalues to be small (ie large and negative) gives a small decrease in the control effort and a small increase in the angle errors.

Minimizing $\kappa(A + BL)$ by choosing the appropriate range space eigenvalues leads to an increase in both the control effort and the angle errors. It would appear, therefore, that a smaller control effort could be obtained simply by choosing the range space eigenvalues to be large and negative, which would have the effect of maximizing the value of $\kappa(A + BL)$.

7.5 Discussion

It is clear from this work that it is possible to minimize either the 2-norm of the linear part of the control, or the condition number of the linear closed-loop feedback system, or in some cases both simultaneously, whilst the closed-loop eigenvalues of the reduced order equivalent system remain in the required sector or disc in the left-hand half-plane. The specialized MATLAB routines seem to work very efficiently when solving these problems, and the difficulties experienced when trying to use a very general MATLAB optimization routine to solve these problems have been overcome.

However, it appears that the effects of these two different minimizations of the linear part of the control are very small, and for some of the examples used here, they are dominated by the effects of the choice of the range space eigenvalues. It is clearly not straightforward to predict these effects on the control effort and performance from the theory, partly due to the complexity of the interactions, and partly because the choice of

the range space eigenvalues affects the non-linear part of the control as well as the linear part of the control. The effects of the minimization of the condition number of the linear feedback system on the control effort and the performance would appear to be as small as the effects of the minimization of the 2-norm of the linear part of the control.

The most critical effect on the performance of the system would appear to be due to the choice of the range space eigenvalues. The following effects of the range space eigenvalues have been deduced from these investigations :

1) If the range space eigenvalues are small and negative, then the 2-norm and the condition number will be minimized, simultaneously, and the resulting control will be increased by about 50% .
2) If the range space eigenvalues are chosen to be large and negative, then the 2-norm and the condition number will be maximized, and the control effort will be decreased.
3) If the 2-norm or the condition number is minimized by design of the sliding mode, and the range space eigenvalues are large and negative, then the control effort may be decreased.

It would appear, therefore, that the most satisfactory way to decrease the effort of the linear part of the control, without increasing the system errors, is to choose the range space eigenvalues so as to maximize the 2-norm or the condition number.

8. CONCLUSIONS AND FURTHER WORK

It has been illustrated in this thesis that the Variable Structure Control approach to the solution of the problem of deterministic control of uncertain time-varying systems compares very well with the method of Lyapunov Control. The accuracy of these two methods has been confirmed by the detailed consideration of a non-linear uncertain model-following control system, a trajectory-tracking robot manipulator.

The design of the sliding hyperplane matrix of a Variable Structure controller, by specifying different regions in the left-hand half-plane in which the closed-loop eigenvalues of the reduced order equivalent system must lie, has been investigated. The method of eigenvalue placement within a vertical strip has necessitated an investigation into the suitability of methods of solution of a real continuous matrix Riccati equation for the particular case when the right-hand side of the equation is equal to zero. The theory for the placement of the closed-loop eigenvalues of a general system within a disc or an infinite vertical strip has been developed for use in the hyperplane matrix design method.

Two new regions of the left-hand half-plane have also been considered, namely a sector and a region bounded by two intersecting sectors. The necessary theory for ensuring that the eigenvalues of a system lie within these regions has been developed, and then extended for use in the design of the sliding hyperplane matrix.

This has involved an investigation into the solution of a complex continuous matrix Riccati equation, and a reliable method leading to a satisfactory solution has been developed. The restrictions on the magnitude of the angle describing the sector, for satisfactory closed-loop eigenvalue placement within the sector, have been established for a general system of the form of equation (2.2.2).

The robustness of the three different regions to changes in the positive definite symmetric R matrix has been investigated. The choice of the appropriate R matrix to give the desired eigenvalues, real or complex, and to specify their positions within the required region have been obtained for a general system of the form of equation (2.2.2). Some further results on the positioning of the eigenvalues within the required region have been proved for a system of a particular specialized form.

The minimization of the magnitude of the control effort has been considered, and two different options have been investigated, namely the minimization of the 2-norm of the linear part of the control, and the minimization of the condition number of the linear closed-loop feedback system. These minimizations have been obtained by choice of the sliding hyperplanes, or by choice of the range space eigenvalues. The results for these two investigations have shown that the magnitude of the range space eigenvalues has a very considerable effect on the magnitude of the control effort, which dominates the effect of the choice of the sliding hyperplanes.

There is clearly scope for further work in this area, and the obvious particular paths to be considered are as follows :

1) Rationale for a 60° limit on the angle describing a sector in the left-hand half-plane whose end point is smaller than the smallest real eigenvalue of the reduced order equivalent system.
2) Full theoretical proof of the method of solution of a complex continuous matrix Riccati equation.
3) Improved accurate method for solving the standard real continuous matrix Riccati equation, with its right-hand side equal to zero.
4) Further investigation into the effect of the range space eigenvalues and the design of the sliding hyperplane matrix on the magnitude of the control effort, and on the performance of a Variable Structure Control system.

REFERENCES

Abdul-Wahab A.A., "Lyapunov-type Equations for Matrix Root-Clustering in Subregions of the Complex Plane", Int. J. Sys. Sci., vol. 21, no. 9, pp. 1819-1830, 1990.

Anderson B.D. and J.B. Moore, "Linear System Optimization with Prescribed Degree of Stability", Proc. IEE, vol. 116, no. 12, pp. 2083-2087, 1969.

Anderson B.D. and J.B. Moore, "Linear Optimal Control",Prentice-Hall, pp. 343-363, 1971.

Barmish B. & G. Leitmann, "On Ultimate Boundedness Control of Uncertain Systems in the Absence of Matching Assumptions", IEEE Trans. Autom. Control, vol. AC-27, no. 1, pp. 153-158, 1982.

Bogachev A.V., V.V. Grigor'ev, V.N. Drozdov and A.N. Korov'yakov, "Analytic Design of Controls from Root Indicators", Autom. Telem., vol. 8, pp. 21-28, 1980.

Burrows S.P. and R.J. Patton, "A Comparison of Some Robust Eigenvalue Assignment Techniques", Optim. Control Appl. & Methods, vol. 11, pp. 355-362, 1990 (a).

Burrows S.P. and R.J. Patton, "Optimal Eigenstructure Assignment for Multiple Design Objectives", American Control Conference, vol. 2, pp. 1678-1683, 1990 (b).

Corless M. & G. Leitmann, "Continuous State Feedback Guaranteeing Uniform Ultimate Boundedness for Uncertain Dynamic Systems", IEEE Trans. Autom. Control., vol. AC-25, no. 5, pp. 1139-1144, 1981.

D'Azzo J.J. and C.H. Houpis, "Linear Control System Analysis and Design", McGraw-Hill, pp. 253-306, 1981.

DeCarlo R.A., S.H. Zak and G.P. Matthews, "Variable Structure Control of Non-Linear Multivariable Systems - a Tutorial", Proc IEEE, vol. 76, pp. 212-232, 1988.

Dorling C.M., "The Design of Variable Structure Control Systems," Manual for VASSYD CAD Package, Sheffield University, 1985.

Dorling C.M. and A.S.I. Zinober, "Two Approaches to Hyperplane Design in Multivariable Variable Structure Control Systems", Int. J. Control, vol. 44, no. 1, pp. 65-82, 1986.

Dorling C.M. and A.S.I. Zinober, "Robust Hyperplane Design in Multivariable Variable Structure Control Systems", Int. J. Control, vol. 48, no. 5, pp. 2043-2054, 1988.

Drazenovic B., "The Invariance Conditions in Variable Structure Systems", Automatica, vol. 5, pp. 287-295, 1965.

Fahmy M.M. and J. O'Reilly, "On Eigenstructure Assignment in Linear Multivariable Systems", IEEE Trans. Autom. Control, vol. AC-27, no. 3, pp. 690-693, 1982.

Foo Y.K. and Y.C. Soh, "Damping Margins of Interval Polynomials", IEEE Trans. Autom. Control, vol. AC-35, no. 4, pp. 477-479, 1990.

Furuta K. & S.B. Kim, "Pole Assignment in a Specified Disc", IEEE Trans. Autom. Control, vol. AC-32, no. 5, pp. 423-427, 1987.

Garofalo F. and L. Glielmo, "Nonlinear Continuous Feedback Control for Robust Tracking," in "Deterministic Control of Uncertain Systems," ed. A.S.I. Zinober, Peter Peregrinus Press, 1991.

Grace A., "Optimization Toolbox Users Guide", Mathworks, pp. 2.4-2.11, 1990.

Grimble M.J. and M.A. Johnson, "Optimal Control and Stochastic Estimation : Theory and Applications", Wiley, Vol 1, pp 256-340, 1988.

Gutman S., "Root Clustering of a Complex Matrix in an Algebraic Region", IEEE Trans. Autom. Control, vol. AC-24, no. 4, pp. 647-650, 1979.

Gutman S. and Z. Palmor, "Properties of Min-Max Controllers in Uncertain Dynamical Systems", SIAM Journal of Control and Optimization, vol. 20, pp. 850-861, 1982.

Gutman S. and F. Vaisberg, "Root Clustering of a Real Matrix in a Sector", IEEE Trans. Autom. Control, vol. AC-29, no. 3, pp. 251-253, 1984.

Harvey C.A. and G. Stein, "Quadratic Weights for Asymptotic Regulator Properties", IEEE Trans. Autom. Control, vol. AC-23, no. 3, pp. 378-387, 1978.

Hohn F.E., "Elementary Matrix Algebra", Macmillan, pp. 350-353, 1964.

Itkis U., "Control Systems of Variable Structure", Wiley, New York, 1976.

Juang Y-T., Z-C. Hong & Y-T. Wang, "Robustness of Pole Assignment in a Specified Region", IEEE Trans. Autom. Control, vol. AC-34, no. 7, pp. 758-760, 1989.

Kailath T., "Linear Systems", Prentice-Hall, pp. 230-237, 1980.

Karanam V.R., "Eigenvalue Bounds for Algebraic Riccati and Lyapunov Equations", IEEE Trans. Autom. Control, vol. AC-27, no. 2, pp. 461-463, 1982.

Kautsky J., N.K. Nichols & P. Van Dooren, "Robust Pole Assignment in Linear State Feedback", Int. J. Control, vol. 41, no. 5, pp. 1129-1155, 1985.

Kawasaki N. and E. Shimemura, "Determining Quadratic Weighting Matrices to Locate Poles in a Specified Region", Automatica, vol. 19, no. 5, pp. 557-560, 1983.

Kawasaki N. & E. Shimemura, "Pole Placement in a Specified Region based on a Linear Quadratic Regulator", Int. J. Control, vol. 48, no. 1, pp. 225-240, 1988.

Kim J-S. and C-W. Lee, "Optimal Pole Assignment into Specified regions and its Application to Rotating Mechanical Systems", Opt. Control Appl. and Methods, vol. 11, pp. 197-210, 1990.

Komaroff N., "Simultaneous Eigenvalue Lower Bounds for the Lyapunov Matrix Equation", IEEE Trans. Autom. Control, vol. AC-33, no. 1, pp. 126-128, 1988.

Kwon B.H., M.J. Youn and Z. Bien, "On Bounds of the Riccati and Lyapunov Matrix Equations", IEEE Trans. Autom. Control, vol. AC-30, no. 11, pp. 1134-1135, 1985.

Laub A., "A Schur Method for Solving Algebraic Riccati Equations", IEEE, Trans Autom. Control, vol. AC-24, no. 6, pp. 913-921, 1979.

Ryan E.P. and M. Corless, "Ultimate Boundedness and Asymptotic Stability of a Class of Uncertain Dynamical Systems via Continuous and Discontinuous Feedback Control", IMA Journal of Math. Control & Information, vol. 1, pp. 223-242, 1984.

Ryan E.P., "A Variable Structure Approach to Feedback Regulation of Uncertain Dynamical Systems", Int. J. Control, vol. 38, no. 6, pp. 1121-1134, 1983.

Ryan E.P., "Adaptive Stabilization of a Class of Uncertain Non-Linear Systems - a Differential Inclusion Approach", Syst. & Control Letters, vol. 10, pp. 95-101, 1988.

Shieh L.S., H.M. Dib & B.C. McInnis, "Linear Quadratic Regulators with Eigenvalue Placement in a Vertical Strip", IEEE Trans. Autom. Control, vol. AC-31, no. 3, pp. 241-243, 1986.

Soh C.B., "Damping Margin of Continuous-Time Systems with Polytope Uncertainties", Int. J. Syst. Sci., vol. 21, no. 4, pp.749-754, 1990.

Utkin V.I., "Variable Structure Systems with Sliding Modes", IEEE Trans. Autom. Control, vol. AC-22, no. 2, pp. 212-222, 1977.

Utkin V.I., "Sliding Modes and their Application in Variable Structure Systems", MIR, Moscow, 1978.

Utkin V.I. and K.D. Yang, "Methods for Constructing Discontinuity Planes in Multidimensional Variable Structure Systems", Autom. Remote Control, vol. 39, no. 10, pp. 1466-1470, 1978.

Wilkinson J.H., "The Algebraic Eigenvalue Problem", Clarendon Press, Oxford, 1965.

Woodham C.A. and A.S.I. Zinober, "New Design Techniques for the Sliding Mode", IEEE International Workshop, Sarajevo, pp. 220-231, 1990.

Woodham C.A. and A.S.I. Zinober, "Eigenvalue Assignment for the Sliding Hyperplanes", IEE Control Conference, Edinburgh, pp 982-988, 1991.

Woodham C.A. and A.S.I. Zinober, "Robust Eigenvalue Assignment Techniques for the Sliding Mode", IFAC Symposium, Zurich, pp 529-533, 1991.

Young K-K.D., "Asymptotic Stability of Model Reference Systems with Variable Structure Control", IEEE Trans. Autom. Control, vol. AC-22, pp. 279-281, 1977.

Young K-K.D., "Controller Design for a Manipulator using Theory of Variable Structure Systems," IEEE Trans. Syst. Man. & Cyb., vol. 8, pp. 101-109, 1978.

Zinober A.S.I., O.M.E. El-Ghezawi and S.A.Billings. "Variable Structure Control of Adaptive Model-Following Systems", IEE Conference Control & Applic., Warwick, pp. 123-127, 1981.

Zinober A.S.I., O.M.E. El-Ghezawi and S.A.Billings. "Multivariable Variable Structure Adaptive Model-Following Control Systems", IEE Proc., vol. 129, part D, no. 1, pp. 6-12, 1982.

Zinober A.S.I., "Properties of Adaptive Discontinuous Model-Following Control Systems," Fourth IMA International Conference, Cambridge, pp. 337-346, 1984.

Zinober A.S.I., "Variable Structure Control of a Robot Manipulator," Fourth IFAC Symposium, Beijing, pp. 175-180, 1988.

Zinober A.S.I., "Deterministic Control of Uncertain Systems," Proc. IEEE ICCON Conference, Jerusalem, WP-6-1, pp. 1-6, 1989.

Zinober A.S.I., "Deterministic Nonlinear Control of Uncertain Systems", Peter Peregrinus Press, 1991.

Zinober A.S.I. and C.A. Woodham, "Deterministic Nonlinear Control of a Robot Manipulator", IEEE Control Conference, Jerusalem, TP-3-8, pp, 1-2, 1989.

Zinober A.S.I. and C.A. Woodham, "Variable Structure Model-Following Control of a Robot Manipulator", IMA Conference, Loughborough, 1989. (Not Yet Published)